UNIWERSYTET
PRZYRODNICZY
WE WROCŁAWIU
WYDZIAŁ PRZYRODNICZO-TECHNOLOGICZNY

Mgr inż. Krzysztof Papuga

Wybrane aspekty analizy składu granulometrycznego gleb metodą pomiaru ciężaru pozornego pływaka zanurzonego w zawiesinie

Selected aspects of the soil particle size analysis by measuring the apparent weight of a float immersed in suspension

Promotor: **Prof. dr hab. inż. Jarosław Kaszubkiewicz**
Instytut Nauk o Glebie, Żywienia Roślin i Ochrony Środowiska
Promotor pomocniczy: **Dr inż. Dorota Kawałko**
Instytut Nauk o Glebie, Żywienia Roślin i Ochrony Środowiska

Wrocław 2022

I z każdym dniem wiedziałem mniej, i z każdym dniem popadałem
w rozpacz, że nigdy nie przeczytam tego, co powinienem przeczytać.
Marek Hłasko

Wykaz publikacji

Autoreferat został przygotowany na podstawie cyklu trzech publikacji, będących opracowaniem wyników badań związanych z rozwijaną metodą oznaczania składu granulometrycznego gleb. Prace zostały opublikowane w czasopismach znajdujących się w wykazie czasopism naukowych i recenzowanych materiałów z konferencji międzynarodowych Ministerstwa Edukacji i Nauki oraz posiadających wskaźnik cytowań *Impact Factor* (IF). Łączna liczba tzw. „punktów ministerialnych" wynosi **440**, a sumaryczny wskaźnik IF jest równy **11.986**. Na cykl publikacji składają się następujące prace:

- Kaszubkiewicz J., Papuga K., Kawałko D., Woźniczka P., 2020. Particle size analysis by an automated dynamometer method integrated with an x-y sample changer. Measurement, 157, 107680. **(Impact Factor: 3,927; liczba punktów: 200)**
- Papuga K., Kaszubkiewicz J., Kawałko D., 2021. Do we have to use suspensions with low concentrations in determination of particle size distribution by sedimentation methods? Powder Technology, 389, 507-521. **(Impact Factor: 5,134; liczba punktów: 140)**
- Papuga K., Kaszubkiewicz J., Kawałko D., Kreimeyer M., 2022. Effect of Organic Matter Removal by Hydrogen Peroxide on the Determination of Soil Particle Size Distribution Using the Dynamometer Method. Agriculture, 12, 226. **(Impact Factor: 2,925; liczba punktów: 100)**

Wszystkie prace dotyczą metody oznaczania składu granulometrycznego za pomocą pomiaru ciężaru pozornego pływaka zanurzonego w sedymentującej zawiesinie, zwanej metodą dynamometryczną. Z racji szerokiego potencjalnego zakresu przygotowywanej pracy, skupiono się na trzech wybranych aspektach. Każda z publikacji stanowi przedstawienie jednego z nich:

- Określenie możliwości zautomatyzowania procesu oznaczania składu granulometrycznego.
- Zniwelowanie wpływu stosowania większych, niż w innych sedymentacyjnych metodach oznaczania składu granulometrycznego, naważek gleby na wyniki.
- Określenie wpływu usuwania materii organicznej na otrzymywane wyniki składu granulometrycznego za pomocą metody dynamometrycznej.

Spis treści

Streszczenie

Mimo, iż podstawy sedymentacyjnych metod oznaczania składu granulometrycznego opracowano przeszło 100 lat temu, to wciąż są one rozwijane. Jedną z metod, która w dużym stopniu eliminuje wady najczęściej stosowanych metod sedymentacyjnych, jednocześnie, zachowująca wysoką dokładność wyników, jest metoda dynamometryczna. Metoda oparta została o pomiary zmian ciężaru pozornego pływaka zawieszonego w sedymentującej zawiesinie glebowej. Celem pracy było uzupełnienie wiedzy z zakresu oznaczania składu granulometrycznego gleb, związanej z nowo powstałą metodą dynamometryczną. W związku z tym przeanalizowano trzy główne aspekty: implementację metody dynamometrycznej do urządzenia z wielostanowiskowym i automatycznym zmieniaczem próbek; wykorzystanie iteracyjnej procedury obliczeniowej w celu zmniejszenia wpływu podwyższonej koncentracji początkowej zawiesiny na wyniki; wpływ usuwania materii organicznej na wyniki.

Na potrzeby pracy wykonano podstawowe analizy gleboznawcze oraz analizy powtarzalności oznaczania składu granulometrycznego, porównano wyniki względem uzyskiwanych za pomocą metody pipetowej, przeprowadzono analizę porównawczą zmierzonej zawartości poszczególnych frakcji w mieszaninach gleb oraz obliczonej teoretycznej zawartości, wykonano analizę wielkości różnic pomiędzy próbkami, w których usunięto materię organiczną, a próbkami bez jej usuwania i analizy statystyczne. W toku badań zostały określone optymalne parametry pomiarów oraz indywidualna metodyka przygotowania próbek glebowych

Stwierdzono, że zastosowanie aparatu wielostanowiskowego z automatycznym zmieniaczem próbek w metodzie dynamometrycznej cechowało się dużą zgodnością z wynikami metody sedymentacyjnej i wysoką powtarzalnością otrzymywanych wyników. Zaproponowana iteracyjna metoda obliczeniowa, wykorzystująca korektę prędkości opadania cząstek w oparciu o równanie Batchelora, pozwala na stosowanie w pomiarach rozkładu wielkości cząstek zawiesin o stężeniu objętościowym do 0,0453. Usuwanie materii organicznej w próbkach glebowych powodować może znaczne zmiany zawartości poszczególnych frakcji mierzonych za pomocą metody dynamometrycznej. Kierunek i wielkość zmian dla poszczególnych próbek jest nieregularny i trudny do przewidzenia. Nie stwierdzono jednoznacznych przesłanek do usuwania materii organicznej w przypadku, gdy jej zawartość w badanej glebie jest na niskim poziomie.

SŁOWA KLUCZOWE: skład granulometryczny, metody sedymentacyjne, metoda dynamometryczna, sedymentacja ziaren gleby

Abstract

Although the basis for sedimentation methods of particle size distribution was developed more than 100 years ago, they are still being improved. One of the methods that eliminates to a large extent the drawbacks of the most commonly used sedimentation methods, while maintaining high accuracy of results, is the dynamometer method. The method was based on measurements of changes in apparent weight of a float suspended in sedimenting soil suspension. The aim of this study was to supplement the knowledge on the determination of the particle size distribution of soils, related to the newly developed dynamometer method. In this regard, three main aspects were analysed: the implementation of the dynamometer method in an device with a multi-station and automatic sample changer; the use of an iterative calculation procedure to reduce the influence of an increased initial suspension concentration on the results; the influence of organic matter removal on the results.

For the purposes of the study, basic soil analyses and repeatability analyses of particle size determination were carried out, the results were compared with those obtained using the pipette method, a comparative analysis of the measured content of individual fractions in soil mixtures and the calculated theoretical content was carried out, as well as an analysis of the magnitude of differences between samples with and without organic matter removal, and statistical analyses. In the study, optimum measurement parameters and an individual soil sample preparation methodology were developed.

It was found that the application of the multi-station automatic sample changer in the dynamometer method was characterised by high agreement with the results of the sedimentation method and high repeatability of the obtained results. The proposed iterative calculation method, using the correction of particle falling velocity based on the Batchelor equation, allows for the use in the measurements of the particle size distribution of suspensions with a volume concentration up to 0.0453. The removal of organic matter in soil samples may cause significant changes in the content of particular fractions measured by the dynamometer method. The direction and magnitude of changes for individual samples is irregular and difficult to predict. There is no unequivocal indication for the removal of organic matter when its content in the tested soil is at a low level.

KEY WORDS: particle size distribution, sedimentation methods, dynamometer method, soil particle sedimentation

1. Wstęp

Skład granulometryczny to podstawowa właściwość gleby (Fan i in., 2021; Ghalib i Hryciw, 1999; Shangguan i in., 2012). Jego poprawne oznaczenie jest kluczowe w pozyskiwaniu informacji wykorzystywanych w różnych działach nauk o glebie. Znajomość składu granulometrycznego jest niezbędna między innymi w przewidywaniu wielkości erozji, systematyce gleb, określaniu wartości użytkowych (Koza i in., 2021; Paluszek i in., 2011; Tong i in., 2018). Istnieje kilka grup metod oznaczania składu granulometrycznego, wykorzystujących różne zjawiska fizyczne. Różnią się one zakresem stosowalności, pracochłonnością, kosztami oraz wielkością błędów pomiarowych. Jedną z głównych grup są metody sedymentacyjne, wykorzystujące zjawisko sedymentacji ziaren glebowych. Do klasycznych metod sedymentacyjnych należą metody: areometryczna opracowana przez Bouyoucos (1927) i pipetowa stworzona niezależnie przez Robinsona (1922) oraz Jenningsa i Gardnera (1922). Obie metody są powszechnie stosowane na świecie (Keller i Gee, 2006; ISO 11277, 2009; Ryżak i Bieganowski, 2010). Metoda areometryczna polega na pomiarze zmian gęstości sedymentującej zawiesiny za pomocą areometru. W przypadku metody pipetowej wymagane jest użycie specjalnej pipety, którą pobierana jest pewna objętość sedymentującej zawiesiny (Bieganowski i Ryżak, 2011; Novák i Hlaváčiková, 2019). W obydwu metodach potrzebne jest określenie odpowiednich czasów, w których następuje pomiar lub pobranie zawiesiny, na podstawie równania Stokesa. Ich niewątpliwą zaletą jest wysoka powtarzalność wyników, prosta procedura wykonywania pomiarów oraz niski koszt wykorzystywanego sprzętu. Do głównych wad należą: znaczna czasochłonność i pracochłonność wykonywania analiz, istotny wpływ czynnika ludzkiego przy odczytywaniu wyników i wyznaczanie krzywej rozkładu granulometrycznego na podstawie kilku punktów. Ponadto w metodzie areometrycznej przy obliczaniu czasów opadania poszczególnych frakcji nie jest uwzględniane zmienne zanurzenie areometru w glebach o różnym składzie (Bieganowski i in., 2018; Bittelli i in., 2019; Di Stefano i in., 2010).

Mimo, iż podstawy sedymentacyjnych metod składu granulometrycznego opracowano przeszło 100 lat temu, to wciąż są one rozwijane. Wpływ na to miało pojawienie się nowych możliwości technicznych (miniaturyzacja i spadek kosztów sensorów) oraz występowanie wad metod innych niż sedymentacyjne m.in. metod dyfrakcji laserowej czy Sedigraphu (Andrenelli i in., 2013; Igaz i in., 2020; Lucke i in., 2015; Polakowski i in., 2021; Yang i in 2019). Obecny rozwój metod kładzie nacisk na cyfryzację wyników, automatyzację procesu oraz skrócenie czasu analizy. W XXI wieku powstały takie metody jak: *The integral suspension pressure method (ISP)* (Durner i Iden, 2021; Durner i in., 2017), połączenie metody sedymentacyjnej ze spektrofotometrią (Ghasemy i in., 2018), zautomatyzowana metoda areometryczna (Murad i in., 2020), metoda z quasi ciągłym pomiarem (Kovács i in., 2004), automatyczna metoda wykorzystująca do pomiaru sedymentującej zawiesiny promieniowanie gamma (Naime i in., 2001), metoda pomiaru zmian natężenia światła laserowego przechodzącego przez cylinder z sedymentującą zawiesiną (Orhan i Kılınç, 2020) czy metoda *Buoyancy weighing-bar* (Obata i in., 2009). Jedną z wielu metod eliminującą w dużym stopniu wady

najczęściej stosowanych metod sedymentacyjnych, jednocześnie zachowującą wysoką dokładność wyników i wpisującą się w obecne trendy rozwoju, jest metoda dynamometryczna.

W 2017 roku zespół profesora Kaszubkiewicza opracował nową metodę oznaczania składu granulometrycznego gleb (Kaszubkiewicz i in., 2017). Metoda oparta została o pomiary zmian ciężaru pozornego pływaka zawieszonego w sedymentującej zawiesinie glebowej. Pomiary wykonywane są za pomocą piezoelektrycznego dynamometru, w związku z tym nową metodę oznaczania składu granulometrycznego nazwano metodą dynamometryczną. Oznaczanie składu granulometrycznego za pomocą metody dynamometrycznej wymaga wykorzystania specjalnego urządzenia, które zaprojektowano, stworzono i opisano (Kaszubkiewicz i in., 2017). Urządzenie zostało opatentowane w Urzędzie Patentowym RP (PL234924B1, 2020). Metoda dynamometryczna składa się z dwóch kluczowych elementów: z opracowanego algorytmu przekształcającego odczytane zmiany ciężaru pozornego pływaka na rozkład granulometryczny oraz urządzenia umożliwiającego poprawny zapis wyników pomiaru. Niniejsza rozprawa doktorska opisuje rozwinięcie obydwu elementów.

Algorytm obliczeniowy metody dynamometrycznej oparty jest na powiązaniu wzoru Stokesa określającego prędkość opadania ziaren gleby w zawiesinie (Stokes, 2009) ze wzorem opisującym zmianę gęstości zawiesiny w czasie sedymentacji. Urządzenie zarówno w wersji jednostanowiskowej, jak i z automatycznym zmieniaczem próbek składa się z podstawowych elementów takich jak: piezoelektryczny dynamometr mierzący ciężar do 50 G (z dokładnością do 0,01 G) wraz z podwieszonym do niego, za pomocą żyłki, pływakiem i mechanicznego ramienia, do którego przymocowany jest dynamometr wraz z termoparą mierzącą temperaturę zawiesiny. Całość jest sterowana przez mikrokontroler, który przesyła sygnały między komputerem a urządzeniem (Rys. 1)

Rys. 1 Urządzenie wykorzystywane w metodzie dynamometrycznej

Metoda dynamometryczna z racji swoich możliwości automatycznej i pełnej cyfryzacji wyników oraz elastyczności pod względem parametrów pomiaru (możliwość pomiarów dowolnej frakcji w zakresie 0,1 – 0,002 mm, dowolna gęstość sedymentujących ziaren czy szeroki zakres możliwej do zastosowania naważki) posiada duży potencjał rozwojowy. W przyszłości za pomocą bardziej zaawansowanych algorytmów obliczeniowych można będzie niwelować wpływ czynników zakłócających proces sedymentacji takich jak: obecność dużej ilości materii organicznej

i węglanów wapnia, zasolenie czy nieregularność kształtu ziaren glebowych. Przykładowo możliwe jest zastosowanie modyfikacji wzoru Stokesa uwzględniającej odbiegający od kulistego kształt ziaren frakcji ilastej (Faroughi i Huber, 2016). Badana metoda pozwala w prosty sposób określać rozkład granulometryczny nie tylko gleby, ale również innych materiałów składających się z cząstek o jednorodnej gęstości i średnicach mieszczących się w wymaganym zakresie.

Ze względu na to, że metoda dynamometryczna należy do grupy metod sedymentacyjnych (wykorzystujących zjawisko sedymentacji) szczególny nacisk położono na odniesienie do innych metod sedymentacyjnych tj. metody pipetowej i areometrycznej. Metoda dynamometryczna została szczegółowo przetestowana, a rezultaty zawarto w publikacji Papuga i in. (2018), która stanowi uzupełnienie niniejszej pracy oraz wiedzy dotyczącej metody dynamometrycznej. Badania przedstawione w powyższym artykule potwierdzają wysoką zbieżność otrzymanych wyników z tymi uzyskanymi metodami areometryczną i pipetową. Niniejsza praca stanowi rozwinięcie wiedzy dotyczącej metody dynamometrycznej oraz przedstawia jej rozwój w ostatnich latach.

2. Cel pracy oraz hipotezy badawcze

Celem pracy było uzupełnienie i rozwinięcie wiedzy z zakresu oznaczania składu granulometrycznego gleb, związanej z nowo powstałą metodą dynamometryczną. W związku z tym postawiono 3 hipotezy badawcze:

- Metodę dynamometryczną można zmodyfikować tak, aby pomiar wykonywany był automatycznie w kilkunastu próbkach w pojedynczym cyklu przy jednoczesnym zachowaniu wysokiej powtarzalności i bez pogorszenia dokładności otrzymywanych wyników.
- Wpływ zwiększonego oddziaływania między sedymentującymi cząstkami glebowymi, wynikający ze stosowania w metodzie dynamometrycznej większej naważki niż w innych metodach sedymentacyjnych, można zniwelować za pomocą iteracyjnej procedury obliczeniowej, wykorzystującej jedno z dostępnych równań korygujących prędkość opadania ziaren glebowych ze względu na gęstość zawiesiny.
- Usuwanie materii organicznej podczas przygotowania zawiesiny glebowej w metodzie dynamometrycznej nie wpływa na pomiary składu granulometrycznego w stopniu większym niż w innych metodach sedymentacyjnych.

3. Materiały i metody

Dla weryfikacji przedstawionych hipotez badawczych dotyczących metody dynamometrycznej zastosowano zróżnicowany materiał glebowy. W przypadku dwóch pierwszych hipotez wykorzystano gleby pochodzące z rejonu Dolnego Śląska o zróżnicowanym składzie granulometrycznym. Próbki pobierano z poziomów glebowych znajdujących się poniżej 50 cm, aby uzyskać materiał pozbawiony materii organicznej, która mogłaby wpływać na wyniki analiz. Do badań nad wpływem usuwania materii organicznej na wyniki oznaczania składu granulometrycznego pobrano próbki glebowe z poziomów powierzchniowych (akumulacyjnych) gleb użytkowanych rolniczo. Łącznie we wszystkich badaniach użyto 65 różnych próbek glebowych oraz 54 mieszaniny wybranych gleb.

W ramach prac wchodzących w skład cyklu publikacji wykonano podstawowe analizy gleboznawcze:

- Oznaczanie składu granulometrycznego gleb za pomocą metody dynamometrycznej;
- Oznaczanie zawartości węglanu wapnia przy użyciu aparatu Scheiblera;
- Oznaczanie pH (w KCl i H_2O) metodą potencjometryczną.

Ponadto w zależności od celu pracy wykonano następujące analizy:

- Oznaczanie składu granulometrycznego gleb za pomocą metody areometryczno-sitowej w modyfikacji Prószyńskiego;
- Oznaczanie składu granulometrycznego gleb za pomocą metody pipetowej;
- Oznaczanie zawartości frakcji d >0,063 metodą sitową na mokro;
- Oznaczanie całkowitej zawartości węgla organicznego w glebie metodą chromatografii gazowej;

- Pomiary gęstości sedymentującej zawiesiny na różnych głębokościach.

W oparciu o uzyskane wyniki przeprowadzone zostały:

- Analiza powtarzalności oznaczania składu granulometrycznego za pomocą metody dynamometrycznej;
- Analiza porównawcza wyników otrzymywanych metodą dynamometryczną względem wyników uzyskiwanych za pomocą metody pipetowej;
- Analiza porównawcza zmierzonej zawartości poszczególnych frakcji w mieszaninach gleb oraz zawartości teoretycznej obliczonej w oparciu o skład granulometryczny składowych mieszaniny i ich udziałów w niej;
- Analiza statystyczna przy wykorzystaniu programu *STATISTICA 12* (obliczanie współczynników determinacji, wartości korelacji Pearsona, wzorów regresji, wartości odchyleń standardowych i RMSE (*Root Mean Square Error*), odległości euklidesowe i inne. Do dopasowywania funkcji krzywych rozkładu (*curve fitting*) wykorzystano program *TableCurve 2D v5.01*

W toku badań zostały opracowane dokładne parametry pomiarów oraz indywidualna metodyka przygotowania próbek glebowych, która wzorowana była na innych metodach sedymentacyjnych. Brak potrzeby wprowadzania dużych zmian w przygotowaniu próbek, względem procedur pochodzących z innych metod sedymentacyjnych, pozwolił na wyeliminowanie potencjalnego wpływu tego etapu na analizę porównawczą otrzymanych wyników. Dobór optymalnych parametrów pomiarów umożliwił zminimalizowanie występujących błędów.

W metodzie dynamometrycznej określono optymalną głębokość pomiarów ciężaru pozornego pływaka, zoptymalizowano kształt pływaka, długość i rodzaj materiału żyłki, na której zawieszony jest pływak oraz ilość dyspergentu dodawanego na etapie przygotowania próbek. Wielostanowiskowe urządzenie wymagało dobrania odpowiednich rozmiarów cylindrów na zawiesinę glebową i przetestowania przydatności ich do pomiarów. Opis urządzenia z automatycznym zmieniaczem próbek został przedstawiony w publikacji Kaszubkiewicz i in. (2020). Podstawy teoretyczne procedury obliczeniowej korygujące odstępstwa wynikające ze stosowania zawiesin o podwyższonej gęstości zostały zawarte w pracy Papuga i in. (2021).

Podsumowanie wybranych elementów metodyki zastosowanej w przeprowadzonych analizach metodą dynamometryczną zostało ujęte w poniższej tabeli. Szczegółowa charakterystyka wykorzystanych próbek glebowych, opisy metodyki oraz sposób przygotowania próbek glebowych zostały przedstawione w pracach wchodzących w skład cyklu publikacji niniejszej rozprawy doktorskiej.

Tabela 1. Wykorzystane próbki glebowe i mierzone frakcje w wykonanych analizach

Analiza	Próbki glebowe	Mierzone frakcje *d* [mm]
Implementacja metody dynamometrycznej do urządzenia z wielostanowiskowym i automatycznym zmieniaczem próbek		
Powtarzalność wyników	4 próbki: piasek, glina pylasta o zawartości iłu 6,2%, glina pylasta o zawartości iłu 22,4% oraz ił. Pomiary wykonano w 6 powtórzeniach.	11 frakcji: <0,002; <0,005; <0,008, <0,010; <0,016; <0,020; <0,032; <0,050; < 0,063, <0,080; <0,100
Zgodność otrzymywanych wyników z teoretycznymi obliczeniami rozkładu granulometrycznego mieszanin	58 próbek: piasek, glina pylasta o zawartości iłu 6,2%, glina pylasta o zawartości iłu 22,4%, ił i ich mieszaniny w proporcjach 90:10, 80:20, 70:30, 60:40, 50:50, 40:60, 30:70, 20:80 i 10:90.	
Porównanie z metodą pipetową	12 próbek: glina pylasta o zawartości iłu 6,2%, glina pylasta o zawartości iłu 22,4%, ił oraz ich mieszaniny w proporcjach 70:30, 50:50 i 30:70.	5 frakcji: <0.002, <0.005, <0.01, <0.02, <0.05 <0.1
Wykorzystanie iteracyjnej procedury obliczeniowej w celu zmniejszenia wpływu podwyższonej koncentracji początkowej zawiesiny na wyniki		
Pomiar gęstości sedymentującej zawiesiny na różnych głębokościach	5 próbek glebowych: 3 próbki gliny pylastej i 2 próbki iłu. Dla każdej próbki wykonano 6 analiz różniących się głębokością zanurzenia pływaka (50, 100, 150, 200, 250, 300 mm poniżej powierzchni zawiesiny).	Brak. Wykonywano pomiary gęstości zawiesiny po określonych czasach.
Wielkości błędów losowych i systematycznych występujących przy zastosowaniu różnych koncentracji początkowych zawiesiny	6 próbek: 3 gliny pylaste, 2 gliny piaszczyste, ił. Dla każdej próbki wykonano 6 analiz różniących się zastosowaną naważką (20, 40, 60, 80, 100, 120 g). Pomiary wykonano w 5 powtórzeniach.	11 frakcji: <0,002; <0,005; <0,008, <0,010; <0,016; <0,020; <0,032; <0,050; < 0,063, <0,080; <0,100
Iteracyjna procedura obliczeniowa		
Wpływ usuwania materii organicznej na wyniki		
Porównanie wyników zawartości frakcji *d* <0,063 pomiędzy metodą dynamometryczną a sitową	50 próbek o zróżnicowanych składach granulometrycznych.	1 frakcja: <0,063
Porównanie wyników oznaczania składu granulometrycznego pomiędzy próbkami w których usunięto materię organiczną a próbkami bez usuwania.		3 frakcje: <0.063, <0.05 <0.002

4. Wyniki

4.1. Poprawność wyników otrzymywanych za pomocą urządzenia z automatycznym i wielostanowiskowym zmieniaczem próbek

W celu sprawdzenia metody pomiarowej wykonano badania składu granulometrycznego sztucznie uzyskanych mieszanin glebowych. Do analizy wybrano cztery monomodalne utwory glebowe o zróżnicowanym składzie granulometrycznym. Różniły się one zarówno wartościami d_{50}, jak i stopniem wysortowania. Zmierzono ich skład granulometryczny (11 frakcji, tabela 1), a następnie sporządzono dwuskładnikowe mieszaniny tych utworów w proporcjach podanych w tabeli 1. Dla każdej z uzyskanych 54 mieszanin (6 par składników po 9 proporcji) oznaczono zawartość 11 frakcji. Następnie dokonano porównania pomiędzy zmierzonymi, a obliczonymi w oparciu o składy granulometryczne próbek (z których utworzono mieszaniny) zawartościami wybranych frakcji w poszczególnych mieszaninach gleb. Największe różnice pomiędzy zmierzonym rozkładem granulometrycznym mieszanin, a obliczonymi na podstawie udziału w mieszanie próbek glebowych i znanych ich składów granulometrycznych stwierdzono dla mieszaniny *Sand-Clay*, czyli mieszanin próbek piasku i iłu. Współczynnik determinacji R^2 wynosił 0,9764 (wartość RMSE wynosiła 4,01%). Dla pozostałych mieszanin, w każdym przypadku współczynnik determinacji był większy niż 0,99 (wartość RMSE wynosiła od 1,77% do 2,71%).

Drugim etapem było zbadanie powtarzalności wyników na podstawie analizy składu granulometrycznego 4 próbek, z których uzyskano wyżej opisane mieszaniny. Najgorszą powtarzalność wyników stwierdzono dla próbki oznaczonej jako *Silt loam 2*, czyli gliny piaszczystej o małej zawartości frakcji ilastej (średnie odchylenie standardowe mierzonych frakcji wynosiło 1,48%). Najlepszą powtarzalność uzyskano w próbce oznaczonej jako *Sand*, czyli piasku (średnie odchylenie standardowe poszczególnych frakcji wynosiło 0,80). W trzech próbkach największe odchylenie standardowe występowało dla wyników pomiarów dotyczących frakcji d <0,1 mm, czyli frakcji o największych mierzonych średnicach cząstek. Jedynie w próbce oznaczonej jako *Clay*, czyli zawierającej najwięcej frakcji d <0,002 mm, największe odchylenie standardowe stwierdzono dla frakcji d <0,032 mm.

Trzecim etapem weryfikacji poprawności otrzymywanych wyników było porównanie wyników otrzymywanych metodą dynamometryczną z wynikami uzyskanymi metodą pipetową. Współczynniki korelacji pomiędzy wynikami otrzymanymi metodami dynamometryczną i pipetową wynosiły od 0,9880 (dla mieszaniny *Silt loam 2-Clay*) do 0,9972 (dla mieszaniny *Silt loam 1-Clay*). Wartości RMSE dla powyższych mieszanin wynosiły odpowiednio 4,15% i 2,65%. Pod względem porównania do metody pipetowej dla poszczególnych mierzonych frakcji największe różnice występowały dla frakcji d <0,1 mm, gdzie RMSE wynosiło 6,05%. Najmniejsze różnice względem metody pipetowej

dla wszystkich przetestowanych próbek obserwowano dla pomiarów frakcji d <0,01 mm, gdzie RMSE wynosiło jedynie 1,89%.

4.2. Wpływ procedury iteracyjnej na krzywe rozkładu granulometrycznego

Wprowadzenie do wyników

Omawiane zagadnienie składa się z trzech części. W pierwszej z nich testowano eksperymentalnie hipotezę, że ziarna glebowe znajdujące się w momencie początkowym blisko powierzchni zawiesiny, poruszają się w warstwie zawiesiny o stałej gęstości i w związku z tym przemieszczają się ze stałą prędkością. Udowodnienie tej hipotezy było konieczne, ponieważ stanowiła ona jedno z założeń, na których oparto iteracyjną procedurę obliczeniową pozwalającą na skorygowanie wyników pomiarów sedymentacyjnych ze względu na wzajemne oddziaływanie opadających w zawiesinie ziaren glebowych. Drugim elementem pracy było pokazanie jak kształtują się błędy przypadkowe (losowe) w pomiarach sedymentacyjnych (metodą dynamometryczną) przy różnych wartościach początkowej koncentracji zawiesiny. Tym samym określono potrzebę zwiększenia koncentracji początkowej zawiesiny (zwiększenie naważki gleby), aby ograniczyć wielkość błędów przypadkowych. Najważniejszym elementem pracy było przedstawienie i wykazanie poprawności działania, iteracyjnej procedury obliczeniowej umożliwiającej uwzględnienie zależności pomiędzy prędkością opadania ziaren glebowych, a koncentracją sedymentującej zawiesiny. Do opisu tej zależności wykorzystano w pracy równanie Batchelora (1982). Dla przetestowania hipotezy o stałej prędkości opadania ziaren, które w momencie początkowym znajdowały się przy powierzchni zawiesiny, zmierzono jej gęstość na 6 wybranych głębokościach po 22 różnych czasach. Następnie w oparciu o uzyskane dwuwymiarowe funkcje $\rho=\rho(z,t)$, wyznaczono czasy po których zawiesina ma tę samą gęstość na różnych głębokościach. Czasy wyznaczono dla poszczególnych próbek dla 3 lub 4 różnych gęstości. Sprawdzano czy warstwy zawiesiny o stałej gęstości przemieszczają się ze stałą prędkością. W tym celu do wyników pomiarów przebytej przez warstwę drogi L w funkcji czasu t dopasowywano funkcję liniową (bez wyrazu wolnego) i obliczano współczynniki korelacji pomiędzy wartościami zmierzonymi i obliczonymi.

Wyniki

Współczynniki korelacji mieściły się w przedziale od 0,9738 do 0,9998. Wśród 17 zmierzonych warstw, dla 12 współczynnik korelacji wyników do dopasowanej funkcji liniowej był większy niż 0,99. Wartości RMSE dla liniowej regresji wynosiły od 4,5 mm do 43,4 mm. Tylko w 3 przypadkach na 17 wartość RMSE była większa niż 20 mm. Przykładowo warstwa o gęstości 1,0218 $g \cdot cm^{-3}$ (utwór A5) przemieszczała się w zawiesinie ze średnią prędkością 0,0543 $mm \cdot s^{-1}$. Interpretując tę wartość według równania Stokesa, należałoby przyjąć, że w warstwie tej znajdowały się cząstki gleby o średnicach $d \leq 0{,}0232$ mm (temperatura 25,4^{o}C). Współczynnik determinacji dla regresji liniowej bez wyrazu wolnego (zależność czas-droga) wynosił 0,9677. Współczynnik korelacji pomiędzy

wartościami zmierzonymi i obliczonymi z regresji liniowej wynosił 0.9863 i był istotny na poziomie α= 1.9E-3. Wartość RMSE wynosiła 16.7 mm.

Wielkości błędów występujących przy zastosowaniu różnych koncentracji początkowych zawiesiny (naważek) obliczono jako odchylenia standardowe od średnich wartości uzyskanych z 5 pomiarów. Odchylenia standardowe obliczano dla każdej z 11 mierzonych frakcji, a następnie obliczano średnią wartość odchylenia standardowego dla danej gleby i koncentracji początkowej. Ze względu na wielowątkowość pracy i ograniczoną objętość, wyniki dotyczące tego zagadnienia zostały przedstawione w publikacji tylko w formie wykresów. Średnie odchylenia standardowe od średnich zawartości poszczególnych frakcji w badanych próbkach dla koncentracji 0,0075 i 0,0453 były następujące:

- W próbce B1, przy koncentracji zawiesiny 0,0075 odchylenie wynosiło 9,1%, a przy koncentracji zawiesiny 0,0453 – 1,2%
- W próbce B2, przy koncentracji zawiesiny 0,0075 odchylenie wynosiło 5,0%, a przy koncentracji zawiesiny 0,0453 – 1,0%
- W próbce B3, przy koncentracji zawiesiny 0,0075 odchylenie wynosiło 3,0%, a przy koncentracji zawiesiny 0,0453 – 1,0%
- W próbce B4, przy koncentracji zawiesiny 0,0075 odchylenie wynosiło 2,3%, a przy koncentracji zawiesiny 0,0453 – 0,8%
- W próbce B5, przy koncentracji zawiesiny 0,0075 odchylenie wynosiło 4,2%, a przy koncentracji zawiesiny 0,0453 – 1,1%
- W próbce B6, przy koncentracji zawiesiny 0,0075 odchylenie wynosiło 12,1%, a przy koncentracji zawiesiny 0,0453 – 0,6%

Wśród 11 mierzonych frakcji odchylenia standardowe od średniej zawartości danej frakcji dla wszystkich próbek (przy koncentracji 0,0075, czyli naważce 20 g) mieściły się w przedziale od 4,8% (dla frakcji d <0,032 mm) do 7,72% (dla frakcji d <0,1 mm). W przypadku zastosowania koncentracji 0,0453 przedział wartości odpowiednich odchyleń standardowych był znacznie mniejszy. Średnie odchylenie standardowe wynosiło od 0,8% dla frakcji d <0,08 mm do 1,1% dla frakcji d <0,008 mm.

Zastosowanie proponowanej iteracyjnej procedury obliczeniowej spowodowało obniżenie we wszystkich przypadkach zawartości mierzonych frakcji. Wartości skorygowane były zatem mniejsze od wartości bez korekty. Wraz ze wzrostem zastosowanej naważki, zwiększała się korekta zawartości wszystkich frakcji. Poniżej przedstawiono wyniki dla koncentracji 0,0453, dla której korekta wynikająca ze stosowania procedury była największa.

- W próbce B1 największa korekta wynosiła 4,63 pp i dotyczyła zawartości frakcji d <0,034 mm
- W próbce B2 największa korekta wynosiła 4,23 pp i dotyczyła zawartości frakcji d <0,100 mm
- W próbce B3 największa korekta wynosiła 2,38 pp i dotyczyła zawartości frakcji d <0,044 mm
- W próbce B4 największa korekta wynosiła 2,06 pp i dotyczyła zawartości frakcji d <0,034 mm

- W próbce B5 największa korekta wynosiła 3,30 pp i dotyczyła zawartości frakcji *d* <0,100 mm
- W próbce B6 największa korekta wynosiła 2,01 pp i dotyczyła zawartości frakcji *d* <0,100 mm

Po zastosowaniu procedury iteracyjnej średnia wartość RMSE rozkładów granulometrycznych zmniejszyła się w 5 z 6 analizowanych próbek. Różnice nie były jednak statystycznie istotne.

4.3. Wpływ usuwania materii organicznej na wyniki pomiarów składu granulometrycznego

W ramach badań nad wpływem usuwania materii organicznej (SOM) na wyniki pomiarów składu granulometrycznego, zmierzono zawartości frakcji *d* <0,063 metodą dynamometryczną i sitową w próbkach zawierających materię organiczną (PM) oraz w próbkach jej pozbawionych poprzez utlenianie na mokro 30% roztworem H_2O_2 (PB). W próbkach zawierających materię organiczną zawartość frakcji *d* <0,063 oznaczonych metodą dynamometryczną była skorelowana z wynikami otrzymanymi metodą sitową na poziomie r=0,9954. Wielkość współczynnika korelacji pomiędzy dwoma metodami przy pomiarze zawartości frakcji *d* <0,063, dla próbek PB była na podobnym poziomie i wynosił 0,9938.

Następnie porównano wyniki oznaczania składu granulometrycznego pomiędzy próbkami, w których usunięto materię organiczną a próbkami bez usuwania. W wyniku usuwania materii organicznej średnia zawartość piasku (0,05 mm – 2,0 mm) zmniejszyła się o 2,41 punktu procentowego (pp). Jednocześnie średnia zawartość pyłu (0,002 mm – 0,05 mm) wzrosła o 1,86 pp, a średnia zawartość iłu (<0,002 mm) o 0,56 pp w PB. Przy odniesieniu średnich zmian zawartości poszczególnych frakcji do ich początkowej zawartości w PM stwierdzone względne zmiany były znacząco większe. Zawartość frakcji piasku zmniejszyła się średnio o 6,3%, średnia zawartość frakcji pyłowej wzrosła o 9,6%, a średnia zawartość frakcji ilastej zwiększyła się o 36,5%. Zmiany zawartości piasku zachodzące po usunięciu SOM były pozytywnie skorelowane z początkową zawartością frakcji piasku oraz negatywnie skorelowane z zawartością frakcji iłu i pyłu. Stwierdzono, że im większa początkowa zawartość iłu w próbce, tym większy wzrost zawartości frakcji pyłu w PB (współczynnik korelacji wynosił 0,6029). Odwrotną korelację stwierdzono dla zawartości iłu. Im większa zawartość iłu w próbkach, tym wzrost zawartości w PB w wyniku usuwania SOM był co raz mniejszy (współczynnik korelacji wynosił -0,4717). Zmiany zawartości frakcji piasku i pyłu były również skorelowane z zawartością materii organicznej w PM. Wraz ze wzrostem jej zawartości w próbkach, następował większy spadek zawartości frakcji piasku i większy wzrost zawartości frakcji pyłu w wyniku usuwania.

Średnia odległość euklidesowa pomiędzy różnicami zawartości frakcji piasku, pyłu i iłu w PM i PB wynosiła 6,6% (wartość minimalna 0,6%, maksymalna 17,1%, odchylenie standardowe 3,6%). Odległość euklidesowa pomiędzy wynikami przed i po usunięciu SOM zwiększała się wraz ze wzrostem początkowej zawartości materii organicznej w próbkach glebowych (Rys. 2, Papuga i in. 2022). Wszystkie wspomniane powyżej zależności były statystycznie istotnie przy p <0,05.

5. Dyskusja

W równaniu Stokesa prędkość opadania cząstki kulistej w zawiesinie jest wprost proporcjonalna do kwadratu średnicy opadającej cząstki. Wyprowadzono je w tak zwanym „modelu pojedynczej cząstki", a zatem nie bierze ono pod uwagę oddziaływania z innymi sedymentującymi cząstkami i wznoszącego przeciwprądu wody, który powstaje skutkiem opadania cząstek o określonej objętości i prędkości ruchu (Winterwerp, 2002). W rzeczywistości koncentracja zawiesiny wpływa na prędkość opadania ziaren. Im większa jest koncentracja zawiesiny, tym bardziej prędkość opadania cząstek jest zredukowana w stosunku do wartości obliczonych na podstawie równania Stokesa. Wraz z jej wzrostem następuje zwiększenie różnic spowodowane większym oddziaływaniem opadających ziaren oraz większą prędkością wytwarzanego przez nie przeciwprądu wody. W literaturze można znaleźć wzory korygujące prędkość opadania cząstek ze względu na koncentrację zawiesiny oraz kształty sedymentujących ziaren glebowych (Ahrens, 2000; Cheng, 1997; Richardson i Zaki, 1997). Dla zawiesin o koncentracji objętościowej mniejszej niż 0,05 można stosować wzór Batchelora (Batchelor, 1982). W związku z tym wyniki otrzymywane przy wykorzystaniu metody dynamometrycznej, w której stosuje się stężenie zawiesiny większe niż w innych metodach sedymentacyjnych, mogą być obarczone błędami wynikającymi z różnicy pomiędzy rzeczywistą prędkością opadania ziaren, a tą wynikającą z równania Stokesa stosowanego do interpretacji pomiarów. Odchylenie od równania Stokesa będzie miało wpływ szczególnie w próbkach ilastych, ze względu na koncentrację frakcji pozostających w zawiesinie przez dłuższy czas. Oczywistym jest, że w celu uniknięcia powyższych odchyleń, naważka powinna być mniejsza. Jednakże, stosowanie mniejszej koncentracji zawiesiny w metodzie dynamometrycznej powoduje pomiary mniejszych zmian gęstości, skutkiem czego jest wzrost błędów losowych.

Odchylenie od kulistego kształtu ziaren ma istotny wpływ na ich prędkość opadania. W literaturze można znaleźć wiele równań empirycznych pozwalających obliczyć rzeczywiste prędkości opadania ziaren gleby (Gibbs i in., 1971; Jiménez i Madsen, 2003; le Roux, 1992). Stosowane są różne wskaźniki opisujące kształt ziaren, takie jak wskaźnik Coreya (Dioguardi i Mele, 2015) lub wskaźnik Jankego (Dietrich, 1982), przy czym każde odchylenie kształtu powoduje zmniejszenie prędkości opadania w stosunku do ziaren kulistych o takiej samej objętości jak badane. Rozwiązaniem problemu kulistości wydaje się być zastosowanie pojęcia średnicy zastępczej rozumianej jako średnica kuli opadającej z prędkością równą prędkości opadania ziaren o rzeczywistym kształcie. Jest to jednak rozwiązanie, które ma znaczący udział w pojawiających się rozbieżnościach pomiędzy metodami sedymentacyjnymi i optycznymi (Faé i in., 2019; Polakowski i in, 2014). Należy jednak zaznaczyć, że nie ma idealnej metody oznaczania składu granulometrycznego, a ich ocena zależy od przyjętych kryteriów (Goossens, 2007).

Wyniki przeprowadzonych badań wskazują, że korekta funkcji skumulowanego rozkładu granulometrycznego (CPSD) związana z zastosowaniem procedury opisanej w pracy Papuga i in.

(2021) przebiega w różny sposób w zależności od badanej gleby. Zróżnicowana jest wielkość korekty, oraz zakres średnic cząstek, dla których obserwuje się największą zmianę kształtu krzywych CPSD (rys. 4 i 5, tab. 4, Papuga in. 2021). Ze względu na fakt, że oddziaływania pomiędzy ziarnami gleby zawsze powodują zmniejszenie prędkości opadania, w rzeczywistości cząstki o określonej średnicy opadają na daną głębokość w czasie dłuższym niż wynika to z równania Stokesa (Concha Arcil, 2009; Dey i in., 2019; Di Felice, 1999). Korekta jest tym większa im większa jest początkowa koncentracja zawiesiny. Największa korekta występuje zawsze dla cząstek o wymiarach większych niż 0,02 mm, a w przypadku 2 z 6 badanych próbek dla cząstek o średnicy 0,1 mm. W większości badanych gleb gwałtowne zmiany gęstości zawiesiny zachodzą w ciągu 10-100 s od rozpoczęcia sedymentacji. W związku z tym nawet niewielka zmiana czasu pomiaru w tym zakresie (spowodowana zastosowaniem proponowanej procedury) powoduje znaczącą zmianę odczytu gęstości zawiesiny, a to skutkuje istotną różnicą pomiędzy obliczonymi wartościami CPSD i CPSD po korekcie. Cząstki gleby o najmniejszych średnicach (rozpoczynające swój ruch od powierzchni) opadają w najbardziej rozrzedzonej zawiesinie, a zatem ich ruch jest bliski opisanego równaniem Stokesa. Oznacza to, że szybko opadające cząstki o średnicach bliskich 0,1 mm w największym stopniu przyczyniają się do tworzenia przeciwprądu, który zmniejsza rzeczywistą prędkość opadania wszystkich pozostałych cząstek (Dankers i Winterwerp, 2007; Xu i in., 2018).

Wychodząc z poczynionych założeń można wnioskować, że cząstka o średnicy *d* znajdująca się w momencie początkowym przy powierzchni zawiesiny będzie opadała tylko w otoczeniu cząstek o średnicach zastępczych $\leq d$. Założenie prawdziwe jest tylko dla cząstek, które w momencie początkowym znajdowały się przy powierzchni zawiesiny. Cząstki o większych średnicach opadają bowiem szybciej i nie ma ich w zawiesinie, w której znajduje się rozpatrywana cząstka o średnicy *d*. Jednocześnie wszystkie cząstki o średnicach mniejszych niż *d* poruszają się wolniej od rozpatrywanej i pozostają w zawiesinie. W warstwie zawiesiny o stałej gęstości, która opada od powierzchni, znajdują się cząstki o średnicach większych niż mierzone dla tej warstwy. Cząstki te, opadając z prędkością większą od prędkości cząstki badanej, szybko opuszczają warstwę i od tego momentu analizowana cząstka porusza się w warstwie o stałej gęstości i ze stałą prędkością. Przykładowo obliczono, że dla cząstek o średnicy 0,016 mm gęstość warstwy, w której się poruszają, stabilizuje się po około 5 s, a dla cząstek o średnicy 0,008 mm po około 20 s od rozpoczęcia sedymentacji. Przy głębokości pomiaru 120 mm cząstki te poruszają się zatem przez kolejne 1800 s w warstwie o stałej gęstości.

Istotnym ograniczeniem w stosowaniu zaproponowanej procedury obliczeniowej jest zakres stosowalności równania Batchelora. Równanie Batchelora może być stosowane dla zawiesin o początkowej koncentracji objętościowej <0,05 (Batchelor, 1972; Silva i in., 2015). Zgodnie z wynikami przeprowadzonych badań, różnica między krzywymi CPSD i CPSD po korekcie, dla stężenia zawiesiny ≤0,0151, jest mniejsza niż 1,51%. Stosunek zawartości poszczególnych frakcji CPSD po korekcie/CPSD nie spada poniżej 0,9820. Wyniki uzyskane przy niskich stężeniach

początkowych zawiesiny charakteryzują się natomiast znacznymi błędami losowymi. W celu ograniczenia losowych błędów występujących podczas oznaczania rozkładu wielkości cząstek, uzasadnione jest stosowanie zawiesin o początkowych stężeniach objętościowych w zakresie 0,0302-0,0453. Dla zawiesin o takich stężeniach odchylenia od równania Stokesa są już istotne. Zastosowanie proponowanej procedury obliczeniowej zmniejsza błędy systematyczne związane ze spadkiem prędkości opadania ziaren wynikającym z ich wzajemnego oddziaływania. Wykorzystane w niniejszej pracy równanie Batchelora jest jednym z kilku możliwych do zastosowania. Procedura analogiczna do opisanej może być przeprowadzona z wykorzystaniem równania Richardsona-Zakiego (Richardson i Zaki, 1954) lub Olivera (Oliver, 1961). Należy zaznaczyć, że równanie Batchelora zaproponowano zostało dla zawiesin o małym zróżnicowaniu wielkości cząstek (Di Felice, 1999), a równanie Richardsona Zaki dla zawiesin prawie monodyspersyjnych (Richardson i Zaki, 1997). Zastosowanie ich do rzeczywistej zawiesiny glebowej jest zatem pewnym przybliżeniem. W literaturze można znaleźć również bardziej złożone równania, które uzależniają prędkość opadania od stężenia zawiesiny, liczby Reynoldsa, mediany średnicy cząstek d_{50} lub kombinacji tych parametrów (Cheng, 1997; Garside i Al-Dibouni, 1977; Gibbs i Matthews, 1971; Ha i Liu, 2008; Rushd i in., 2019). Ich zastosowanie w proponowanej procedurze jest możliwe, jednak ze względu na konieczność obliczania skorygowanej prędkości osobno dla każdej średnicy cząstek, bardzo utrudnione.

Na podstawie przeprowadzonych analiz można stwierdzić, że korekta uzyskana w trakcie stosowania proponowanej procedury dla najwyższej zastosowanej początkowej koncentracji zawiesiny z wykorzystaniem wzorów Batchelora i Richardsona-Zakiego jest zbliżona i nie przekracza wartości 0,055. Równanie Olivera, ze względu na największą redukcję prędkości opadania cząstek, daje znacznie wyższe wartości poprawki, które sięgają aż 0,09 dla próbki B1 (Rys. 7. Papuga i in., 2021). Przy niższych koncentracjach początkowych zawiesiny wartości korekty były mniejsze. Celem zaproponowanej procedury iteracyjnej było uwzględnienie wpływu wzajemnych oddziaływań cząstek sedymentujących na ich prędkość opadania. Procedura zmniejsza błąd systematyczny wynikający z założenia zbyt dużej prędkości opadania cząstek, natomiast ma znacznie mniejszy wpływ na błędy przypadkowe. Są one związane ze specyfiką pomiarów i z zastosowaniem różnych funkcji wygładzających krzywą rozkładu granulometrycznego dla różnych początkowych stężeń zawiesiny (Rys. 4 i 5 Papuga i in. 2021). Proponowana procedura obliczeniowa pozwala na zastosowanie różnych równań, dając w rezultacie podobną korektę krzywych CPSD obliczonych na podstawie zmian gęstości zawiesiny.

Materia organiczna w glebie (*soil organic matter*, SOM), mająca istotny wpływ na wyniki oznaczania składu granulometrycznego gleb, występuje w dwóch formach: *particulate organic matter* (POM) i *mineral-associated organic matter* (MAOM). MAOM i POM różnią się gęstością i wielkością cząstek. MAOM związana jest z frakcją pyłową i ilastą, a jej cząstki są mniejsze niż 0,057 mm. POM składa się z cząstek materii organicznej o rozmiarach w zakresie 0,0057-2,0 mm i nie jest związana w mikroagregatach glebowych (Cotrufo i in., 2019; Six i in., 2002; Totsche i in., 2018).

Różnią się one właściwościami, a tym samym mogą różnić się wpływem na wyniki analizy składu granulometrycznego metodami sedymentacyjnym (Benbi i in., 2014; Lavallee i in., 2020). Różne właściwości obu form SOM znacznie komplikują określenie wpływu jej usuwania na wyniki oznaczania wielkości cząstek gleby metodami sedymentacyjnymi. Zmiany zawartości poszczególnych frakcji wynikające z usunięcia SOM mogły być spowodowane dwoma czynnikami.

Pierwszy czynnik dotyczy mineralizacji materii organicznej podczas stosowania perhydrolu. W trakcie pomiarów składu granulometrycznego próbek z materią organiczną, jej cząstki są traktowane jak ziarna mineralne gleby. Materia organiczna charakteryzuje się mniejszą gęstością niż części mineralne, w związku z tym ich cząstki i agregaty mineralno-organiczne opadały z mniejszą prędkością niż wynikałoby to z ich średnic zastępczych. Tym samym podczas analizy granulometrycznej określane były jako drobniejsze frakcje, niż są w rzeczywistości. Wyniki badań tylko częściowo potwierdziły tę obserwację. Średnia suma frakcji d <0,063 mm mierzonych metodą dynamometryczną i frakcji d >0,063 mm mierzonych metodą sitową była wyższa dla próbek z SOM (98,51%) niż dla próbek po usunięciu SOM (96,33%), to w obu przypadkach było to poniżej 100%. Cząstki SOM o średnicy nieco większej niż 0,063 mm będą oznaczone jako <0,063 mm w analizie sedymentacyjnej i jednocześnie jako >0,063 mm w analizie sitowej. W rezultacie suma frakcji d <0,063 mm zmierzonej dynamometrem sedymentacyjnym i frakcji d >0,063 mm zmierzonej analizą sitową powinna być większa niż 100%. Nie znajduje to jednak potwierdzenia w uzyskanych wynikach. Możliwe są dwa wytłumaczenia. Pierwszym z nich jest to, że cząstki SOM mają na ogół mniejszą średnicę niż 0,063 mm, więc podczas analizy pojawiałyby się tylko raz. Jest to zgodne z danymi pochodzącymi z literatury. Największą ilość w glebie stanowi MAOM, w tym materia o średnicy cząstek mniejsze niż 0,02 mm (Barthès i in. 2008; Haddix i in., 2020; Samson i in., 2020). Drugim wyjaśnieniem jest niedoszacowanie frakcji przez metodę dynamometryczną. Jest bardzo prawdopodobne, że oba efekty mogą występować jednocześnie.

Drugim czynnikiem powodującym zmiany odczytów zawartości poszczególnych frakcji w procesie usuwania SOM jest wpływ samego usuwania materii organicznej na cząstki mineralne związane z materią organiczną. Cząstki SOM występują w glebie w postaci związanej z różnymi frakcjami granulometrycznymi, co wpływa na interpretację ich średnic zastępczych w pomiarach sedymentacyjnych. Niektóre cząstki SOM mogą być odpowiedzialne za zdolność cząstek gleby i agregatów do sklejania się (Oades, 1988; Puget i in., 2000; Yang i in., 2009). Prosty proces dyspersji nie wpływa znacząco na ich stabilność. Proces utleniania SOM z użyciem H_2O_2 może je rozbijać, powodując rozpad agregatów na mniejsze fragmenty, co zmienia prędkość sedymentacji związanych z nimi cząstek mineralnych (Schmidt i in., 1999; Steinhardt i in., 1980). Kompleksy organiczno-mineralne zawierające MAOM mają mniejszą średnią gęstość niż mineralne cząstki gleby. Mineralizacja ich frakcji organicznej powoduje wzrost gęstości, a tym samym wzrost prędkości sedymentacji w zawiesinie. Cząstki takie można zatem interpretować w analizie sedymentacyjnej jako większe niż były pierwotnie, i to pomimo utraty pewnej masy. Na wyniki analizy sedymentacyjnej

mogło również wpłynąć ogrzewanie zawiesiny i czas kontaktu z wodnym roztworem dyspergentu, który był dłuższy niż w przypadku próbek, z których nie usunięto SOM. Standardowe przygotowanie próbek mogło nie doprowadzić do rozpadu wszystkich agregatów, które rozpadły się później w procesie usuwania materii organicznej.

Usunięcie SOM spowodowało zatem względny wzrost zawartości frakcji mineralnych i spadek zawartości ziaren o wymiarach odpowiadających średnicom ziaren zastępczych POM i MAOM. Rezultaty tych procesów są złożone i zależą nie tylko od zawartości SOM, ale także od wielkości cząstek SOM, ich powiązania z różnymi frakcjami mineralnymi oraz rozkładu wielkości cząstek frakcji mineralnych. Oczywistym jest, że taki efekt powinien mieć coraz mniejsze znaczenie w miarę zmniejszania się początkowej zawartości SOM. Beuselinck i in. (1998) stwierdzili, że proces usuwania SOC z próbek zawierających <1% SOC (ok. 1,7% SOM) nie miał istotnego wpływu na wyniki badań. Jeszcze wyższą wartość podali Jensen i in. (2017), którzy stwierdzili, że wartość graniczna zawartości węgla organicznego, powyżej której należy usunąć materię organiczną, wynosi 2%. Ponadto, powyżej tej zawartości następuje znaczny wzrost niedoszacowania frakcji pyłu i iłu w próbkach, z których nie usunięto materii organicznej. Do podobnych wniosków doszli Hereter i in (2002). SOM należy usunąć, jeżeli jej zawartość jest większa niż 2%, a próbka ma zawartość frakcji <0,002 mm większą niż 25%. Takie właściwości próbki prowadzą do niedoszacowania frakcji ilastej w próbkach, które nie zostały poddane obróbce wstępnej. Nasze wyniki nie potwierdziły jednak tej obserwacji. Z kolei Zimmermann i Horn (2020) odnotowali w swoich badaniach znaczące różnice w różnych frakcjach, przy czym usunięcie SOM powodowało wzrost zawartości frakcji ilastej i spadek zawartości frakcji pyłu i piasku. Wyniki badań przeprowadzonych w niniejszej pracy są częściowo zbieżne z przedstawionymi w literaturze.

6. Wnioski

1. Zastosowanie wielostanowiskowego automatycznego zmieniacza próbek w metodzie dynamometrycznej umożliwiło analizy wielu próbek jednocześnie bez udziału osób, ujednolicenie procesu mieszania próbek przed pomiarem oraz skrócenie czasu analizy w stosunku do innych metod sedymentacyjnych. Wprowadzone rozwiązanie zachowało możliwość analizy wielu frakcji o dowolnie wybranych zakresach średnic oraz zapis wyników w postaci cyfrowej. Utrzymano dobrą zgodność rezultatów pomiarów z wynikami metody pipetowej,
2. Metoda dynamometryczna wykorzystująca urządzenie z automatycznym i wielostanowiskowym zmieniaczem charakteryzuje się wysoką powtarzalnością otrzymywanych wyników dla próbek o zróżnicowanym składzie granulometrycznym. Automatyzacja metody nie wpłynęła negatywnie na otrzymywane wyniki. Metoda została zweryfikowana poprzez oznaczenie składu granulometrycznego mieszanin gleb (o znanych proporcjach) i znanym składzie granulometrycznym składników mieszanin. Różnice między zmierzonymi i obliczonymi skumulowanymi rozkładami granulometrycznymi nie przekraczały dla poszczególnych mieszanin ok. 2,5% (dla mediany) i 14% (dla błędu maksymalnego).
3. Różnica w porównaniu z metodą pipetową jest największa przy pomiarze frakcji $d < 0{,}1$ mm, kiedy czas od zakończenia mieszania do pomiaru gęstości jest najkrótszy, a wpływ różnych odchyleń losowych największy. Zaobserwowany rozkład wyników wskazuje na brak istotnych błędów systematycznych w metodzie dynamometrycznej oraz na występowanie pewnych błędów przypadkowych, które wymagają usunięcia lub ograniczenia w trakcie dalszego rozwoju metody.
4. Stosowanie zawiesin o małych stężeniach objętościowych w pomiarach rozkładu wielkości cząstek gleby powoduje powstawanie znacznych błędów przypadkowych. Wyniki charakteryzują się znacznym stopniem rozrzutu, a uzyskanie zadowalających rezultatów wymaga przestrzegania ściśle określonych reżimów pomiarowych. Z drugiej strony, wzrost stężenia zawiesiny sprawia, że wzajemne oddziaływania cząstek zaczynają mieć istotny wpływ na ich prędkość opadania, a zastosowanie równania Stokesa do opisu tej prędkości wiąże się ze znacznym błędem systematycznym.
5. Zaproponowana iteracyjna metoda obliczeniowa, wykorzystująca korektę prędkości opadania cząstek w oparciu o równanie Batchelora, pozwala na stosowanie w pomiarach rozkładu wielkości cząstek zawiesin o stężeniu objętościowym do 0,0453. Przy zwiększonym stężeniu zawiesiny błędy przypadkowe ulegały zmniejszeniu. Ograniczenia prezentowanej metody wynikają jedynie z zakresu stosowalności równania użytego w obliczeniowej procedurze iteracyjnej.
6. Usuwanie materii organicznej w próbkach glebowych może powodować znaczne zmiany zawartości poszczególnych frakcji mierzonych za pomocą metody dynamometrycznej. Kierunek i wielkość tych zmian dla poszczególnych próbek jest nieregularny i trudny do przewidzenia. W związku z tym, podczas przygotowania próbek do oznaczania składu granulometrycznego za

pomocą metody dynamometrycznej, nie stwierdzono jednoznacznych przesłanek do usuwania materii organicznej w przypadku, gdy jej zawartość w badanej glebie jest mniejsza niż 2%.

7. Literatura

1. Ahrens, J.P., 2000. A Fall-Velocity Equation. J. Waterway, Port, Coastal, Ocean Eng. 126, 99–102. https://doi.org/10.1061/(ASCE)0733-950X(2000)126:2(99)
2. Andrenelli, M.C., Fiori, V., Pellegrini, S., 2013. Soil particle-size analysis up to 250 μm by X-ray granulometer: Device set-up and regressions for data conversion into pipette-equivalent values. Geoderma 192, 380–393. https://doi.org/10.1016/j.geoderma.2012.06.011
3. Barthès, B.G., Brunet, D., Hien, E., Enjalric, F., Conche, S., Freschet, G.T., d'Annunzio, R., Toucet-Louri, J., 2008. Determining the distributions of soil carbon and nitrogen in particle size fractions using near-infrared reflectance spectrum of bulk soil samples. Soil Biology and Biochemistry 40, 1533–1537. https://doi.org/10.1016/j.soilbio.2007.12.023
4. Batchelor, G.K., 1972. Sedimentation in a dilute dispersion of spheres. J. Fluid Mech. 52, 245–268. https://doi.org/10.1017/S0022112072001399
5. Batchelor, G.K., 1982. Sedimentation in a dilute polydisperse system of interacting spheres. Part 1. General theory. J. Fluid Mech. 119, 379–408. https://doi.org/10.1017/S0022112082001402
6. Benbi, D.K., Boparai, A.K., Brar, K., 2014. Decomposition of particulate organic matter is more sensitive to temperature than the mineral associated organic matter. Soil Biology and Biochemistry 70, 183–192. https://doi.org/10.1016/j.soilbio.2013.12.032
7. Beuselinck, L., Govers, G., Poesen, J., Degraer, G., Froyen, L., 1998. Grain-size analysis by laser diffractometry: comparison with the sieve-pipette method. CATENA 32, 193–208. https://doi.org/10.1016/S0341-8162(98)00051-4
8. Bieganowski, A., Ryżak, M., 2011. Soil Texture: Measurement Methods, in: Gliński, J., Horabik, J., Lipiec, J. (Eds.), Encyclopedia of Agrophysics, Encyclopedia of Earth Sciences Series. Springer Netherlands, Dordrecht, pp. 791–794. https://doi.org/10.1007/978-90-481-3585-1_157
9. Bieganowski, A., Ryżak, M., Sochan, A., Barna, G., Hernádi, H., Beczek, M., Polakowski, C., Makó, A., 2018. Laser Diffractometry in the Measurements of Soil and Sediment Particle Size Distribution, in: Advances in Agronomy. Elsevier, pp. 215–279. https://doi.org/10.1016/bs.agron.2018.04.003
10. Bittelli, M., Andrenelli, M.C., Simonetti, G., Pellegrini, S., Artioli, G., Piccoli, I., Morari, F., 2019. Shall we abandon sedimentation methods for particle size analysis in soils? Soil and Tillage Research 185, 36–46. https://doi.org/10.1016/j.still.2018.08.018
11. Bouyoucos, G.J., 1927. THE HYDROMETER AS A NEW METHOD FOR THE MECHANICAL ANALYSIS OF SOILS: Soil Science 23, 343–354. https://doi.org/10.1097/00010694-192705000-00002
12. Cheng, N.-S., 1997. Simplified Settling Velocity Formula for Sediment Particle. Journal of Hydraulic Engineering 123, 149–152. https://doi.org/10.1061/(ASCE)0733-9429(1997)123:2(149)
13. Concha Arcil, F., 2009. Settling Velocities of Particulate Systems. KONA 27, 18–37. https://doi.org/10.14356/kona.2009006
14. Cotrufo, M.F., Ranalli, M.G., Haddix, M.L., Six, J., Lugato, E., 2019. Soil carbon storage informed by particulate and mineral-associated organic matter. Nat. Geosci. 12, 989–994. https://doi.org/10.1038/s41561-019-0484-6
15. Dankers, P.J.T., Winterwerp, J.C., 2007. Hindered settling of mud flocs: Theory and validation. Continental Shelf Research 27, 1893–1907. https://doi.org/10.1016/j.csr.2007.03.005
16. Dey, S., Zeeshan Ali, S., Padhi, E., 2019. Terminal fall velocity: the legacy of Stokes from the perspective of fluvial hydraulics. Proc. R. Soc. A. 475, 20190277. https://doi.org/10.1098/rspa.2019.0277

17. Di Felice, R., 1999. The sedimentation velocity of dilute suspensions of nearly monosized spheres. International Journal of Multiphase Flow 25, 559–574. https://doi.org/10.1016/S0301-9322(98)00084-6
18. Di Stefano, C., Ferro, V., Mirabile, S., 2010. Comparison between grain-size analyses using laser diffraction and sedimentation methods. Biosystems Engineering 106, 205–215. https://doi.org/10.1016/j.biosystemseng.2010.03.013
19. Dietrich, W.E., 1982. Settling velocity of natural particles. Water Resour. Res. 18, 1615–1626. https://doi.org/10.1029/WR018i006p01615
20. Dioguardi, F., Mele, D., 2015. A new shape dependent drag correlation formula for non-spherical rough particles. Experiments and results. Powder Technology 277, 222–230. https://doi.org/10.1016/j.powtec.2015.02.062
21. Durner, W., Iden, S.C., 2021. The improved integral suspension pressure method (ISP+) for precise particle size analysis of soil and sedimentary materials. Soil and Tillage Research 213, 105086. https://doi.org/10.1016/j.still.2021.105086
22. Durner, W., Iden, S.C., von Unold, G., 2017. The integral suspension pressure method (ISP) for precise particle-size analysis by gravitational sedimentation: ISP METHOD FOR PARTICLE-SIZE ANALYSIS. Water Resour. Res. 53, 33–48. https://doi.org/10.1002/2016WR019830
23. Faé, G.S., Montes, F., Bazilevskaya, E., Añó, R.M., Kemanian, A.R., 2019. Making Soil Particle Size Analysis by Laser Diffraction Compatible with Standard Soil Texture Determination Methods. Soil Sci. Soc. Am. j. 83, 1244–1252. https://doi.org/10.2136/sssaj2018.10.0385
24. Fan, X., Xue, Q., Liu, S., Tang, J., Qiao, J., Huang, Y., Sun, J., Liu, N., 2021. The influence of soil particle size distribution and clay minerals on ammonium nitrogen in weathered crust elution-deposited rare earth tailing. Ecotoxicology and Environmental Safety 208, 111663. https://doi.org/10.1016/j.ecoenv.2020.111663
25. Faroughi, S.A., Huber, C., 2016. A theoretical hydrodynamic modification on the soil texture analyses obtained from the hydrometer test. Géotechnique 66, 378–385. https://doi.org/10.1680/jgeot.14.P.267
26. Garside, J., Al-Dibouni, M.R., 1977. Velocity-Voidage Relationships for Fluidization and Sedimentation in Solid-Liquid Systems. Ind. Eng. Chem. Proc. Des. Dev. 16, 206–214. https://doi.org/10.1021/i260062a008
27. Ghalib, A.M., Hryciw, R.D., 1999. Soil Particle Size Distribution by Mosaic Imaging and Watershed Analysis. Journal of Computing in Civil Engineering 13, 80–87. https://doi.org/10.1061/(ASCE)0887-3801(1999)13:2(80)
28. Ghasemy, A., Rahimi, E., Malekzadeh, A., 2019. Introduction of a new method for determining the particle-size distribution of fine-grained soils. Measurement 132, 79–86. https://doi.org/10.1016/j.measurement.2018.09.041
29. Gibbs, R.J., Matthews, M.D., 1971. The Relationship Between Sphere Size And Settling Velocity. SEPM JSR Vol. 41. https://doi.org/10.1306/74D721D0-2B21-11D7-8648000102C1865D
30. Goossens, D., 2007. Techniques to measure grain-size distributions of loamy sediments: a comparative study of ten instruments for wet analysis. Sedimentology 0, 070921101149001-??? https://doi.org/10.1111/j.1365-3091.2007.00893.x
31. Ha, Z., Liu, S., 2008. Settling Velocities of Polydisperse Concentrated Suspensions. Can. J. Chem. Eng. 80, 783–790. https://doi.org/10.1002/cjce.5450800501
32. Haddix, M.L., Gregorich, E.G., Helgason, B.L., Janzen, H., Ellert, B.H., Francesca Cotrufo, M., 2020. Climate, carbon content, and soil texture control the independent formation and persistence of particulate and mineral-associated organic matter in soil. Geoderma 363, 114160. https://doi.org/10.1016/j.geoderma.2019.114160
33. Hereter, A., Josa, R., Candela, X., 2002. Changes in particle-size distribution influenced by organic matter and mechanical or ultrasonic dispersion techniques. Communications in Soil Science and Plant Analysis 33, 1351–1362. https://doi.org/10.1081/CSS-120003892
34. Igaz, D., Aydin, E., Šinkovičová, M., Šimanský, V., Tall, A., Horák, J., 2020. Laser Diffraction as An Innovative Alternative to Standard Pipette Method for Determination of Soil Texture Classes in Central Europe. Water 12, 1232. https://doi.org/10.3390/w12051232
35. ISO 11277., 2009. Soil quality—Determination of particle size distributionin mineral soil material—Method by sieving and sedimentation, Reference Number ISO 11277:2009(E). Geneva, Switzerland.

36. Jennings, D.S., Gardner, W., 1922. A NEW METHOD OF MECHANICAL ANALYSIS OF SOILS: Soil Science 14, 485. https://doi.org/10.1097/00010694-192212000-00011
37. Jensen, J.L., Schjønning, P., Watts, C.W., Christensen, B.T., Munkholm, L.J., 2017. Soil texture analysis revisited: Removal of organic matter matters more than ever. PLoS ONE 12, e0178039. https://doi.org/10.1371/journal.pone.0178039
38. Jiménez, J.A., Madsen, O.S., 2003. A Simple Formula to Estimate Settling Velocity of Natural Sediments. J. Waterway, Port, Coastal, Ocean Eng. 129, 70–78. https://doi.org/10.1061/(ASCE)0733-950X(2003)129:2(70)
39. Kaszubkiewicz J., 2020. Patent PL. Urządzenie do pomiaru składu granulometrycznego materiału drobnoziarnistego. PL234924B1. Warszawa, Urząd Patentowy RP.
40. Kaszubkiewicz, J., Papuga, K., Kawałko, D., Woźniczka, P., 2020. Particle size analysis by an automated dynamometer method integrated with an x-y sample changer. Measurement 157, 107680. https://doi.org/10.1016/j.measurement.2020.107680
41. Kaszubkiewicz, J., Wilczewski, W., Novák, T.J., Woźniczka, P., Faliński, K., Belowski, J., Kawałko, D., 2017. Determination of soil grain size composition by measuring apparent weight of float submerged in suspension. International Agrophysics 31, 61–72. https://doi.org/10.1515/intag-2016-0027
42. Keller, J.M., Gee, G.W., 2006. Comparison of American Society of Testing Materials and Soil Science Society of America Hydrometer Methods for Particle-Size Analysis. Soil Sci. Soc. Am. j. 70, 1094–1100. https://doi.org/10.2136/sssaj2005.0303N
43. Kovács B., Czinkota I., Tolner L., Czinkota G., 2004. The determination of particle size distribution (PSD) of clayey and silty formations using the hydrostatic method. Acta Mineralogica-Petrographica 45, 29-34
44. Koza, M., Schmidt, G., Bondarovich, A., Akshalov, K., Conrad, C., Pöhlitz, J., 2021. Consequences of chemical pretreatments in particle size analysis for modelling wind erosion. Geoderma 396, 115073. https://doi.org/10.1016/j.geoderma.2021.115073
45. Lavallee, J.M., Soong, J.L., Cotrufo, M.F., 2020. Conceptualizing soil organic matter into particulate and mineral-associated forms to address global change in the 21st century. Glob Change Biol 26, 261–273. https://doi.org/10.1111/gcb.14859
46. le Roux, J.P., 1992. Settling velocity of spheres: a new approach. Sedimentary Geology 81, 11–16. https://doi.org/10.1016/0037-0738(92)90053-T
47. Lucke, B., Bäumler, R., Schmidt, M. (Eds.), 2015. Soils and sediments as archives of landscape change: geoarchaeology and landscape change in the subtropics and tropics, Erlanger geographische Arbeiten. Sonderband. Selbstverlag der Fränkischen Geographischen Gesellschaft in Kommission bei Palm & Enke, Erlangen.
48. Murad, M.O.F., Jones, E.J., Minasny, B., 2020. Automated soil particle-size analysis using time of flight distance ranging sensor. Soil Sci. Soc. Am. j. 84, 690–699. https://doi.org/10.1002/saj2.20053
49. Naime, J.M., Vaz, C.M.P., Macedo, A., 2001. Automated soil particle size analyzer based on gamma-ray attenuation. Computers and Electronics in Agriculture 31, 295–304. https://doi.org/10.1016/S0168-1699(00)00188-5
50. Novák, V., Hlaváčiková, H., 2019. Basic Physical Characteristics of Soils, in: Novák, V., Hlaváčiková, H. (Eds.), Applied Soil Hydrology. Springer International Publishing, Cham, pp. 15–28.
51. Oades, J.M., 1988. The retention of organic matter in soils. Biogeochemistry 5, 35–70. https://doi.org/10.1007/BF02180317
52. Obata, E., Ohira, Y., Ohta, M., 2009. New measurement of particle size distribution by a buoyancy weighing-bar method. Powder Technology 196, 163–168. https://doi.org/10.1016/j.powtec.2009.07.015
53. Oliver, D.R., 1961. The sedimentation of suspensions of closely-sized spherical particles. Chemical Engineering Science 15, 230–242. https://doi.org/10.1016/0009-2509(61)85026-4
54. Orhan, U., Kılınç, E., 2020. Estimating soil texture with laser-guided Bouyoucos. Automatika 61, 1–10. https://doi.org/10.1080/00051144.2019.1654283

55. Paluszek J. 2011. Kryteria oceny jakości fizycznej gleb uprawnych Polski. Rozprawy i Monografie, Wyd. Instytut Agrofizyki PAN, Lublin 2, 139 s.
56. Papuga, K., Kaszubkiewicz, J., Kawałko, D., 2021. Do we have to use suspensions with low concentrations in determination of particle size distribution by sedimentation methods? Powder Technology 389, 507–521. https://doi.org/10.1016/j.powtec.2021.05.060
57. Papuga, K., Kaszubkiewicz, J., Kawałko, D., Kreimeyer, M., 2022. Effect of Organic Matter Removal by Hydrogen Peroxide on the Determination of Soil Particle Size Distribution Using the Dynamometer Method. Agriculture 12, 226. https://doi.org/10.3390/agriculture12020226
58. Papuga, K., Kaszubkiewicz, J., Wilczewski, W., Staś, M., Belowski, J., Kawałko, D., 2018. Soil grain size analysis by the dynamometer method – a comparison to the pipette and hydrometer method. Soil Science Annual 69, 17–27. https://doi.org/10.2478/ssa-2018-0003
59. Polakowski, C., Ryżak, M., Sochan, A., Beczek, M., Mazur, R., Bieganowski, A., 2021. Particle Size Distribution of Various Soil Materials Measured by Laser Diffraction—The Problem of Reproducibility. Minerals 11, 465. https://doi.org/10.3390/min11050465
60. Polakowski, C., Sochan, A., Bieganowski, A., Ryżak, M., Földényi, R., Toth, J., 2014. Influence of the Sand Particle Shape on Particle Size Distribution Measured by Laser Diffraction Method. International Agrophysics 28, 195–200. https://doi.org/10.2478/intag-20014-0008
61. Puget, P., Chenu, C., Balesdent, J., 2000. Dynamics of soil organic matter associated with particle-size fractions of water-stable aggregates: Dynamics of soil organic matter in water-stable aggregates. European Journal of Soil Science 51, 595–605. https://doi.org/10.1111/j.1365-2389.2000.00353.x
62. Richardson, J.F., Zaki, W.N., 1997. Sedimentation and fluidisation: Part I. Chemical Engineering Research and Design 75, S82–S100. https://doi.org/10.1016/S0263-8762(97)80006-8
63. Richardson, J.F., Zaki, W.N., 1954. The sedimentation of a suspension of uniform spheres under conditions of viscous flow. Chemical Engineering Science 3, 65–73. https://doi.org/10.1016/0009-2509(54)85015-9
64. Robinson, G.W., 1922. A new method for the mechanical analysis of soils and other dispersions. J. Agric. Sci. 12, 306–321. https://doi.org/10.1017/S0021859600005360
65. Rushd, S., Hassan, I., Sultan, R.A., Kelessidis, V.C., Rahman, A., Hasan, H.S., Hasan, A., 2019. Terminal settling velocity of a single sphere in drilling fluid. Particulate Science and Technology 37, 943–952. https://doi.org/10.1080/02726351.2018.1472162
66. Ryzak, M., Bieganowski, A., 2010. Determination of particle size distrubution of soil using laser diffraction – comparison with areometric method. Int. Agrophys. 24, 177–181.
67. Samson, M.-E., Chantigny, M.H., Vanasse, A., Menasseri-Aubry, S., Royer, I., Angers, D.A., 2020. Management practices differently affect particulate and mineral-associated organic matter and their precursors in arable soils. Soil Biology and Biochemistry 148, 107867. https://doi.org/10.1016/j.soilbio.2020.107867
68. Schmidt, M.W.I., Rumpel, C., Kögel-Knabner, I., 1999. Particle size fractionation of soil containing coal and combusted particles: Particle size fractionation of soil containing coal and combusted particles. European Journal of Soil Science 50, 515–522. https://doi.org/10.1046/j.1365-2389.1999.00254.x
69. Shangguan, W., Dai, Y., Liu, B., Ye, A., Yuan, H., 2012. A soil particle-size distribution dataset for regional land and climate modelling in China. Geoderma 171–172, 85–91. https://doi.org/10.1016/j.geoderma.2011.01.013
70. Silva, R., Garcia, F.A.P., Faia, P.M.G.M., Rasteiro, M.G., 2015. Settling Suspensions Flow Modelling: A Review. KONA 32, 41–56. https://doi.org/10.14356/kona.2015009
71. Six, J., Conant, R.T., Paul, E.A., Paustian, K., 2002. Stabilization mechanisms of soil organic matter: Implications for C-saturation of soils. Plant and Soil 241, 155–176. https://doi.org/10.1023/A:1016125726789
72. Steinhardt, G.C., Franzmeier D.P., Valentine S.C., 1980. Effects of hydrogen peroxide pretreatment on particle-size analysis (soil samples). Proc. Indiana Acad. Sci. 90: 428-434.

73. Stokes, G.G., 2009. Mathematical and physical papers, Volume 3.
74. Tong, C.-X., Burton, G.J., Zhang, S., Sheng, D., 2018. A simple particle-size distribution model for granular materials. Can. Geotech. J. 55, 246–257. https://doi.org/10.1139/cgj-2017-0098
75. Totsche, K.U., Amelung, W., Gerzabek, M.H., Guggenberger, G., Klumpp, E., Knief, C., Lehndorff, E., Mikutta, R., Peth, S., Prechtel, A., Ray, N., Kögel-Knabner, I., 2018. Microaggregates in soils. J. Plant Nutr. Soil Sci. 181, 104–136. https://doi.org/10.1002/jpln.201600451
76. Winterwerp, J.C., 2002. On the flocculation and settling velocity of estuarine mud. Continental Shelf Research 22, 1339–1360. https://doi.org/10.1016/S0278-4343(02)00010-9
77. Xu, S., Sun, R., Cai, Y., Sun, H., 2018. Study of sedimentation of non-cohesive particles via CFD–DEM simulations. Granular Matter 20, 4. https://doi.org/10.1007/s10035-017-0769-7
78. Yang, X.M., Drury, C.F., Reynolds, W.D., MacTavish, D.C., 2009. Use of sonication to determine the size distributions of soil particles and organic matter. Can. J. Soil. Sci. 89, 413–419. https://doi.org/10.4141/cjss08063
79. Yang, Y., Wang, L., Wendroth, O., Liu, B., Cheng, C., Huang, T., Shi, Y., 2019. Is the Laser Diffraction Method Reliable for Soil Particle Size Distribution Analysis? Soil Sci. Soc. Am. j. 83, 276–287. https://doi.org/10.2136/sssaj2018.07.0252
80. Zimmermann, I., Horn, R., 2020. Impact of sample pretreatment on the results of texture analysis in different soils. Geoderma 371, 114379. https://doi.org/10.1016/j.geoderma.2020.114379

Załączniki

1. Kaszubkiewicz J., Papuga K., Kawałko D., Woźniczka P., 2020. Particle size analysis by an automated dynamometer method integrated with an x-y sample changer. Measurement, 157, 107680. https://doi.org/10.1016/j.measurement.2020.107680
2. Papuga K., Kaszubkiewicz J., Kawałko D., 2021. Do we have to use suspensions with low concentrations in determination of particle size distribution by sedimentation methods? Powder Technology, 389, 507-521. https://doi.org/10.1016/j.powtec.2021.05.060
3. Papuga K., Kaszubkiewicz J., Kawałko D., Kreimeyer M., 2022. Effect of Organic Matter Removal by Hydrogen Peroxide on the Determination of Soil Particle Size Distribution Using the Dynamometer Method. Agriculture, 12, 226. https://doi.org/10.3390/agriculture12020226

Aktywność naukowa

Staże naukowe i warsztaty:

- Staż naukowy od 16 marca do 14 kwietnia 2019 r. na Uniwersytecie w Debreczynie (Węgry) w ramach międzynarodowej wymiany stypendialnej doktorantów i kadry akademickiej. Program Prom (NAWA)
- Udział w warsztatach glebowych w ramach The Freely Accessible Central European Soil (FACES), 1-7 lipca 2018

Publikacje:

- Papuga, K., Kaszubkiewicz, J., Wilczewski, W., Staś, M., Belowski, J., Kawałko, D., 2018. Soil grain size analysis by the dynamometer method – a comparison to the pipette and hydrometer method. Soil Science Annual 69, 17–27. https://doi.org/10.2478/ssa-2018-0003

Udział w konferencjach

- K. Papuga, A. Kałuża, J. Kaszubkiewicz, Przebieg procesu naturalnego odsalania gleb o zróżnicowanym składzie granulometrycznym, III Toruńskie Sympozjum Doktorantów Nauk Przyrodniczych, 1-2 kwietnia 2017, poster
- K. Papuga, J. Kaszubkiewicz, Bioconcentration factors and determination of daily intake of heavy metals by man, for selected agricultural produce from the area of ząbkowicki county, VIII Międzynarodowa Konferencja Naukowa Toxic Substances In The Environment, Kraków, 14-15 września 2017, poster
- K. Papuga, J. Kaszubkiewicz, Sedimentation method for determining the content of soil fractions with diameters from 0.05 to 1.0 mm, Annual Congress on Soil Sciences Theme: "Awareness on Innovations in Soil Science and Soil Management Challenges, Madryt, 4-5 grudnia 2017, poster
- J. Kaszubkiewicz, K. Papuga, P. Woźniczka, Comparison of the dynamometric method with the pipette and hydrometer method used in the grain size analysis, 3rd International Symposium Of Soil Physics, Kraków, 14-15 lutego 2018, prezentacja
- K. Papuga, J. Kaszubkiewicz, The float apparent weight measurement for particle-size analysis by sedimentation, 7th International Conference for Young Researchers, Kraków, 16-17 kwietnia 2018, prezentacja
- K. Papuga, J. Kaszubkiewicz, Oznaczanie składu granulometrycznego gleb i osadów rzecznych za pomocą pomiarów zmian ciężaru pozornego pływaka zanurzonego w zawiesinie, Przyrodnicze, Techniczne I Gospodarcze Aspekty Rozwoju Odrzańskiej Drogi Wodnej, Wrocław, 14 czerwca 2018, poster

- K. Papuga, J. Kaszubkiewicz, Settling velocity of soil particles in water depending on the composition and concentration of suspension, 3rd International Conference Of Young Scientists, Poronin, 16-19 września 2018, poster
- J. Kaszubkiewicz, P. Woźniczka, K. Papuga, D. Kawałko, Device for measuring of the soil granulometric composition with an integrated mixer with sample changer, 4th International Symposium Of Soil Physics, Lublin 13-14 lutego, 2019, poster
- K. Papuga, J. Kaszubkiewicz, D. Kawałko. Wpływ koncentracji zawiesiny i głębokości pomiaru w oznaczaniu składu granulometrycznego gleb za pomocą metody dynamometrycznej, 30. Kongres Polskiego Towarzystwa Gleboznawczego, Lublin, 2-7 września 2019r, prezentacja

Pozostała aktywność:

Wolontariat:

- Warsztaty edukacyjne Wydziału Przyrodniczo-Technologicznego, Wrocław, 13 kwietnia 2018

Organizacja:

- Konferencja naukowa „Przyrodnicze, Techniczne I Gospodarcze Aspekty Rozwoju Odrzańskiej Drogi Wodnej", Wrocław, 14 czerwca 2018
- Konferencja naukowa „Polskie gleboznawstwo na forum międzynarodowym" połączona z Jubileuszem 70-lecia Prof. dr. hab. J. Webera, Wrocław, 21-23 października 2018

Measurement 157 (2020) 107680

Contents lists available at ScienceDirect

Measurement

journal homepage: www.elsevier.com/locate/measurement

Particle size analysis by an automated dynamometer method integrated with an x-y sample changer

Jarosław Kaszubkiewicz, Krzysztof Papuga *, Dorota Kawałko, Przemysław Woźniczka

Institute of Soil Science and Environment Protection, Wrocław University of Environmental and Life Sciences, Grunwaldzka 53, 50-357 Wrocław, Poland

ARTICLE INFO

Article history:
Received 9 October 2019
Received in revised form 23 December 2019
Accepted 26 February 2020
Available online 28 February 2020

Keywords:
Particle size distribution
Dynamometer method
Pipette method
Particle settling velocity

ABSTRACT

Methods for determining the particle size distribution (PSD) of soils have been developed for many years and we now have a wide range at our disposal. Despite this, the question of their usefulness and the quality of the results obtained by using particular methods is still open. Among them, historically, the oldest sedimentation methods are still very much employed. The paper presents, developed and consistently modernized by the authors, a method of determining the PSD based on changes in the apparent weight of the float submerged in sedimenting suspension. The apparent weight measurement is performed using a sensitive dynamometer with the piezoelectric effect. Then, it is recalculated into cumulative PSD (CPSD) on the basis of Stoke's law. The method allows the measurement of PSD in a range of grain diameters from 2 μm to 120–130 μm. The integration of the vertically displacing dynamometer and float with the mixer made it possible to automate. Moving the measuring head in the horizontal plane permitted automatic examination of several samples in one measuring cycle. The device works independently after starting. Of note, the method allows for the determination of many different fractions selected by the user. The results of the tests are saved in the form of a report in pdf or xls format. Verification of the method was carried out by comparing the measured and calculated CPSD values of soils, created by mixing in specified proportions of two components with known particle size distribution. The results obtained by this method show a high repeatability and accuracy. Good agreement with the reference method (pipette) is expressed by the RMSE value of 3.36%.

1. Introduction

Sedimentary, or more precisely, sieve-sedimentary methods for determining the particle size distribution (PSD) of soils have been used for roughly 90 years [10,32,12]. Their modern versions are characterized by high repeatability of results and simplicity of the measurement process [53,21,48]. In recent decades, other methods based on optical properties of suspensions [43,26,41], X-ray absorption [40], impedance measurements, gamma absorption [54], terahertz radiation transmission [20] or computer image analysis [13,49,18] have been dynamically developed. Despite this extension of the set of research tools, sedimentation methods are still being developed and improved. They are based on the measurement of suspension density at a specified depth and after a specified period of time from the start of the sedimentation process. With the pipette method, considered as exemplary, the suspension density is determined by the evaporation of the collected suspension [21]. With other sedimentation methods, it can be determined indirectly by measuring the hydraulic pressure exerted by a column of suspension at a certain depth [56,19] or by measuring the hydraulic pressure difference between the suspension and control fluid [33]. There are also proposals for methods using more than one physical phenomenon to determine PSD [23]. Of course, in the range of diameters larger than 0.1 mm, owing to the short falling time of the grains, sedimentation methods have to be supplemented by sieve analysis. Many authors point to other disadvantages of sedimentation methods, such as small range and limited number of size classes, long analysis time [7], lack of reliable data for smaller grain sizes (<2 μm) owing to the influence of Brownian movements on sedimentation times [35,25] or lack of standardization of the suspension mixing process. The usefulness of individual optical and sedimentation methods is evaluated differently [36,9,47] however most authors agree that none of them can be considered ideal [26,7,16].

Recently, a new method has been proposed Kaszubkiewicz et al. [31] for determining the density of a suspension, and hence soil PSD. The method is based on measuring the apparent weight of a float immersed in a suspension at a given depth. The apparent weight measurement is carried out a sensitive dynamometer

* Corresponding author.
E-mail address: krzysztof.papuga@upwr.edu.pl (K. Papuga).

https://doi.org/10.1016/j.measurement.2020.107680
0263-2241/

utilizing the piezoelectric effect. The change of the float's anchor point position at this measurement is at a fraction of a millimeter. Such measurements of the density of the suspension with a float can therefore be performed at a selected depth with a frequency of up to 10 s^{-1}. In the latter part of the work, we will describe this method as a dynamometer method. The repeatability of the results obtained in the above method and compliance with the pipette method has been positively verified and the results of this verification are presented by Papuga et al. [42].

In order to automate the method, increase its efficiency, reduce human errors and standardize the measurement conditions, the authors of this work found it necessary to integrate the measuring device with the sample changer and automatic mixing system. The use of the new measurement method requires checking: comparability of results, magnitude of accidental and systematic errors and repeatability of test results. The first tests of the method demonstrated its satisfactory compliance with the results obtained with the pipetting method and the correctness of results for artificially prepared soil mixtures. The presented work includes a description of an automated device for measuring soil grain composition and analysis of the results obtained, including repeatability and compliance with the pipette method that was adopted as a reference for sedimentation methods [28].

2. Materials and methods

2.1. Theoretical basis of the device's operation

To describe the theoretical basis of the proposed measurement method, it is necessary to recognize physical forces affecting the float immersed in a water suspension of soil particles with different equivalent diameters. The float has a higher density than the soil suspension and it hangs on a thin line connected to a high-resolution dynamometer. The net force $G(z,t)$ acting on the float immersed to depth, z, in soil suspension after time, t, from the start of sedimentation is equal to:

$$G(z,t) = \left(M_f - V_f \rho(z,t)\right)g \tag{1}$$

where M_f is the mass of the float, V_f is the volume of the float, $\rho\,(z,t)$ is the density of suspension on the depth, z, after time, t, and g is the acceleration of gravity. Eq. (1) is based on changes in the density of the suspension at the height of the float.

It is assumed in Eq. (1) that the density of particles of varying sizes is constant or slightly different, and it is possible to approximate this with the single value of ρ_{so}.

The mass of soil solid phase, $\partial M_{so}(z,t)$, in the suspension layer with a thickness of ∂z at depth, z, at time, t, can be calculated from the equation:

$$\partial M_{so}(z,t) = s\partial z \frac{M}{V_z} F(z,t) \tag{2}$$

where M and V_z are the total mass and total volume of the suspension and $F(z,\,t)$ is the fraction of particles that did not fall below depth, z, after time, t and s is the cross-sectional area of the vessel in which sedimentation takes place.

Therefore, the density of the suspension at depth, z, after time, t, can be described as:

$$\rho(z,t) = \rho_w + \frac{M}{V_z} F(z,t)\left(1 - \frac{\rho_w}{\rho_s}\right) \tag{3}$$

where ρ_w is the density of water.

After modification of Equation (3) to calculate function $F(z,\,t)$ we obtain:

$$F(z,t) = \frac{V_z}{M} \frac{\rho_s(\rho(z,t) - \rho_w)}{(\rho_s - \rho_w)} \tag{4}$$

After the rearrangement of Eq. (1) to calculate $\rho\,(z,\,t)$ and substituting it into Equation (4), one can yield:

$$F(z,t) = \frac{V_z}{M} \frac{\rho_s}{(\rho_s - \rho_w)} \left(\frac{M_f g - G(z,t)}{V_f g} - \rho_w\right) \tag{5}$$

Equation (5) defines the relationship between the apparent weight of the float, submerged to depth z below the suspension surface at time t from the beginning of sedimentation (mixing) and the cumulative fraction content $F(z,t)$ of particles that fall to depth z, by time t. In fact, the density of water depends on the temperature and can be calculated from the appropriate regression equation [19].

On the other hand, the settling velocity of a spherical particle of diameter d and density ρ_S in a fluid with density ρ_w and dynamic viscosity η can be calculated from the equilibrium condition of the forces acting on it [39,52,37]:

$$v = \frac{d^2 g}{18\eta}(\rho_s - \rho_w) \tag{6}$$

Equation (6) can be applied to spherical particles of homogeneous density [15] within the range of the laminar flow (Reynolds number < 0.25), and to the diameter of the container (cylindrical) wherein the sedimentation that occurs is much greater than the diameter of falling particles. In real conditions, hydrodynamic and molecular interactions take place between the molecules [5], and Equation (6) supplies accurate results exclusively for diluted suspensions [45,4,2]. In addition, for particles with a higher Reynolds number, the dependence of the settling velocity on their shape is revealed [17,27,57].

The distance that particles overcome in time t during sedimentation with settling velocity v is:

$$z = vt = \frac{d^2 g}{18\eta}(\rho_s - \rho_w)t = \alpha d^2 t \tag{7}$$

where $\alpha = \alpha(\tau) = \frac{g}{18\eta}(\rho_s - \rho_w)$

In fact, $\alpha(\tau)$ is a function of temperature because both ρ_w and η depend on it. The dependence of η on temperature can be found, for example, in Durner et al. [19]

Equation (7) defines the depth to which, after time t, a particle with the equivalent diameter d, located close to the surface of suspension at the initial time t, *of* sedimentation has fallen. The use of a dynamometer to measure the force acting on the float submerged in the soil suspension, $G(z,\,t)$ (the apparent weight of the float), at desired depth z with times $t_1, t_2, \ldots t_n$, calculated with the transformed formula (7):

$$t_i = \sqrt{\frac{z}{\alpha d_i^2}} \tag{8}$$

Therefore, it is possible, on the basis of Eq. (5), to determine values of function $F(z,\,t)$ for times t_i and therefore for the selected values of d_i.

2.2. Construction of a measuring device

The measuring device is a development of the apparatus shown in Kaszubkiewicz et. al. [31]. The mechanical base of the structure (guide rails, drive belts, rollers) is made with a widely used, easily accessible "open builds" system. A trolley moving along the X-axis is attached to the movable beam of the system that moves in the Y-axis. A trolley moving along the X-axis is attached to the movable beam of the system that moves along the Y-axis. The trolley is equipped with a measuring head that permits vertical (Z-axis)

movement of the float, thermometer and agitator. Vertical movements of individual head systems are carried out independently by stepper motors operated from the controller by power regulators. The rotational speed of the motors is regulated by the frequency of impulses sent by the power controllers. The step of the motors is 1.8° and corresponds to 2 pulses from the power controller. The drive from the stepper motors is transmitted to the actuators by rubber toothed belts. The rotary movement of the mixer is carried out by a current-controlled DC motor and a reduction gear. The heads (measuring and mixing) are set on the "open builds" system rail, and their movement in the x-y plane facilitates automatic movement from cylinder to cylinder, and is realized in a similar way as vertical movement - stepper motors with transmission of drive through toothed belts and control from the controller through power controllers (Fig. 1).

The controller is placed in the housing of the device and communicates with the computer via the "Bluetooth" adapter. The entire measuring system is additionally equipped with a barcode scanner which enables the identification of cylinders. A key element of the analysis is the measurement of the sedimenting suspension density after a specified time and at a particular depth. In the developed solution, it is performed by measuring the apparent weight of a float suspended on a sensitive dynamometer. The float may be made of glass or acrylic glass (Fig. 2). It is important that the average density of the float is greater than that of the suspension and the total weight must not exceed the measuring range of the dynamometer. The cross-sectional area of the float should be much smaller than the cross-sectional area of the cylinder with suspension. The exact size of the float may change depending on the nature of the analysis; the number of fractions to be measured, expected performance and precision of the measurement. The float is hanged to the dynamometer by a very thin wire or a low-stretch fishing line.

The apparent weight of the float is measured using a dynamometer with resolution 0.01 gf (gram of force) (approximately 0.0001 N) and with a maximum capacity of 50 gf. The required measuring range depends on the float design and is approximately 0,01 gf to 50 gf (9.81E-5–4.91E-1 N). The dynamometer measures the apparent weight of the float after the time of the individually measured fractions, determined by Eq. (8). A cylindrical float ending with two cones with an apex angle of 60° was used. The volume of the float was 38.82 cm^3 and the density of the material from which it was made (acrylic glass) was 1.18 $g \bullet cm^{-3}$. The measuring cylinders had a volume of 1000 cm^3 and an internal diameter of 78 mm. The dynamometer

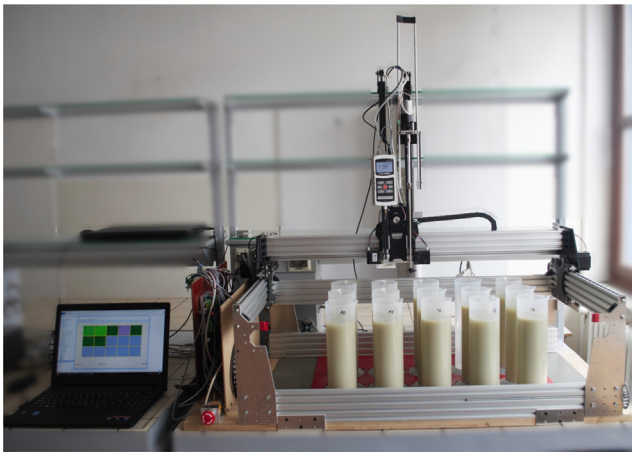

Fig. 1. The device used in the dynamometer method with the integrated x-y sample changer.

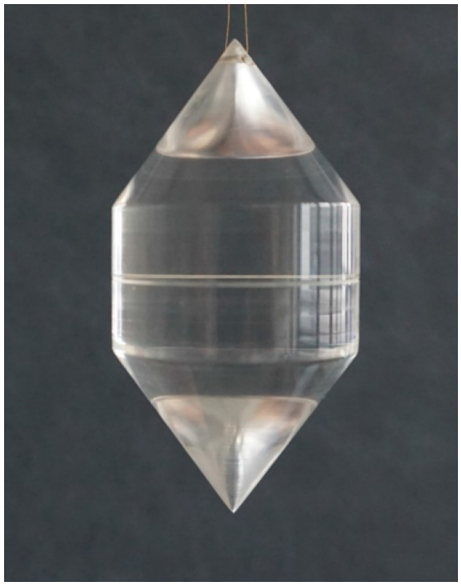

Fig. 2. Acrylic glass float.

with the attached float is mounted on a movable arm of the tripod and positioned vertically with an accuracy of 0.3 mm (one step of the motor). The use of a digital piezoelectric dynamometer and precision vertical-positioning system enables accurate depth control at which the apparent weight of the float is measured. A sensor to measure the temperature of the soil suspension is mounted on the movable arm of the tripod. The time of measurement of a given fraction is determined by the measured temperature values (Eq. (7)).

The entire mechanical system is mounted on a stable, solid base equipped with legs made of a material suppressing vibrations from the ground and a system that permits levelling. The currently implemented system allows for simultaneous analysis in 14 cylinders. A cylinder with water is placed on the 15th stand to calibrate the float and rinse it while transferring it between cylinders with suspension during the analysis. Cylinders are placed in 3 rows and 5 columns.

The software of the device consists of two parts. The first is the main software installed in the computer, which controls the whole process. It is written in the Java language, which ensures interoperability and portability (architecture-neutral) with all operating systems of computers. Its functions are to run tests, define test diagrams, define cylinders using a keyboard or read data from a barcode reader, send commands to the controller to run elementary steps in the measurement procedure and record test results.

The controller's software was made in the C+ language with a version dedicated to "Arduino" series controllers. It takes commands from the main program and controls executive devices: moving the heads using stepper motors to a specific place, making initial settings and starting reading from the dynamometer, detecting the thermometer and temperature measurements (including temperature control inside the device), starting the mixer and determining the direction as well as speed of rotation.

The horizontal movement of the tripod arm is through the use of the speed acceleration mechanism (soft start). There is a gradual change from a minimum to a specified value. The same mechanism is used to stop the arm. A similar approach was applied to vertical movements of the head. The measurement time for the individual fractions is calculated on the basis of their equivalent diameter and the measured temperature of the suspension using the formulae

previously provided (8). It is important that the room temperature where the apparatus is located is constant during measurements. In order to limit the influence of random errors in the float weight reading, the device control software calculates the result of a single measurement at the moment, t, as the average of 11 consecutive measurements made at intervals of 150 ms, starting from the moment, *t-750* ms to *t + 750* ms. Such a procedure, according to the authors, permitted reading the float weight with an accuracy of 0.001 gf.

The software includes a module that allows one to select and edit measurement schemes. Through the measurement scheme, we mean here the number and diameters of the measured fractions and the immersion depth of the float. This software module also performs functions related to the selection of the sequence of measurements in individual cylinders and verifying if there is no overlap in the analysis of different fractions in various cylinders at the same time. As a result of this control, the maximum number of samples that can be analysed simultaneously with the number and dimensions of the fraction is given in advance.

The operator can select a suspension mixing mode that determines parameters, such as mixing time, speed of the mixing element, immersion depth, speed and acceleration in the vertical movement of the agitator. At the end of the mixing process, the system briefly changes direction of rotation in order to extinguish the gyration of the suspension in the cylinder.

The software using Eq. (5) converts the float weight *G(t)* measured at the moment, t, corresponding to the given depth, h, equivalent diameter, d, into the cumulated fraction, *F(d)*, with diameters smaller than d. Based on the *F(d)* function, the content of individual fractions is calculated.

After the measurements are completed, a report is created and saved containing all necessary information concerning the identification of the tested sample, analysis parameters and the results obtained. The report is produced separately for each of the analysed samples. The control computer database also stores information surrounding the course of measurements, including results of partial measurements, exact measurement times, temperature values and messages about possible system errors.

2.3. Material and methodology of research

In order to test the proposed measurement method, the particle size distribution of the artificially obtained soil mixtures was evaluated. In the samples, the PSD was determined using the Köhn pipette method [32,22] and the described dynamometer method. In the case of the pipette method, the methodology described in the paper by Ryżak et al. [46] was applied. Four monomodal soils with different particle size distribution were selected as components of the mixtures. They differed in both d_{50} values and degree of sorting. None of them contained organic matter. The presence of calcium carbonate was also not found. The specific gravity of the test soils was 2.65 g cm^{-3} across all cases. In terms of classification to granulometric groups, they were: sand, silt loam with higher clay content (silt loam 1), silt loam with a lower clay content (silt loam 2) and clay. Data regarding the mentioned soils, among others the content of the main fractions and the functions fitted to the CPSD curve (cumulative particle size distribution curve) in the range of 0.002–0.1 mm are summarized in Table 1. The equation fitted to CPSD curve was selected using iterative nonlinear regression by verifying it through a correlation coefficient (CC) and standard error of estimation (SEE).

Prior to the analysis, selected soil samples were air dried and sieved through a 2-mm mesh screen. The mentioned soils were mixed in pairs (six variants) in percentage proportions: 90:10, 80:20, 70:30, 60:40, 50:50, 40:60, 30:70, 20:80 and 10:90. Therefore, 6x9 = 54 variants of mixtures and four "pure soils" were analysed. Measurements of the PSD of "pure soils" were made in six replications, and, as a result, the arithmetic mean of measurements was taken for each fraction. Preparation for the analysis of the PSD was made in the same way as the hydrometric method.

By means of the apparatus described earlier for each of the tested mixtures and for "pure" samples, the cumulative content of the fraction with equivalent diameters <0.002, <0.005, <0.008, <0.010, <0.016, <0.020, <0.032, <0.050, < 0.063, <0.080 and <0.100 mm was measured. In a single cycle, six samples were assessed using a 12-cm float depth below the suspension level in the measuring cylinder. The mixtures were evaluated without replications. The measurement results for each mixture were compared with the values calculated on the basis of the measurement for "pure" soils and their percentage content in the mixture. The statistical evaluation of the results obtained was conducted using the values calculated as reference values.

To assess compliance with the pipette method the fractions, <0.002, <0.005, <0.01, <0.02, <0.05 and <0.1 mm, were determined directly via the pipette method. The determinations were made for mixtures of three pure samples: silt loam 1, silt loam 2 and clay, and for their mixtures in the selected proportions: 70:30, 50:50 and 30:70, respectively. In total, 12 samples (three "pure" samples and nine mixtures) were evaluated, each for the content of the six previously specified fractions. The "pure" sample of sand was omitted based on the difficulty of determining the content of the 0.1–0.15 mm fraction in the pipetting method.

3. Results

3.1. Reproducibility of test results

The reproducibility of the obtained results was examined for the four tested "pure" soils by performing the analysis in six replications. The CPSDs were analysed, and therefore the share of all

Table 1
Cumulative PSD functions – *F(d)*, fitted to the measuring points of the soils used to made the mixtures and PSD functions – *f(d)* calculated as a derivative of CPSD.

Soil	F(d) - curve fitting equation	Parameters values	CC	SEE	f(d) = F'(d)
1	*2*	*3*	*4*	*5*	*6*
Sand	$F(d)=\frac{a+cd^2}{1+bd^2}$	a = -0.00436 b = 1506.49 c = 1585.40	0.9925	3.41	$x=\frac{2(c-ab)d}{(bd^2+1)^2}$
Silt loam 1	$F(d)=\frac{a+cd^2}{1+bd^2}$	a = 0.99783 b = 744.125 c = 799185	0.9996	0.97	$x=\frac{2(c-ab)d}{(bd^2+1)^2}$
Silt loam 2	$F(d)=\frac{a+cd}{1+bd}$	a = -0.00883 b = 18.6539 c = 24.3517	0.9978	1.49	$x=\frac{c-ab}{(bd+1)^2}$
Clay	$F(d)=\frac{a+cln(d)}{1+bln(d)}$	a = 1.01105 b = 0.11723 c = 0.12969	0.9988	0.26	$x=\frac{c-ab}{d(bln(d)+1)^2}$

grains with substitute diameters below that tested was investigated. It was decided to use the CPSD – *F(d)* owing to the dependence of the function PSD *f(d) = F'(d)* on the selection of the fractions being evaluated. It was found that for individual soils, mean values of standard deviation from six repetitions calculated for individual readings of accumulated fraction content differ slightly and remain within 0.80 for sand to 1.48 for silty clay.

The maximum standard deviation values remain below 2.73 (silt loam 2, fraction d < 0.1 mm). It was determined that the largest results scattering occurred precisely when measuring the fraction, d < 0.1 mm, when the time from the end of mixing to measurement is roughly 12 s (depth of measurement 12 cm) and there are still turbulent movements of the suspension. Thus, as can be seen, the method allows obtaining results with high repeatability regardless of the nature of the analysed soils. Table 1 lists the equations of functions fitted to the results of CPSD measurements in the four examined soils, along with the parameters defining the quality of the fit in the form of correlation coefficients (CC) and standard estimation errors (SEE). Table 1 also lists PSD function equations calculated as a derivative of matched CPSD functions.

Matching functions with three parameters, selected from the libraries of several curve-fitting programs, were used. The matched CPSD functions were not, therefore, among the most frequent and described in the subject literature [11,55].

Graphs of CPSD curves together with standard errors and PSD curves (calculated as derivatives of CPSD functions) are presented

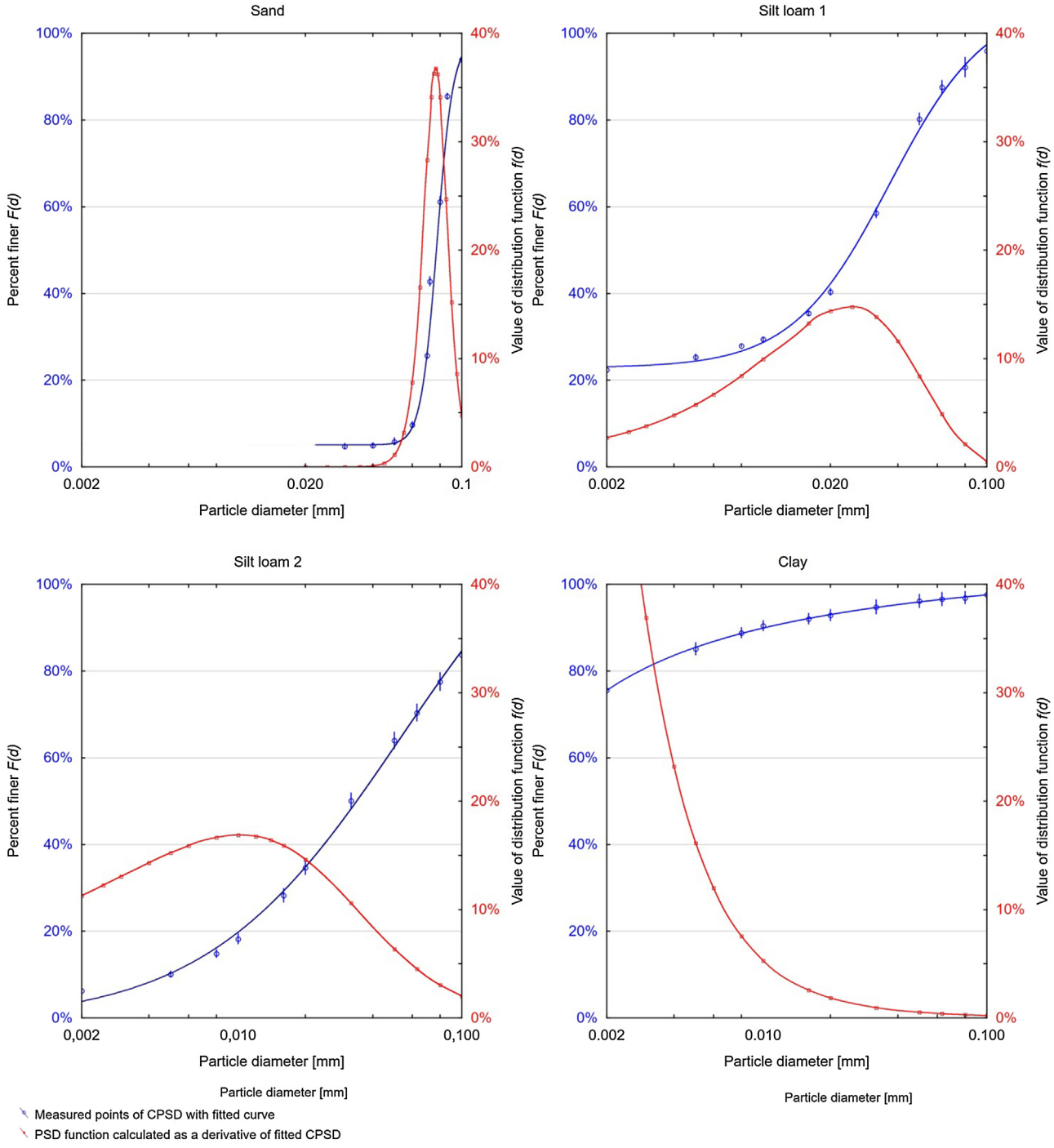

Fig. 3. Cumulative and differential particle size distribution functions for analysed individual soils.

in Fig. 3 and some data about measured PSD for "pure" soils and repeatability of measurement results are collected in Table 2.

3.2. Compatibility of measurement results with calculations

The quality assessment of the obtained PSD results encounters serious problems related to the presence of errors in all methods used. None of them is perfect [26], and their assessment depends essentially on the criteria employed. Of course, it is possible and often practiced to compare the results of research obtained by different methods [6,51], however, it does not ultimately determine which of them and to what extent it is responsible for the observed differences [26]. To limit this problem when assessing the proposed method, a comparison of the measured course of CPSD curves, $F_m(d)$, was made for mixtures with curves calculated based on the share of both mixed components and the known CPSD of "pure" soils. The authors are aware that the PSD measurements of "pure" soil, despite their performance in six replicates are also affected by errors.

Using four components, six possible types of mixtures were obtained, and each type of mixture was prepared in nine different, previously mentioned proportions. The results of the comparisons are summarized in Table 3 and illustrated in Figs. 4–6.

Table 2 and Fig. 4(a-f) outlines the collective results for the individual mixtures taking into account all analysed proportions and all fractions together. For the statistical evaluation of the obtained results, it was assumed that the real value is the one calculated from the proportion of the components' share and the relevant F (d) values for both components.

With this assumption, RMSE values and individual quartile values were calculated for errors understood as $\Delta = ((F_m(d) - Fcal(d))^2)^{0.5}$. The value of the II quartile is obviously equal to the median, and the fourth quartile is the maximum error value. As can be seen from Table 3, the root mean square error (RMSE) of the values Δ for all 6 mixtures did not exceed 4.01% with the five mixtures falling below 2.7%. The highest RMSE value was found for a mixture of clay and sand, i.e., particles with the largest grain size difference. The most likely effect here is the formation based on the falling of particles with large diameters, ascending current, which reduces the rate of settlement of fine particles in relation to the walls of the cylinder. Consequently, for the sand and clay mixture, the highest maximum error – 13.9% - and the highest median error – 2.5% – were found.

For the remaining mixtures, the maximum error did not exceed 9.6% and the median of error was 2.1% (Table 3). It is known that under real conditions during sedimentation, each particle experiences a different fluid resistance because of: variable arrangements of neighbouring particles [14], local pressure gradients appearing, eddies caused by rapidly falling larger grains, water countercurrents and wall effects [53,38].

Owing to the phenomena described, it cannot be expected that for a mixture of components, with the use of sedimentation analysis, we will yield results exactly corresponding to the theoretical forecasts, however this is a way to verify the consistency of the method without referring to results obtained using other methods.

It was also found that the trend lines for the relationship between $F_{cal}(d)$ and $F_m(d)$ for individual mixtures have slopes close to unity (from 0.9658 to 1.0009) and vertical intercepts within the range of –0.37 to 2.06 (Table 3).

Values of RMSE, calculated separately for individually measured fractions, were also assessed. Although it was found that the mean value of RMSE was the highest for the fraction d < 0.1 mm where it was 3.21, the differences with respect to the other fractions were not statistically significant at a significance level of $\alpha = 0.05$.

Analysing the individual curves $F(d)$, it can be concluded that the largest differences between the calculated and measured values occur when the curve $F(d)$ exhibits rapid changes, and

Table 2
Statistical analysis of measurement repeatability for selected fractions of "pure" soils.

Soil definition	N	Mean measured fraction content [%]				d_{50} diameter [mm]	Mean STD	Max STD d (mm)
		<0.002 [mm]	<0.02 [mm]	<0.05 [mm]	<0.1[mm]			
1	*2*	*3*	*4*	*5*	*6*	*7*	*8*	*9*
Sand	6	n.o.	4.6	5.8	93.9	0.077	0.80	1.18 0.100
Silt loam 1	6	22.4	40.4	80.2	95.9	0.026	1.10	2.73 0.100
Silt loam 2	6	6.2	34.6	64.0	83.7	0.033	1.48	2.48 0.100
Clay	6	75.6	92.8	96.1	97.6	<0.002	1.23	1.44 0.032

N – number of measurement replication.
STD – the standard deviation was calculated from 6 replications, separately for each of the 11 measured fractions.

Table 3
Statistical characteristics of differences between $F_m(d)$ and $F_{cal}(d)$ for individual mixture variants.

Mixture components	n	R^2	RMSE	error Δ				Linear trend equation
				I	II (median)	III	IV (max)	
1	*2*	*3*	*4*	*5*	*6*	*7*	*8*	*9*
Sand-Silt loam 1	99	0.9942	2.47	0.47	1.19	2.15	9.56	y = 0.9658x + 0.36
Sand-Silt loam 2	99	0.9960	2.36	0.75	1.36	1.96	6.62	y = 0.9835x + 1.28
Sand-Clay	99	0.9764	4.01	1.06	2.52	3.36	13.92	y = 0.9693x + 1.97
Silt loam 1-Silt loam 2	99	0.9986	2.18	1.00	1.61	2.58	5.95	y = 0.9850x-1.17
Silt loam 1-Clay	99	0.9931	1.77	0.82	1.41	2.11	4.21	y = 0.9842x + 1.70
Silt loam 2-Clay	99	0.9957	2.71	1.12	2.10	3.23	6.82	y = 1.0009x + 2.06

RMSE – root mean square error.
n - number of mixtures (9), multiplied by the number of fractions analysed for each mixture (11).

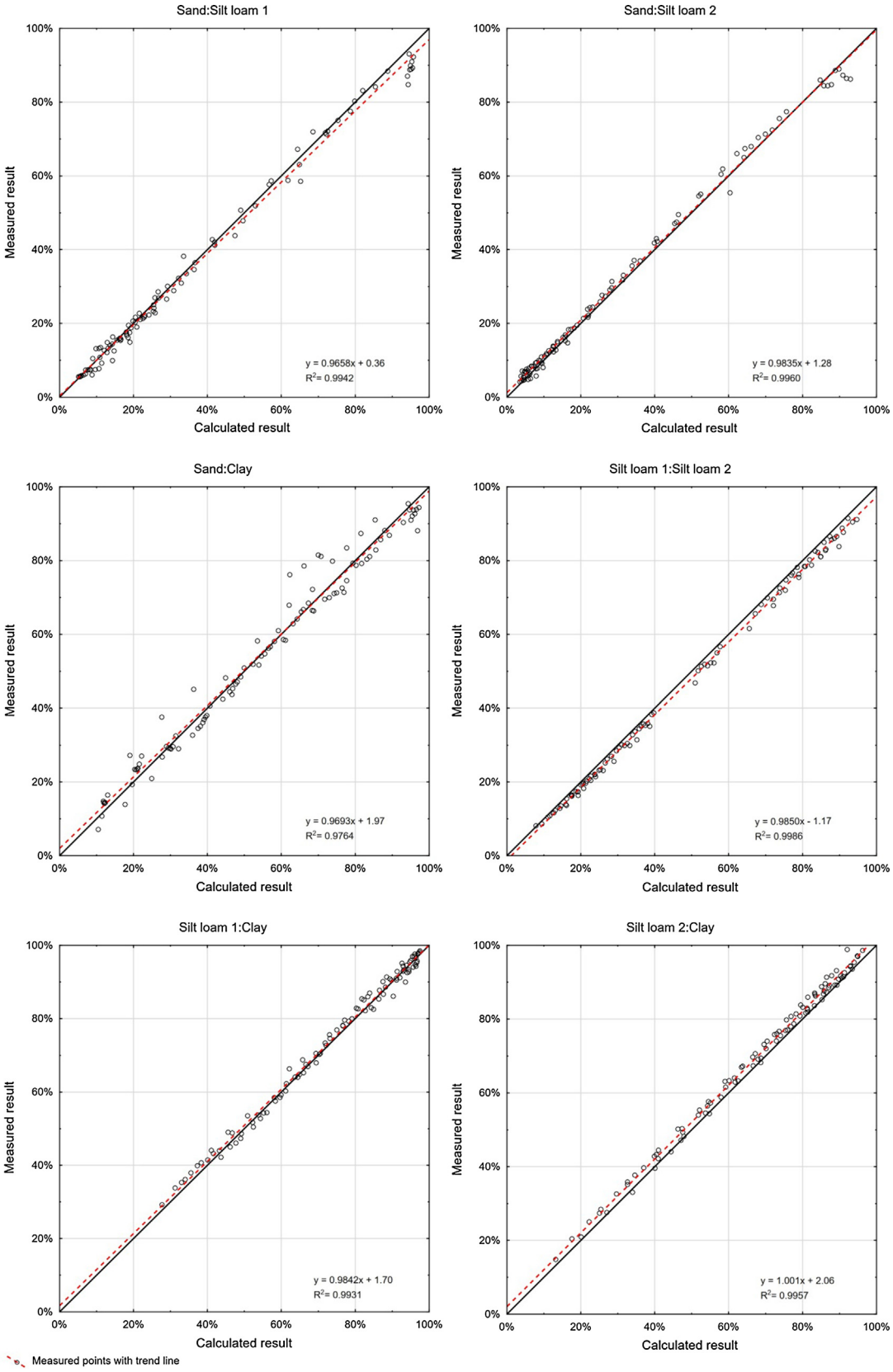

Fig. 4. Comparison of calculated and measured cumulative particle fraction content for particulate mixtures. All fractions.

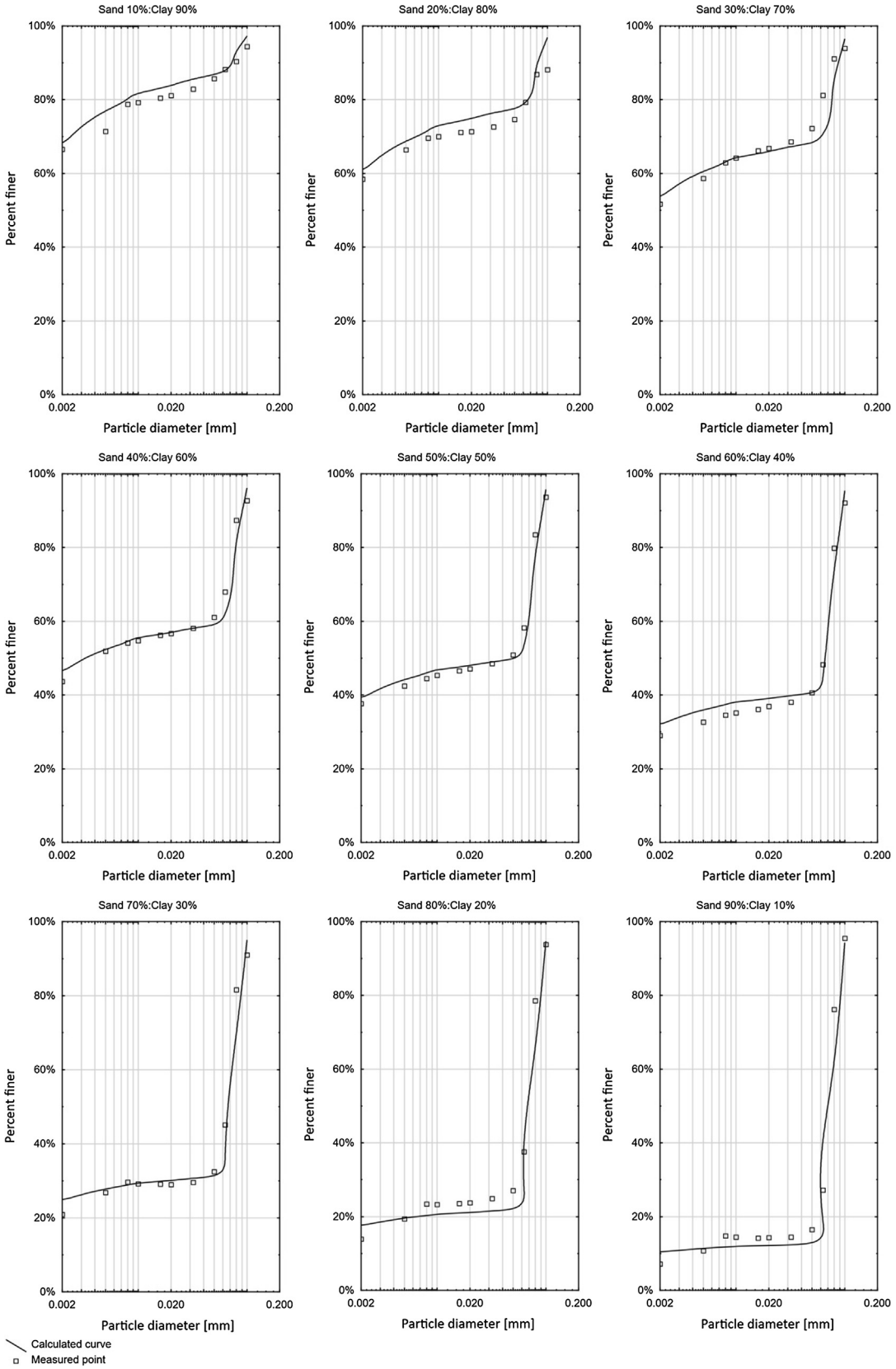

Fig. 5. Mixtures of sand and clay. CPSD calculated at the basis of pure components contents.

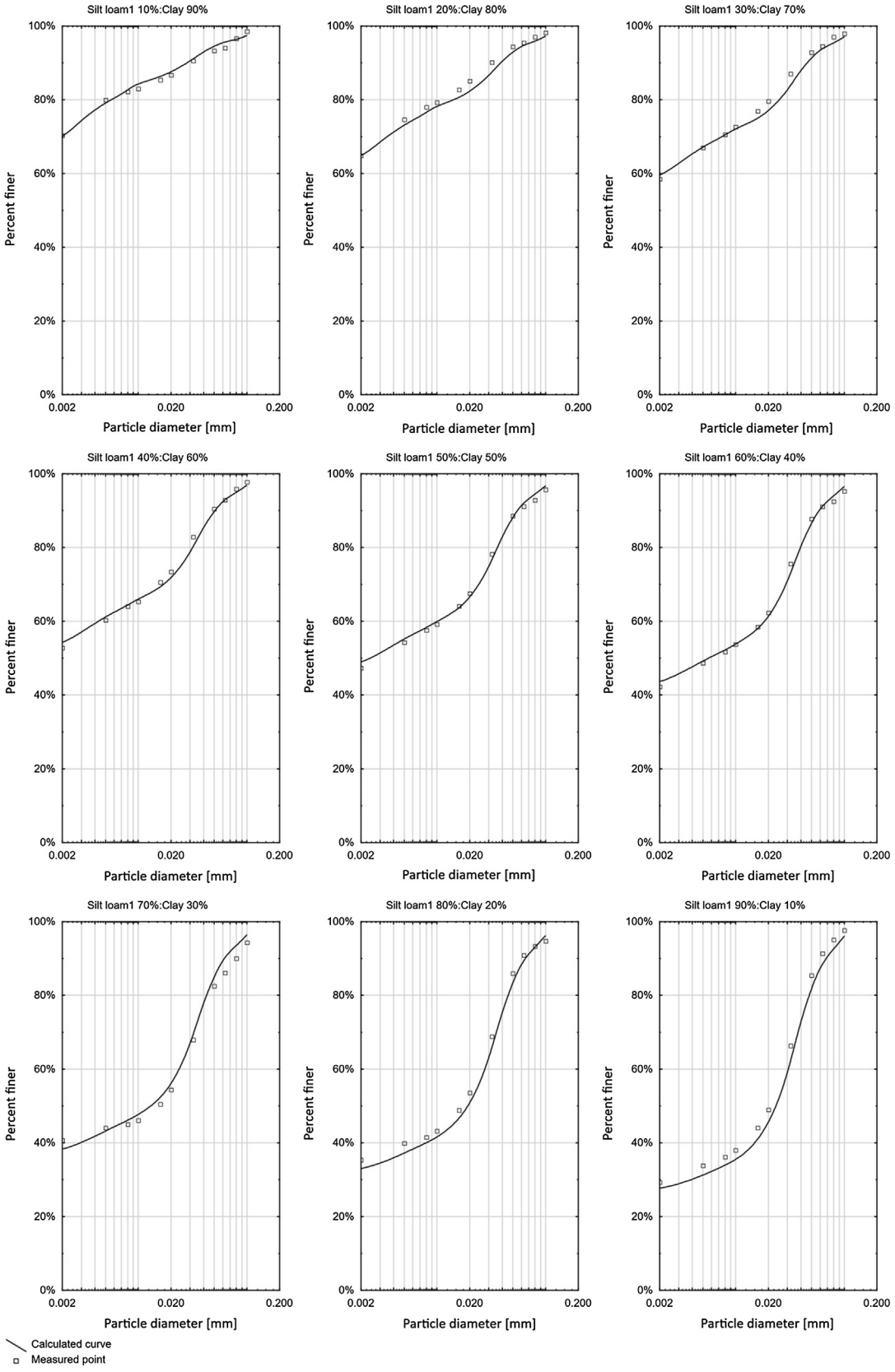

Fig. 6. Mixtures of silt loam 1 and clay. CPSD calculated at the basis of pure components contents.

therefore at high values $f(d) = F'(d)$ (Fig. 6). This is because of the fact that a small error in determining the measurement time is then associated with large differences in the obtained CPSD values.

For example in Figs. 5 and 6, CPSD, calculated on the basis of the "pure" components' share in the mixture, are presented in the form of continuous lines, and measurement results for the same mixtures are presented in the form of points.

Fig. 5 shows the results for the mixture of sand and clay, for which the greatest differences between the measured and calculated values were found: RMSE – 4.01%, median error – 2.52%, maximum error – 13.9%. However, Fig. 6 shows the results for the mixture of clay and silt loam 1, for which the smallest differences were found: RMSE – 1.77%, median error – 1.41%, maximum error – 4.21%.

3.3. Compatibility with the pipette method

The pipette method is considered the reference method for determining PSD [28]. It is essentially used to validate other methods [53,51,34]. The results obtained with it are characterized by high repeatability and reproducibility.

It employs a simple and understandable mathematical model of the single particle sedimentation phenomenon [52,17]. Its shortcomings are being considerably labour-consuming and time-consuming. In the presented work, it was also treated as a reference method.

Suspensions for measurements with the use of dynamometer and pipette methods were prepared separately. The results of the comparison for the pipette and dynamometer methods are presented in Fig. 7 in the form of pairs of x-y points; on the x-axis,

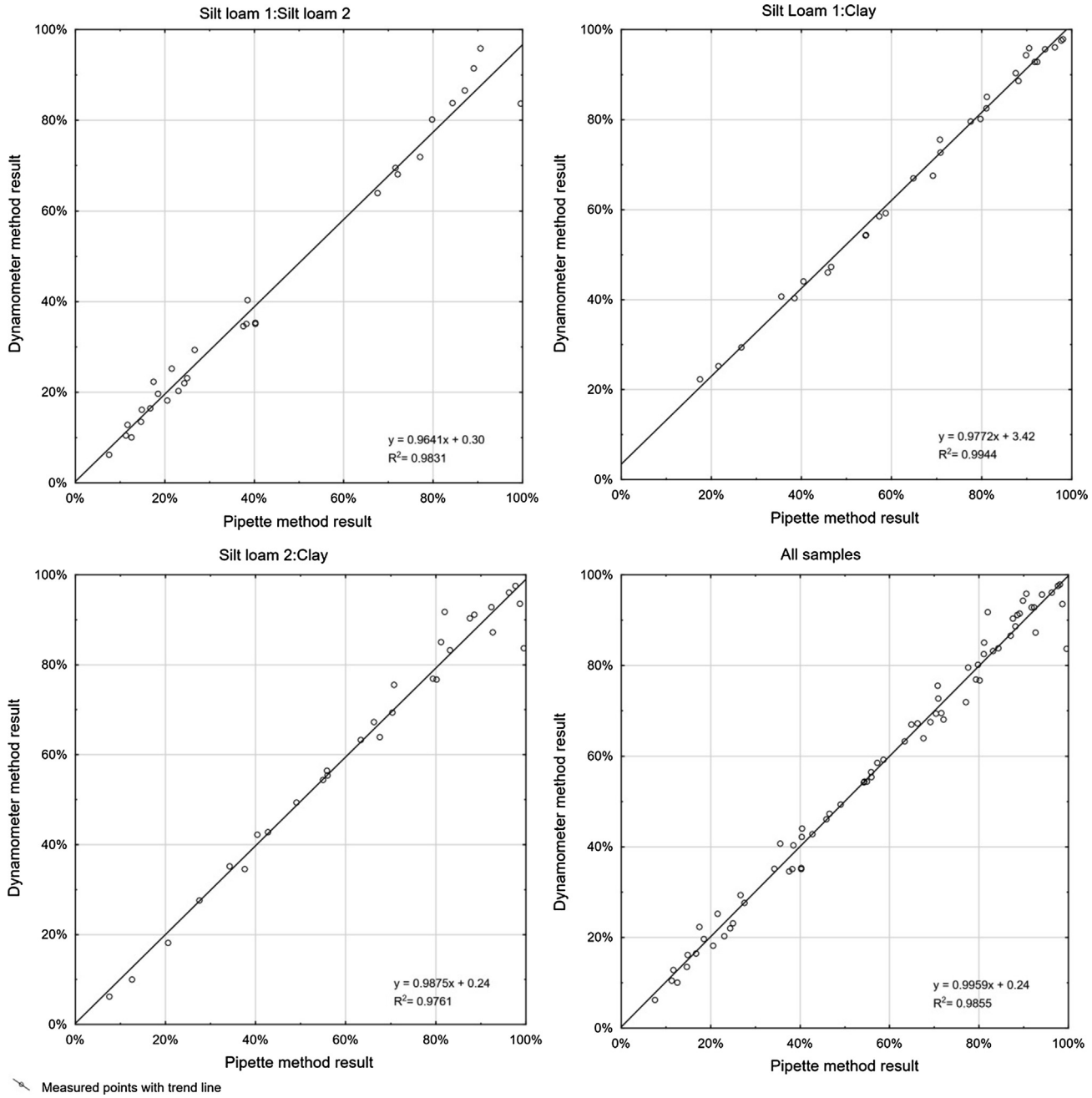

Fig. 7. Comparison of cumulative particle fraction content measured with the pipette and dynamometer method for chosen mixtures separately and for all of them together. All fractions.

the results of the pipette method, and on the y-axis, the results of the measurement using the dynamometer method along with the trend line for the $y = y(x)$ relationship. Selected statistical parameters are summarized in Table 4.

The trend lines for the relationship between the results of both methods deviate only slightly from the line $y = x$. Coefficients of slope are within 0.9641 and 0.9959, and vertical intercepts from 0.24 to 3.42. Taking into account all fractions together, for 25% of measurements the absolute difference between the results obtained by both methods was <0.53, for 50% of the results not exceeding 1.71, and for 75% of the measurements, it was <3.18. The maximum difference found was 15.83.

When considering the individual fractions separately the values of root mean square error and error assumed as a absolute value of the difference between result of the pipette and dynamometer method presented in the Table 5 were found.

Thus, it is apparent that the difference between the methods is greatest when measuring fraction < 0.1 mm, when the time from the end of mixing to measuring density is the shortest and the impact of different random deviations is the largest. The observed pattern of results indicates the lack of major systematic errors in the dynamometer method and the occurrence of some random errors requiring elimination or at least reduction during the course of further development of the method (see Fig. 7).

4. Discussion

Variable drag of fluid owing to the presence of other particles and, caused by them, ascending water streams infers that the settling velocity of particles depends on the concentration of suspension and PSD of measured soil. The actual settling velocity, ω is therefore different from that calculated from the Stokes equation, ω_0, and the difference is greater when the concentration of the suspension is higher. In the literature there are many equations describing the relationship between ω_0, and ω considering the concentration of the suspension as well as the size and shape of sedimenting particles [45,14,1]. Particularly, for suspensions at a volumetric concentration < 0.05, the Batchelor formula [4,50] may be used.

Therefore, it can be expected that the results obtained with sedimentation methods, where volumetric suspension concentrations used are at the level of 0.01–0.03, will depend on the applied sample weight determining the concentration of the suspension and thus the actual particles' settling velocities. The deviation of real settling velocity from that calculated with the Stokes equation will be greater in clay soils based on the higher concentration of fractions remaining in the suspension for a long time. The phenomenon has a complicated nature because the settling velocity of particles depends on their concentration, and this depends on the PSD, which would be just measured.

The obvious solution to the problem would be to diminish the soil weight and hence the concentration of the suspension, but this would require measuring smaller than the current changes in density. This would reduce the value of the signal:noise ratio and increase random errors. A possible solution to the problem may be the diversity of the soil sample based on the initial organoleptic assessment of the PSD. As a result, uniform sedimentation conditions for samples with different PSD can be achieved. The exact approach to determining particle falling times would also require determining the specific density of soil. It can be assumed that at low levels of organic matter or after its removal, its impact on density is small [8]. The effect of differentiated mineral composition and hence the varying density of fractions included in a single soil [30] is not featured in any of the available methods.

On the other hand, effects related to the particle's movement phase should not be expected when they accelerate after mixing until reaching the terminal settling velocity. According to [21], the time it takes for a particle with a diameter of 5 μm to reach 99% of the terminal settling velocity is 0.017 ms, and for a particle of 1000 μm, the same time is 1000 ms. The deviation from the spherical shape of grains has a significant influence on its settling velocity. In the literature on the subject, many empirical equations can be found to calculate the settling velocity of real soil grains [1,24,30]. Various indices describing the shape of grains are used, such as the Corey index [30] or Janke index [29], with each deviation of the shape resulting in a decrease of the falling velocity in relation to the spherical grain of the same volume as the tested ones. On the other hand, the surface roundness and smoothness

Table 4
Comparison of results obtained using the pipette and dynamometer methods.

Mixture	Number of fractions being compared	Regression equation	Correlation coefficient	Root mean square error RMSE	Standard regression error	Critical value CV**
1	*2*	*3*	*4*	*5*	*6*	*7*
Silt loam 1-Silt loam 2	30*	y = 0,9641x + 0,30	0.9915	4.07	3.29	−0.41
Silt loam 1-Clay	30*	y = 0.9772x + 3.42	0.9972	2.65	5.48	−3.50
Silt loam 2-Clay	30*	y = 0.9875x + 0.24	0.9880	4.15	5.12	−0.24
All samples	72	y = 0.9959x + 0.24	0.9927	3.36	4.86	−0.24

* 3 mixtures + 2 "pure" soils = 5. Multiplied by 6 fractions for each soil = 30. The "pure" samples were taken into account twice.
** CV – value of x for which y = 0.

Table 5
Statistical characteristics of differences between the results of the pipette and dynamometer methods for individual fractions.

Fraction diameter *d* [mm]	No of repetition in different mixtures	RMSE [%]	Quartile [%]			
			I	II median	III	IV (max)
1	*2*	*3*	*4*	*5*	*6*	*7*
<0,1	12	6,05	0.47	2.55	5.10	15.83
<0,05	12	2,92	0.49	1.77	3.66	5.35
<0,02	12	2,68	0.91	1.99	2.97	5.14
<0,01	12	1,89	0.65	1.83	2.46	2.87
<0,005	12	2,19	0.31	1.18	2.77	3.96
<0,002	12	2,68	0.77	1.30	2.62	5.17

[3] turns out to be less important. The solution of the sphericity problem seems to be the application of the concept of the equivalent diameter as the diameter of the sphere falling at the velocity equal to the settling velocity of the real shape grain. However, this is a solution that has a significant role in the emerging discrepancies between sedimentation and optical methods [44].

5. Conclusions

From a wide range of PSD analysis methods, none can be considered as ideal [26], and their evaluation depends on the criteria used. The proposed method for the determination of PSD, which is a development of the dynamometer method proposed by Kaszubkiewicz et al. [31], allows for automatic analysis of many samples simultaneously within the range of diameters 2–120 μm, performed without staff involvement. The proposed method, owing to standardization of mixing and complete elimination of the human factor, exhibits very robust reproducibility of results with the relatively highest dispersion of results found in the determination of the cumulative fraction of <0.1 mm measured in suspensions after a dozen or so seconds following the completion of the mixing process.

The method has been positively verified by determining the composition of mixtures of reference soils (with known proportions). Differences between measured and calculated CPSD did not exceed approximately, for individual mixtures, 2.5% - for median - and 14% - for maximum - error. The method shows satisfactory agreement of results with those of the pipette method considered as reference. There is no need to calibrate the dynamometer method to achieve convergent results with the pipette method. The disagreements observed in relation to the reference method are accidental; meanwhile, no systematic differences were observed.

Further improvements of the method both in terms of its physical aspects and the utility of improved computational algorithms should lead to further improvement of compliance with the reference method and repeatability of results. The current advantages of the developed method are: strong compliance with the results of the reference sedimentation method, the ability to analyse multiple fractions with arbitrarily chosen diameters ranges, analysis of many samples at the same time without the participation of staff, recording results in digital form, unification of sample mixing before measurement and shortening the analysis time in relation to other sedimentation methods.

CRediT authorship contribution statement

Jarosław Kaszubkiewicz: Conceptualization, Methodology, Resources, Supervision, Writing - review & editing. **Krzysztof Papuga:** Conceptualization, Methodology, Validation, Formal analysis, Investigation, Visualization, Writing - original draft, Writing - review & editing. **Dorota Kawałko:** Investigation, Writing - original draft. **Przemysław Woźniczka:** Investigation, Writing - original draft.

Declaration of Competing Interest

The authors declare that they have no known competing financial interests or personal relationships that could have appeared to influence the work reported in this paper.

Acknowledgments

This work was financially supported by The Polish National Agency for Academic Exchange (POWR.03.03.00-00-PN13/18).

References

[1] J.P. Ahrens, The fall-velocity equation, J. Waterw. 2000, Port, Coastal, Ocean Eng., 126(2) 99-102.
[2] T. Allen, Powder sampling and particle size measurement. In particle size and measurement, Allen T. 5th ed. Allen T. Chapman and Hall, London, UK, 1997, 216-219.
[3] J. Baba, P.D. Komar, 1981 Settling velocity of irregular grains at low Reynolds numbers, J. Sed. Petrology 51 (1) (1981) 121–128.
[4] G.K. Batchelor, Sedimentation in a dilute dispersion of spheres, J. Fluid Mech. 52 (2) (1972) 245–268.
[5] G.K. Batchelor, Sedimentation in a dilute polydisperse system of interacting spheres. Part 1. General Theory, J. Fluid Mech. 119 (1982) 379–408.
[6] A. Bieganowski, M. Ryżak, A. Sochan, A. Mako, G. Barna, H. Harnadi, M. Beczek, C. Polakowski, Laser diffractometry in the measurement of soils and sediment particle size distribution, Adv. Agron. 151 (2018) 215–279.
[7] M. Bittelli, M.C. Andrenelli, G. Simonetti, S. Pellegrini, G. Artioli, I. Piccoli, F. Morari, Shall we abandon sedimentation methods for particle size analysis in soils?, Soil Tillage Res. 185 (2019) 36–46.
[8] G.R. Blake, K.H. Hartge, Particle density in methods of soil analysis. In: A. Klute (ed.) Methods of Soil Analysis: Part 1. Physical and Mineralogical Methods. 2nd ed. Agron. Monogr. 9. ASA and SSSA Madison, USA, 1986, 363-375.
[9] S.J. Blott, K. Pye, Particle size distribution analysis of sand-sized particles by laser diffraction: an experimental investigation of instrument sensitivity and the effects of particle shape, Sedimentology 53 (3) (2006) 671–685.
[10] G.J. Bouyoucos, The hydrometer as a new method for the mechanical composition of soils, Soil Sci. 23 (1927) 319–335.
[11] G.D. Buchan, K.S. Grewal, J.J. Claydon, R.J. McPherson, A comparison of sedigraph and pipette methods for soil particle-size analysis, Australian J. Soil Res. 31 (4) (1993) 407–417.
[12] A. Casagrande, Die Areometr Methode zur Bestimmung der Kornverteilung von Böden, Berlin, 1934.
[13] H. Chen, H. Tang, Y. Liu, H. Wang, G. Liu, Measurement of particle size based on digital imaging technique, J. Hydrodyn. 25 (2) (2013) 242–248.
[14] N.S. Cheng, A simplified settling velocity formula for sediment particle, J. Hydraulic Eng. 123 (2) (1997) 149–152.
[15] J. Clifton, P. Mc Donald, A. Plater, F. Oldfield, An investigation into the efficiency of particle size separation using Stokes' measurement, Earth Surf. Process. Landf. 24 (1999) 725–730.
[16] G.F. Coates, C.A. Hulse, A comparison of four methods of size analysis of fine-grained sediments, N. Z. J. Geol. Geophys. 28 (2) (1985) 369–380.
[17] W. Dietrich, Settling velocity of natural particles, Water Res. Res. 18 (6) (1982) 1615–1626.
[18] N. Dipowa, Determining the grain size distribution of granular soils using image analysis, Acta Geotech. Slov. 1 (2017) 29–37.
[19] W.S.C. Durner, S.C. Iden, G. von Unold, The integral suspension pressure method (ISP) for precise particle-size analysis by gravitational sedimentation, Water Resour. Res. 53 (2017) 33–48.
[20] V. Dworak, B. Mahns, J. Selbeck, R. Gebbers, C. Weltzien, Terahertz Spectroscopy for Proximal Soil Sensing: An Approach to Particle Size Analysis, Sensors 17 (10) (2017) 2387.
[21] G.W. Gee, D. Or, Particle-size analysis. In: Methods of Soil Analysis, Part 4: Physical Methods, JH Dane & GC Topp., SSSA, Inc., Madison, USA, 2002, 255-293.
[22] G.W. Gee, J.W. Bauder, Particle-size analysis. In: A. Klute (ed). Methods of Soil Analysis: Part 1. Physical and Mineralogical Methods. 2nd ed. Agron. Monogr. 9. ASA and SSSA Madison, USA, 1986, 383-411.
[23] A. Ghasemy, E. Rahimi, A. Malekzadeh, Introduction of a new method for determining the particle-size distribution of fine-grained soils, Measurement 132 (2019) 79–86.
[24] R.J. Gibbs, M.D. Matthews, D.A. Link, The relationship between sphere size and settling velocity, J. Sed. Res. 41 (1) (1971) 7–18.
[25] M. Gomboš, A. Tall, J. Trpčevská, B. Kandra1, D. Pavelkova1, L. Balejčíková, Sedimentation rate of soil microparticles. Arabian, J. Geosci. 11 (2018) 635.
[26] D. Goossens, Techniques to measure grain-size distributions of loamy sediments: a comparative study of ten instruments for wet analysis, Sedimentology 55 (1) (2008) 65–96.
[27] A. Haider, O. Levenspiel, Drag coefficient and terminal velocity of spherical and nonspherical particles, Powder Technology 58 (1989) 63–70.
[28] International Standards, ISO 11277, Determination of Particle size Distribution in Mineral Soil Material, Method by Sieving and Sedimentation, 2009.
[29] N.C. Janke, Effect of shape upon the settling velocity of regular convex geometric particles, J. Sed. Petrology 36 (1966) 310–376.
[30] José A. Jiménez, Ole S. Madsen, A Simple Formula to Estimate Settling Velocity of Natural Sediments, J. Waterway, Port, Coastal, Ocean Eng. 129 (2) (2003) 70–78, https://doi.org/10.1061/(ASCE)0733-950X(2003)129:2(70).
[31] J. Kaszubkiewicz, W. Wilczewski, T.J. Nowak, P. Woźniczka, K. Faliński, J. Belowski, D. Kawałko, Determination of soil grain size composition by measuring apparent weight of float submerged in suspension, Int. Agrophys. 31 (1) (2017) 61–72.
[32] M. Köhn, Beitrage zur Theorie und Praxis der mechanischen Bodenanalyse, Landw. Jahrbuch. (1928,) 67.
[33] B. Kovács, I. Czinkota, L. Tolner, G. Czinkota, The determination of particle size distribution (PSD) of clayey and silty formations using the hydrostatic method, Acta Mineralogica-Petrographica 2004 (45) (2004) 29–34.

[34] A. Kun, O. Katona, G. Sipos, K. Barta, Comparison of pipette and laser diffraction methods in determining the granulometric content of fluvial sediment samples, J. Environ. Geography 6 (3–4) (2013) 49–54.
[35] P.J. Loveland, W.R. Whalley, Particle size analysis, in: K.A. Smith, C.E. Mullins (Eds.), Soil and Environmental Analysis, Physical Methods, Marcel Dekker Inc., New York, 2001, pp. 281–314.
[36] I.N. McCave, R.J. Bryant, H.F. Cook, C.A. Coughanowr, Evaluation of a laser-diffraction-size analyzer for use with natural sediments, J. Sediment. Res. 56 (1986) 561–564.
[37] I.N. McCave, J.P.M. Syvitski, Principles and methods of geological particle size analysis. In: J.P.M. Syvitski (ed.) Principles, Methods and Applications of Particle Size Analysis, Cambridge University Press, Cambridge, 1991, 3-21.
[38] N.-Q. Nguyen, A.J.C. Ladd, Sedimentation of hard-sphere suspensions at low Reynolds number, J. Fluid Mech. 525 (2005) 73–104.
[39] Y. Odén, Eine neue Methode zur mechanischen Bodenanalyse; Int. Mitt. Für Bodenkunde, 1915, Band 5, Heft 4, 257 - 311.
[40] J.M.C. Oliveira, C.M.P. Vaz, K. Reichardt, D. Swartzendruber, Improved soil particle-size analysis by gamma-ray attenuation, Soil Sci. Soc. Am. J. 61 (1997) 23–26.
[41] M. Ozer, O. Mehmet, S.I. Nihat, Effect of particle optical properties on size distribution of soils obtained by laser diffraction environment, Eng. Geosci. 16 (2) (2010) 163–173.
[42] K. Papuga, J. Kaszubkiewicz, W. Wilczewski, J. Belowski, D. Kawałko, Soil grain size analysis by the dynamometer method - a comparison to the pipette and hydrometer method, Soil Sci. Ann. 69 (1) (2018) 17–27.
[43] L. Pieri, M. Bittelli, P. Rossi Pisa, Laser diffraction, transmission electron microscopy and image analysis to evaluate a bimodal Gaussian model for particle size distribution in soils, Geoderma 135 (2006) 118–132.
[44] C. Polakowski, A. Sochan, A. Bieganowski, M. Ryżak, R. Földényi, J. Tóth, Influence of the sand particle shape on particle size distribution measured by laser diffraction method, Int. Agrophys. 28 (2014) 195–200.
[45] J.F. Richardson, W.N. Zaki, Sedimentation and fluidisation. Part 1, Trans. Inst. Chem. Eng. 32 (1954) 35–53.
[46] M. Ryżak, P. Bartmiński, A. Bieganowski, Methods for determination of particle size distribution of mineral soils, Acta Agrophys. 4 (175) (2009) 5–84.
[47] M. Ryżak, A. Bieganowski, Determination of particle size distribution of soil using laser diffraction - comparison with areometric method, Int. Agrophys. 24 (2) (2010) 177–181.
[48] S. Rząsa, W. Owczarzak, Methods for the granulometric analysis of soil for science and practice, Polish J. Soil Sci. 46 (1) (2013) 1–50.
[49] C. Shanthi, R. Kingsley Porpatham, N. Pappa, Image analysis for particle size distribution, Inte. J. Eng. Technolog. 6 (3) (2014) 1340–1344.
[50] R. Silva, F. Garcia, P. Faia, M. Rasteiro, Settling suspension flow modelling: A review, KONA Powder Particle J. 32 (2015) 41–56.
[51] M. Šinkovičová, I. Dušan, E. Kondrlová, M. Jarošová, Soil particle size analysis by laser diffractometry: result comparison with pipette method, Conf. Series: Materials Sci. Eng. 245 (2017) 072025.
[52] G.G. Stokes, On the effect of the internal friction of fluids on the motion of pendulums, Trans. Cambridge Philos. Soc. 9 (1850) 8–106.
[53] J.P.M. Syvitski, Principles, methods and application of particle size analysis, Cambridge University Press, Cambridge, 1991, p. 371.
[54] C.M.P. Vaz, J. de Mendonca Naime, A. Macedo, Soil particle size fraction determined by gamma – ray attenuation, Soil Sci. 164 (6) (1999) 403–410.
[55] L. Yong, H. Chengmin, W. Baoliang, T. Xiafei, L. Jingjing, A unified expression for grain size distribution of soils, Geoderma 288 (2017) 105–119.
[56] Z. Zhang, M.T. Tumay, Granulometric evaluation of particle size using suspension pressure during sedimentation, Geotech. Test. J. 18 (1) (1995) 121–129.
[57] S. Zhiyao, W. Tingting, X. Fumin, L. Ruijie, A simple formula for predicting settling velocity of sediment particles, Water Sci. Eng. 1 (1) (2008) 37–43.

UNIWERSYTET
PRZYRODNICZY
WE WROCŁAWIU

Wrocław 04.04.2022

Prof. Dr hab. Jarosław Kaszubkiewicz
Instytut Nauk o Glebie, Żywienia Roślin
i Ochrony Środowiska
Uniwersytet Przyrodniczy we Wrocławiu

OŚWIADCZENIE

Oświadczam, że w pracy: Kaszubkiewicz J., Papuga K., Kawałko D., Woźniczka P., 2020. Particle size analysis by an automated dynamometer method integrated with an x-y sample changer. Measurement, 157, 107680 (doi: 10.1016/j.measurement.2020.107680) mój udział polegał na nadzorowaniu przy opracowaniu koncepcji, metodologii i doboru analiz laboratoryjnych. Nadzór merytoryczny obejmował także poprawność interpretacji wyników oraz przygotowanie treści manuskryptu.

.....
Podpis

UNIWERSYTET
PRZYRODNICZY
WE WROCŁAWIU

INSTYTUT NAUK O GLEBIE, ŻYWIENIA ROŚLIN I OCHRONY ŚRODOWISKA

Wrocław 04.04.2022

Mgr inż. Krzysztof Papuga
Instytut Nauk o Glebie, Żywienia Roślin
i Ochrony Środowiska
Uniwersytet Przyrodniczy we Wrocławiu

OŚWIADCZENIE

Oświadczam, że w pracy: Kaszubkiewicz J., Papuga K., Kawałko D., Woźniczka P., 2020. Particle size analysis by an automated dynamometer method integrated with an x-y sample changer. Measurement, 157, 107680 (doi: 10.1016/j.measurement.2020.107680) mój udział polegał na opracowaniu koncepcji, metodologii, wykonaniu analiz laboratoryjnych i obliczeniowych, opracowaniu merytorycznym i graficznym rezultatów analiz oraz przygotowaniu treści manuskryptu.

.....Papuga.....
Podpis

UNIWERSYTET
PRZYRODNICZY
WE WROCŁAWIU

INSTYTUT NAUK O GLEBIE, ŻYWIENIA ROŚLIN I OCHRONY ŚRODOWISKA

Wrocław 04.04.2022

Dr inż. Dorota Kawałko
Instytut Nauk o Glebie, Żywienia Roślin
i Ochrony Środowiska
Uniwersytet Przyrodniczy we Wrocławiu

OŚWIADCZENIE

Oświadczam, że w pracy: Kaszubkiewicz J., Papuga K., Kawałko D., Woźniczka P., 2020. Particle size analysis by an automated dynamometer method integrated with an x-y sample changer. Measurement, 157, 107680 (doi: 10.1016/j.measurement.2020.107680) mój udział polegał na nadzorowaniu przy opracowaniu metodologii, doboru analiz laboratoryjnych oraz przygotowaniu treści manuskryptu.

Dorota Kawałko
Podpis

UNIWERSYTET PRZYRODNICZY WE WROCŁAWIU
INSTYTUT NAUK O GLEBIE, ŻYWIENIA ROŚLIN I OCHRONY ŚRODOWISKA
UL. GRUNWALDZKA 53, 50-357 WROCŁAW
tel. 71 320 56 04
e-mail: igleb@upwr.edu.pl • https://ingos.upwr.edu.pl/

Powder Technology 389 (2021) 507–521

Contents lists available at ScienceDirect

Powder Technology

journal homepage: www.elsevier.com/locate/powtec

Do we have to use suspensions with low concentrations in determination of particle size distribution by sedimentation methods?

Krzysztof Papuga, Jarosław Kaszubkiewicz *, Dorota Kawałko

Institute of Soil Science and Environment Protection, Wrocław University of Environmental and Life Sciences, Grunwaldzka 53, 50-357 Wrocław, Poland

ARTICLE INFO

Article history:
Received 8 October 2020
Received in revised form 10 March 2021
Accepted 16 May 2021
Available online 19 May 2021

Keywords:
Particle size distribution
Dynamometer method
Particle settling velocity
Sedimentation

ABSTRACT

The Stokes equation used in the measurement of particle size distribution is based on the assumption that there are no interactions between settling soil particles. This requirement is fulfilled by using a low-concentration suspension. Therefore a highly precise determination of the suspension density is needed and makes that the measurement is sensitive to temperature changes and other random factors. In the presented paper, we attempted to overcome this problem by using increased initial suspension concentrations and at the same time taking into account the mutual interactions of sedimenting particles. The Batchelor equation was used to calculate the hindered settling velocity of the particles. The problem of mutual dependence among the concentration of particles and measurement times for individual fractions was solved by applying a simple iterative procedure. Application of the procedure caused the results obtained with the use of various initial suspension concentrations to become more similar than without it.

1. Introduction

Methods of measuring the particle size composition of soils require suspension density measurements during the sedimentation process. Repeatedly performed density measurements make it possible to determine the concentration of particles with specific diameters that remain in the suspension after dropping particles with larger equivalent diameters. A single particle model developed by Stokes [1,2] is used to interpret the results. In this model it is assumed, among other things, that there are no interactions between particles settling in suspension.

This condition is assumed to be met when using diluted suspensions with a volume concentration of $c < 0.02–0.03$. In the pipette method, suspensions with a concentration of between 0.006 and 0.008 are generally used [3–5], while in the hydrometer method suspensions at concentrations between 0.017 and 0.019 are typically used [6–9]. Generally, even lower concentrations of suspensions should be used. For example, at a concentration of only 0.015, assuming that all particles have a uniform diameter of 0.02 mm, a return flow of water with a velocity of 1.5% of the particle fall rate is formed.

The mentioned effect of water counter-currents is only one of several responsible for slowing down the process of settling particles in suspension. The others are related to the interaction of particles, the effects of vessel walls [10], deviations of particles from a spherical shape [11] and differentiation of density of individual fractions [8,12,13]. Together, these various factors cause the rate of fall to decrease by up to several percent, compared to values resulting from the Stokes equation. These effects increase as the density of the suspension used increases [14,15].

Lower concentrations would be beneficial in reducing the interactions of sedimentary particles. However, they are also concomitant with smaller changes in the density of the sedimentary suspension, meaning that their measurement requires more accurate methods [16]. Additionally, lower concentrations would be expected to increase the significance of accidental errors resulting from changes in the temperature of the suspension (change in water density), vibrations of measuring systems, inaccuracies in the equipment used to measure density (balance, hydrometer, dynamometer), the influence of the dispersant on the density and viscosity of water, and other factors of a random nature. Thus, on the one hand, reduction in suspension concentration limits the influence of interactions between particles and allows the use of a single particle model based on the Stokes equation, but on the other hand, causes a decrease in the signal-to-noise ratio and an increase in the significance of accidental errors. The magnitude of the second effect may differ based on the method used for determining suspension density [17].

The problem described above also occurred in the dynamometer method of determining particle size composition, developed for several years by the authors of this paper. In this method, the suspension density is determined by measuring the apparent weight of a float suspended at a certain depth in the suspension. The weight of the float, suspended by a thin thread in a sedimentary suspension, is measured by a sensitive piezoelectric dynamometer. A detailed description of the method can be found in [18–20]. In this paper, an attempt has

* Corresponding author.
E-mail address: jaroslaw.kaszubkiewicz@upwr.edu.pl (J. Kaszubkiewicz).

https://doi.org/10.1016/j.powtec.2021.05.060

been made to account for the interactions between sedimentary particles in equations used to determine the velocity and time of settling soil particles.

Taking this effect into account should allow for the use of higher densities of suspensions than those used thus far in methods of particle size distribution measurement. The proposed solution does have a limited scope of application, in terms of the density of suspensions. However, in the authors' opinion, it should make it possible to at least partially eliminate systematic errors associated with the interaction of particles, enabling the use of suspensions with densities up to c = 0.05. The solution is based on the use of equations known from the literature which correct the particle settling velocity calculated using the Stokes equation by taking into account the concentration of suspension.

In the experimental part of this study, the influence of suspension density on the magnitude of random and systematic errors in the process of measuring particle size distribution using the dynamometer method was evaluated. Then, the influence of proposed theoretical solutions on the results of particle size analysis was tested and evaluated.

2. Theoretical basis

Let us assume that the sedimenting suspension meets the conditions required by the Stokes equation [2,12], that the dimensions of sedimenting particles are much smaller than the dimensions of the vessel in which sedimentation takes place, and that the Reynolds number is less than 1 ($Re < 1$), which according to Allen [16] means that the particles must be smaller than 60.6 μm. Let us also assume that the temperature during the process of sedimentation is constant, that there are no significant effects of vessel walls, that the density of all soil particles is equal, and that the density of the suspension is measured at a considerable distance from the vessel bottom. Finally, let us assume that the suspension is homogeneous at the initial moment, *i.e.* particles of all diameters are evenly distributed throughout the space. Let us consider a soil particle which has an equivalent diameter d and at $t_0 = 0$ is localized at the surface of a homogeneous suspension. For the purposes of sedimentation analysis of particle size distribution, we can assume that the value of the volume concentration of suspension c is less than 0.05. In our considerations, let us ignore the very short period in which the particle accelerates before it reaches its terminal velocity [21,22]. Moreover, let us assume that particles with larger diameters fall in the water suspension with settling velocities greater than those of particles with smaller diameters at the same level in the suspension.

Based on the assumptions made, we conclude that the previously mentioned particle with a diameter d, located at the initial moment at the surface of the suspension, will be surrounded only by particles with equivalent diameters (≤d) during sedimentation. This is a very important finding, true only for the particles that were initially at the surface of the suspension. Particles with larger diameters fall faster, and are not present in the suspension in which the particle with diameter d is located. At the same time, all particles with diameters smaller than d fall with a settling velocity lower than the considered one and remain in the suspension in which it moves. The situation of a particle with a diameter d, which was initially at the surface, can therefore be perceived as if there were no particles with diameters greater than d in the suspension at all.

From the above considerations, it follows directly that the particle which was initially at the surface of the suspension will fall in a suspension of constant density at a constant settling velocity. Thus, a suspension layer with fixed density will move downward from the surface at a constant velocity. This conclusion will be experimentally verified later in this paper. Thus, the examined particle with the equivalent diameter d, which at the initial moment was at the surface of the suspension, is permanently moving in a suspension with a constant density equal to:

$$c(d) = cF(d) \tag{1}$$

where $c(d)$ is the density of the suspension containing only particles with diameters less than or equal to d, c is the volumetric density of the suspension at the initial moment, and $F(d)$ is the proportion of particles with diameters less than or equal to d in the total soil formation as described by the cumulative particle size distribution (CPSD). The fact that the described particle moves in a suspension of constant density also means that it moves at a constant velocity $v(d)$ [23].

The observation of the constant density of the suspension does not apply to particles of diameter d that were initially below the surface of the suspension. Such particles, during their movement, are captured and overtaken by particles with diameters greater than d. They fall in a suspension of variable density and consequently have time-variable settling velocities. During the sedimentation process, the settling particle experiences interactions with other particles [21], settles in the return flow of water produced by the remaining particles [24,25], experiences buoyancy modified by the proportion of the solid phase in the suspension [26,27], and moves in a liquid with a viscosity higher than that of the water itself [25,28,29].

In order to account for the above effects, empirical and semi-empirical equations are used to link the actual settling velocity of soil particles (hindered settling velocity) in the suspension of concentration c with the velocity calculated on the basis of the Stokes equation. For a diluted ($c < 0.05$) bidisperse colloidal suspension, Batchelor [30,31] proposed an approximate equation describing the hindered settling velocity of particles depending on the concentration of the suspension in the form:

$$v = v_S(1-mc) \tag{2}$$

where m is an empirical coefficient ranging from 4 to 6, c is the volume concentration of the suspension as before, and v_S is the settling velocity calculated from the Stokes equation (single particle model). The predictions using Batchelor's model are in good agreement with the experimental data for monodisperse and bidisperse colloidal suspensions [32] and even for tridisperse noncolloidal suspensions [33,34]. It has been previously shown that each particle of diameter d, which was initially at the surface of suspension, falls in a constant density suspension containing only particles with diameters less than or equal to d. Therefore, it can be written that the density of the suspension in which a particle with a diameter d falls (starting from the surface) is $cF(d)$, and for a polydisperse suspension eq. (2) can be replaced by:

$$v(d) = v_S(d)(1-mcF(d)) \tag{3}$$

where $v(d)$ is the hindered settling velocity measured from the walls of the sedimentation vessel, corrected for the existence of different particle-to-particle and vessel wall interaction effects. The parameter m in eq. (3) also takes into account the existence of a water return flow and the interaction between molecules. The proposed eq. (3) is one of a few that are available in the literature and can be used [35–37]. The authors of this paper do not aim to obtain another equation linking the hindered settling velocity of a particle in a suspension of a given concentration with its settling velocity calculated on the basis of the Stokes equation. Instead, we intend to show that the accuracy of sedimentation methods can be improved by using suspensions with higher concentrations, for which hindered settling velocity should be used (rather than the settling velocity calculated from the Stokes formula).

It is useful to emphasize once again that the above eq. (3) is valid only for particles that were initially at the surface of the suspension. Such particles move in a suspension of constant density and therefore their velocity is also constant. The hindered settling velocity $v(d)$, calculated with reference to the walls of the sedimentation vessel, thus depends on the CPSD described by the function $F(d)$. Therefore, in sedimentation methods we deal with an unfavourable situation in

which, in order to accurately determine the settlement times of individual fractions, it is necessary to know the cumulative particle size distribution function $F(d)$, and at the same time the exact settlement times of individual fractions are necessary to determine the value of the function $F(d)$.

To solve this problem, the authors propose to use the following iterative procedure:

- With the selected (constant) measurement depth L, for the fraction with diameters d_i ($i = 1, 2, 3, \ldots, n$) we determine the initial measurement times $t^{(0)}(d_i)$ ($i = 1, 2, 3, \ldots, n$) based on the Stokes equation:

$$t^{(0)}(d_i) = \frac{L}{v_S(d_i)} = \frac{L}{\frac{d_i^2}{18}\frac{g}{\eta}(\rho_s - \rho_w)} = \frac{18\eta L}{d_i^2 g(\rho_s - \rho_w)} \tag{4}$$

where ρ_S is a density of particles, settling in a fluid with density ρ_w and dynamic viscosity η and g is the acceleration of gravity.

- We measure the density of the suspension at the depth L at the times $t^{(0)}(d_i)$ established above, obtaining a series of values $\rho_z(t^{(0)}(d_i))$. Then we fit the function $\overline{\rho_z}(t)$ to the obtained set of points $(t^{(0)}(d_i); \rho_z(t^{(0)}(d_i)))$.
- Then, for the smallest value $d_i = d_1$ we calculate the initial value of the cumulative distribution function $F^{(0)}(d_1)$ based on the equation:

$$F^{(0)}(d_1) = \frac{\overline{\rho_z}(t^{(0)}(d_1)) - \rho_w}{c(\rho_s - \rho_w)} \tag{5}$$

- Thus, for the content of fractions with diameters smaller than d_1 equal to $F^{(0)}(d_1)$ based on the eq. (3) we obtain the hindered settling velocity:

$$v^{(1)}(d_1) = v_S(d_1)\left(1 - kcF^{(0)}(d_1)\right) \tag{6}$$

- And then the corrected settlement time to depth L for a particle with diameter d_1.

$$t^{(1)}(d_1) = \frac{L}{v^{(1)}(d_1)} \tag{7}$$

- For the new settlement time of the particle with diameter d_1 to depth L, we calculate from the fit equation the new value of the suspension density $\overline{\rho_z}(t^{(1)}(d_1))$ and the new corrected value of the cumulative particle size distribution function:

$$F^{(1)}(d_1) = \frac{\overline{\rho_z}(t^{(1)}(d_1)) - \rho_w}{c(\rho_s - \rho_w)} \tag{8}$$

- Using the eqs. (6), (7) and (8) again, we calculate the next corrected values $v^{(2)}(d_1)$, $t^{(2)}(d_1)$ and $F^{(2)}(d_1)$. We repeat the calculations until the values obtained from subsequent iterations differ by a value smaller than the predetermined accuracy ε. The calculations show that after 3 iteration steps, the differences between the values of the successive distribution functions $F^{(3)}(d_1) - F^{(2)}(d_1)$ are less than 0.001. Next, we use diameter value $d_2 = d_1 + \Delta d$. The value of the parameter Δd should be selected to be small enough that no effects related to the numerical procedure appear. Eq. (6) now takes the equivalent form:

$$v^{(1)}(d_2) = v_S(d_2)\left(1 - kcF^{(0)}(d_2)\right) \tag{9}$$

- The value of $t^{(1)}(d_2)$ is calculated in the same way as before from the equation:

$$t^{(1)}(d_2) = \frac{L}{v^{(1)}(d_2)} \tag{10}$$

- The value of $F^{(1)}(d_2)$ is calculated from the equivalent form of eq. (8):

$$F^{(1)}(d_2) = \frac{\overline{\rho_z}(t^{(1)}(d_2)) - \rho_w}{c(\rho_s - \rho_w)} \tag{11}$$

- We perform calculations described by eqs. (9), (10) and (11) again and repeat until we obtain values from subsequent iterations that differ by a value lower than the value set in advance. For subsequent values of diameters $d_3 \ldots d_n$ we repeat the calculations using the formulas analogous to (9), (10) and (11), where for the ith value of the diameter d_i and for the jth iteration the equivalent of formula (9) has the following form:

$$v^{(j)}(d_i) = v_S(d_i)\left(1 - kcF^{(j-1)}(d_i)\right) \tag{12}$$

As a result of the application of the iterative procedure presented above, we obtain a corrected cumulative particle size distribution (CPSDC) and values of the hindered settling velocity of particles with different diameters d (those initially located at the surface of the suspension). The procedure described above can be applied to those sedimentation methods that allow a quasi-continuous measurement of the density [18,20,38,39] or hydrostatic pressure of the suspension column [22,40] as a function of time.

In the next part of this paper, we attempt to use experimental results to demonstrate that the application of the above procedure and the correction of the CPSD function allow the use of suspensions with volume concentrations up to 0.05. The limitation in the scope of application of the procedure results from limitations on the use of Batchelor Eq. [30]. We emphasize once again that the aim of the authors is not to find an equation linking hindered settling velocity with concentration and CPSD of soil, but to use existing equations for determining particle size composition within the scope of average concentrations of measured suspensions. As the equations describing the hindered settling velocity of particles in polydisperse suspensions with average concentrations less than 0.05 develop, they can be used as part of the proposed procedure.

3. Materials and methods

The samples for research were taken from the subsurface horizons of soils with different particle size composition and without calcium carbonate. The collected soil samples were dried, then ground and sifted through a 2 mm sieve. Analyses of the following parameters influencing

the sedimentation of soil particles were performed on the collected material: organic carbon content (measured by loss on ignition) and calcium carbonate content (analysed using volumetric method on Scheibler apparatus).

In the first part of the research, the suspension density was measured at different depths and at different intervals in order to check the assumption of constant velocity of the suspended solids layer of a certain density. The test was performed with the use of Digital Casagrande® device described in the paper by Kaszubkiewicz et al. [18] in 5 soil samples (A1-A5). The granulometric classification of the samples were as follows: silty loam with different clay content (A1-A3) and clay with different clay content (A4, A5). The basic soil properties are presented in Table 1.

The soil suspension was prepared according to the standard hydrometer method. The soil was dried at the temperature of 105 °C, crushed in a mortar and sieved through a 2 mm mesh sieve. Sixty grams of the sieved soil were weighed and transferred to a 1000 cm^3 glass beaker, to which 25 cm^3 of dispersant (sodium hexometaphosphate) and 700 cm^3 of distilled water were added. The contents of the beaker was stirred in a laboratory stirrer for 15 min and then transferred to a measuring cylinder with a capacity of 1000 cm^3. The suspension was filled to the volume of 1000 cm^3 with distilled water which was at ambient laboratory temperature. Suspension density was measured at depths of 50, 100, 150, 200, 250 and 300 mm below the surface. Measurement times varied at individual depths and ranged from 20 to 74,700 s. In total, the suspension density was analysed for each depth at 22 different times. An acrylic glass float with a volume of 39.005 cm^3 and a density of 1.188 g·cm^{-3} was used. Measurements were taken in glass cylinders with a diameter of 61 mm, which made it possible to omit the effect of walls [41]. The height of the suspension pole was 342 mm. Then, based on the obtained two-dimensional functions $\rho = \rho(z,t)$, the times after which the suspension had the same density at different depths were determined. These times were determined for individual samples for 3 or 4 different densities (Table 2). The results are presented in the next section.

In the second stage of research, the dynamometer method developed by the authors [18,19] and described in [20] was used to conduct analyses of soil particle size composition. Dynamometer method of determining the PSD is based on changes in the apparent weight of the float submerged in sedimenting suspension. The apparent weight measurement is performed using a sensitive dynamometer with the piezoelectric effect. Then, it is recalculated into cumulative PSD (CPSD) on the basis of Stokes law. The method allows the measurement of PSD in a range of grain diameters from 0.002 mm to 0.130 mm. The integration of the vertically displacing dynamometer and float with the mixer made it possible to automate. Moving the measuring head in the horizontal plane permitted automatic examination of several samples in one measuring cycle. The method allows for the continuous determination of many different fractions preselected by the user.

The first aim of these studies was to verify the thesis that the measurement results are characterized by greater random errors when using lower density suspensions. The second aim was to verify the developed iterative calculation procedure described in the previous chapter, which would allow for the use of suspensions with volume densities up to 0.045. Six soil samples were used in these studies. The granulometric classifications of these samples were silty loam with different clay content (B1-B3), sandy loam with different clay content (B4, B5) and clay (B6). The content of fractions with equivalent diameters $d < 0.1$, <0.008, 0.063, 0.05, 0.032, 0.02, 0.016, 0.01, 0.008, 0.005 and 0.002 mm was measured. Soil dry weights of 20, 40, 60, 80, 100 and 120 g·dm^{-3} of the suspension were used, which, assuming that the density of soil material is 2.65 g·cm^{-3}, corresponds to the following volume concentrations: 0.0075, 0.0151, 0.0226, 0.0302, 0.0377, 0.0453. Each measurement was taken 5 times by immersing the float so that the sedimentation path of particles from the surface to the level of the buoyancy centre of the float was 120 mm. The results were interpreted using the procedure described above in the Theoretical Basis section. A 38.885 cm^3 float made of acrylic glass with a density of 1.189 g·cm^{-3} was used. The measurements were made in PE cylinders with a diameter of 78 mm and a suspension height of 209 mm. The basic soil properties are presented in Table 1.

The influence of soil suspension concentration on the results of particle size distribution measurements was analysed. The magnitude of random errors and systematic errors in relation to the suspension concentration was tested.

Table 1
Properties of tested soils.

Soil sample	Soil type[a]	Horizon	Granulometric group	Organic carbon content [%][b]	Content of $CaCO_3$ [%][d]	pH[e]
1	2	3	4	5	6	7
A1	Luvisol	B	silty loam	bdl[c]	bdl	6.1
A2	Luvisol	C	silty loam	bdl	bdl	6.5
A3	Luvisol	Bt	silty loam	bdl	bdl	6.7
A4	Gleysol	Cox	clay	bdl	bdl	6.1
A5	Gleysol	G	clay	bdl	bdl	6.0
B1	Luvisol	B/C	silty loam	bdl	bdl	6.4
B2	Luvisol	BC	silty loam	bdl	bdl	6.7
B3	Luvisol	EB	silty loam	bdl	bdl	6.9
B4	Fluvisol	C	sandy loam	bdl	bdl	6.0
B5	Fluvisol	C	sandy loam	bdl	bdl	6.1
B6	Gleysol	G	clay	bdl	bdl	6.2

[a] Soil types were classified according to the World Reference Base for Soil Resources 2014.
[b] Measured by loss on ignition.
[c] Below detection limit.
[d] Analysed using volumetric method on Scheibler apparatus.
[e] Measured in water, using pH meter.

4. Results

4.1. Experimental studies

To verify the theoretical assumptions, the movement of a suspension layer with specific, constant density during the sedimentation process was analysed. Changes in position of layers with densities from 10,081 g·cm^{-3} to 10,320 g·cm^{-3} (corresponding to float apparent weights of 7.0 gF to 6.1 gF, respectively) were analysed. The assumption that movement of a constant density layer is a linear function of time was confirmed.

According to the data in Table 2, the determination coefficients for linear regression (y-intercept is equal to zero), for the time-distance relationship, exceeded 0.90 in 15 and 0.95 in 14 cases (out of 17 test cases). At the same time, the RMSE value for linear regression in 16 out of 17 test cases did not exceed 24.5 mm, and in 14 cases did not exceed 16.7 mm. The differences between the measured values and those predicted on the basis of the linear time-distance relationship were random.

For example, a layer with a density of 1.0218 g·cm^{-3} (sample A5) moved in suspension at an average velocity of 0.0543 mm·s^{-1}. Interpreting this value according to the Stokes equation, it would be assumed that this layer contained soil particles with diameters $d \leq$ 0.0232 mm (temperature 25.4 °C). The coefficient of determination for linear regression without constant term (time-distance relation) was 0.9677. The correlation coefficient between measured and calculated values from linear regression was 0.9863 and was significant at $\alpha =$ 1.9E-3. RMSE value was 16.7 mm.

At the same time, a layer with a density of 1.0235 g·cm^{-3} (sample A2) moved in suspension at an average velocity of 1.4460 mm·s^{-1}. When interpreting this value according to the Stokes equation it would be assumed that this layer contained soil particles with diameters $d \leq$ 0.1207 mm (temperature 24.6 °C). The coefficient of determination for linear regression without constant term (time-distance

Table 2
Statistical parameters of linear regression in the process of movement of constant density layers during sedimentation.

Soil sample	Suspension density in the layer [g·cm^{-3}]	Apparent float weight corresponding to the suspension density	Linear regression equation for relationships time (t) - depth(y) (without constant term)	The diameter of the largest particles [mm]. corresponding to the settling velocity calculated according to the Stokes equation.	Coefficient of determination for linear regression without constant term R^2	Correlation coefficient between measured and predicted settling time r	Significance of correlation p	RMSE for linear regression [mm]
1	2	3	4	5	6	7	8	9
A1	1.0235	6.40	$y = 1.0269 \cdot t$	0.1017	0.9930	0.9965	1.8E-5	7.2
	1.0183	6.60	$y = 0.5901 \cdot t$	0.0771	0.9921	0.9961	2.3E-5	7.6
	1.0132	6.80	$y = 0.2931 \cdot t$	0.0546	0.9868	0.9934	6.5E-5	9.8
	1.0081	7.00	$y = 0.0804 \cdot t$	0.0285	0.9864	0.9960	3.0E-4	10.8
A2	1.0235	6.40	$y = 1.4460 \cdot t$	0.1207	0.9972	0.9987	3.0E-6	4.5
	1.0183	6.60	$y = 0.8793 \cdot t$	0.0941	0.9949	0.9978	8.0E-6	6.1
	1.0132	6.80	$y = 0.4911 \cdot t$	0.0704	0.9886	0.9948	4.0E-5	9.1
A3	1.0223	6.50	$y = 1.5129 \cdot t$	0.1198	0.9875	0.9950	3.8E-5	9.5
	1.0197	6.60	$y = 1.2096 \cdot t$	0.1071	0.9953	0.9979	7.0E-6	5.8
	1.0172	6.70	$y = 0.8925 \cdot t$	0.0920	0.9951	0.9979	7.0E-6	6.0
	1.0146	6.80	$y = 0.6237 \cdot t$	0.0769	0.9936	0.9972	1.2E-5	6.9
A4	1.0320	6.10	$y = 0.0648 \cdot t$	0.0253	0.6556	0.9825	1.8E-2	43.4
	1.0308	6.15	$y = 0.0199 \cdot t$	0.0140	0.8902	0.9854	1.5E-2	24.5
	1.0295	6.20	$y = 0.0087 \cdot t$	0.0093	0.9104	0.9738	2.6E-2	22.1
A5	1.0295	6.20	$y = 2.1516 \cdot t$	0.1459	0.9677	0.9896	1.3E-3	16.7
	1.0243	6.40	$y = 0.2298 \cdot t$	0.0477	0.9876	0.9998	3.0E-6	10.3
	1.0218	6.50	$y = 0.0543 \cdot t$	0.0232	0.9677	0.9863	1.9E-3	16.7

relation) was 0.9972. The correlation coefficient between measured and calculated values from linear regression was 0.9987 and was significant at $\alpha = 3.6E\text{-}6$. RMSE value was 4.5 mm. The lowest values of determination coefficients and the highest RMSE error values were found for sample A4, which was characterized by a clayey granulometric composition and thus low falling velocities.

Therefore, the data presented in Table 2 confirm the hypothesis, put forward in the previous section, that layers of constant density – and thus particles of a fixed size starting their movement from the surface of the suspension – move at a constant velocity (linear distance-time relationship). Different compositions correspond to different particle diameters, so the velocities of layers with the same density but different compositions were different. For example, layers of density 1.0235 from A1 and A2 samples moved with velocities of 1.0269 mm·s^{-1}and 1.4460 mm·s^{-1}, respectively. Of course, when interpreting the results according to Stokes equation, the same velocities of layer movement would correspond to the same dimensions of sedimentary particles. It has been shown that the settling velocity of particles with specific diameters (starting their movement from the surface of the suspension) is constant over time, but this does not change the fact, highlighted in the literature, that the interaction of particles in the suspension reduces their settling velocity, making this value lower than predicted by the Stokes Eq. [42–44].

The results of the measurements therefore confirm the assumption that the position of each of the analysed layers changes linearly with time, so that a layer of suspension with a constant density moves downwards at a constant velocity (Fig. 1).

4.2. Random and systematic errors

The second aim of the laboratory studies was to determine the magnitude of random and systematic errors that occurred, depending on the applied soil weight (initial suspension concentration). The research hypothesis was verified that, for small weights and low concentrations of suspensions, the observed density changes associated with the sedimentation process are similar to random errors resulting from temperature fluctuations, surface vibrations, zero drift in an electronic dynamometer, *etc.*

Measurements of particle size distribution made in 5 repetitions showed that for small soil concentrations (0.0075 and 0.0151), the values of standard deviation of all tested fractions are significantly higher than for concentrations ≥0.0226. Fig. 2 shows the standard deviation for 3 sample fractions ($d < 0.063$, 0.02, 0.002 mm), depending on the weight applied. For all 6 tested soils there is a trend of decreasing standard deviation with an increasing applied weight (and thus increasing suspension concentration). Moreover, Fig. 2 shows averaged values of standard deviations for all 11 measured fractions. These values also show clear improvement in the convergence of results with an increase in the applied soil weight, with the lowest average standard deviation values observed for concentrations of 0.0377 and 0.0453.

The reasons for the observed trend are apparent. In the previously discussed dynamometer method, the current suspension density is determined from the apparent weight of the float immersed in it. The non-systematic errors in measuring the apparent weight of a float are due to several random factors, such as surface vibrations, air movements and temperature changes. It can be assumed that these errors remain constant. However, the total change of suspension concentration and apparent weight of the float during sedimentation increases with an increase in the initial concentration of the suspension. The latter fact is illustrated in Table 3, in which the ranges of change of suspension density during measurements at individual initial concentrations are listed.

The second aim of the research also involved determining the occurrence of systematic errors associated with the interaction of sedimentary particles. This phenomenon causes the actual settling velocity for a given equivalent diameter to be lower than that resulting from the Stokes equation. We tested the hypothesis that the application of the presented calculation procedure described in the Theoretical Basis section allows for the reduction of systematic errors caused by the use of suspensions with increased concentration.

4.3. Results of the calculation procedure

The calculation procedure described in the Theoretical Basis section was applied to the obtained results of the cumulative particle size distribution (CPSD), which was measured as described in the Materials and Methods section. Example results of direct measurements with CPSD curves (black lines) plotted and corrected by using the proposed procedure (CPSDC, red lines) are shown in Fig. 3. The error bars show a significant spread of results obtained with a small concentration (0.0075) and very good repeatability of results with a high concentration (0.0453). It

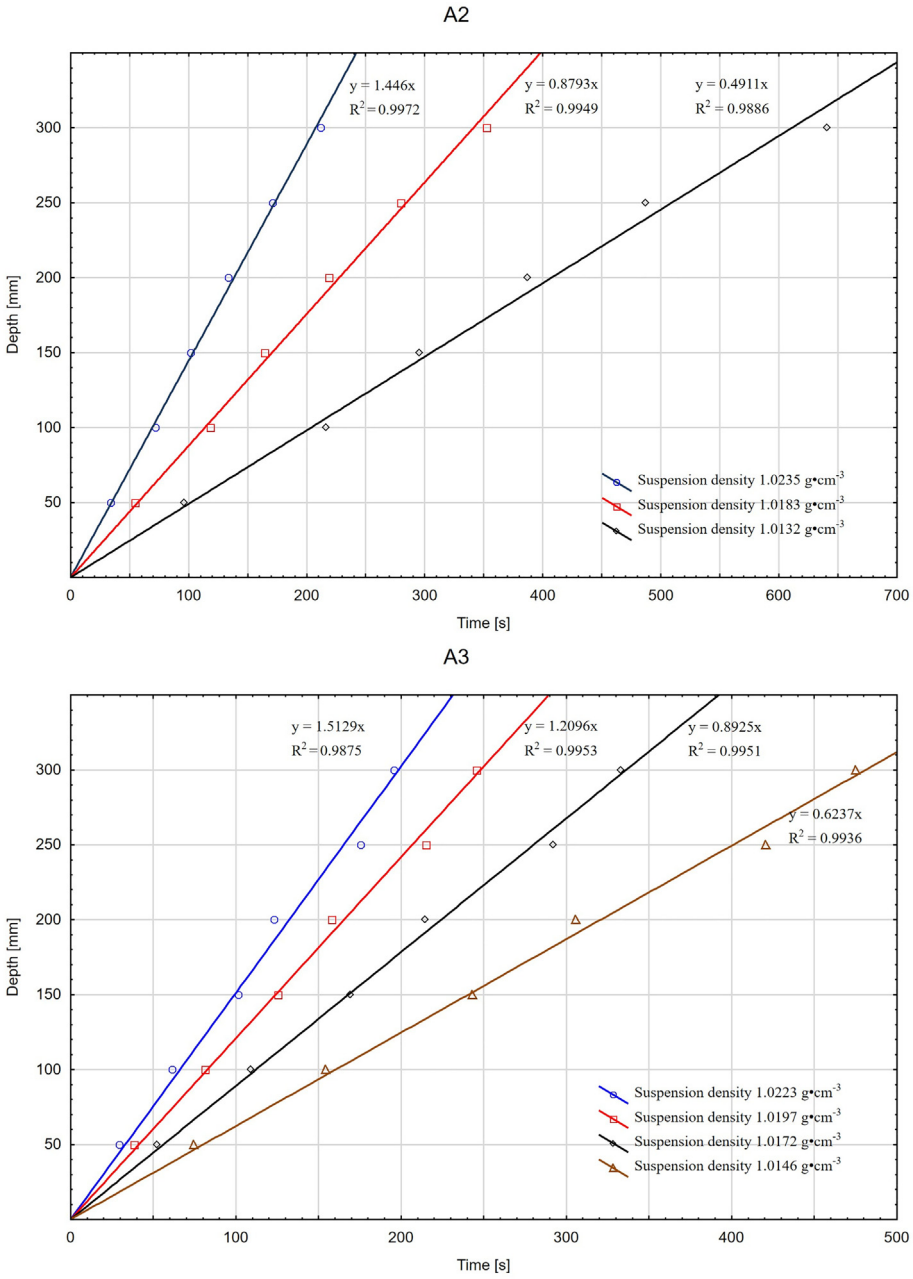

Fig. 1. The distance dependence on time for layers with selected constant densities in A2 and A3 samples (for x = 0, y = 0).

can also be seen that the application of the proposed procedure for a 0.0075 initial concentration has practically no influence on the results obtained. However, in all cases for 0.0453 (Fig. 3 and others), the difference in the shape of the curve, before and after the correction resulting from the applied procedure is clearly visible.

The results of the procedure in quantitative terms for all 6 examined soil formations and for all analysed concentrations are illustrated in Figs. 4 and 5. Fig. 4 shows the ratio of CPSDC/CPSD values as a function of particle diameter *d*. However, the difference between CPSD and CPSDC, also as a function of particle diameter, is shown in Fig. 5. It should be noted that for comparison it was not the direct results of the CPSD curve that were used, but the values from the curve matched to the measurement results.

Based on Figs. 5 and 6 and the data presented in Table 3, it can be seen that the maximum correction of CPSD curves (both in terms of minimum CPSDC/CPSD and maximum CPSD-CPSDC) occurs for particle diameters greater than the mode value and value d_{50}. It is also visible that the correction causes only a slight (within the limits of calculation errors) shift of d_{50} and mode values. Evaluating the magnitude of the correction resulting from the procedure used at different concentrations, one can see that for an initial volume density of 0.0075 (20 g sample weight) the value of the CPSDC/CPSD ratio does not decrease for the 6 samples tested below 0.9894 (0.077 mm fraction, sample B6), while the CPSD-CPSDC difference does not increase above 0.0087 (0.077 mm fraction, sample B6). The maximum correction for both minimum CPSDC/CPSD value and maximum CPSD-CPSDC value was observed for the highest initial suspension concentration (0.0453, 120 g sample weight). The lowest CPSDC/CPSDC value was observed for sample B5 and was 0.9411 (fraction <0.034 mm), while the CPSD/CPSDC difference was the highest for sample B1 and was 0.0463 for the fraction <0.100 mm. It is worth mentioning that due to large random errors in the measurement of CPSD curves when using a 0.075 density

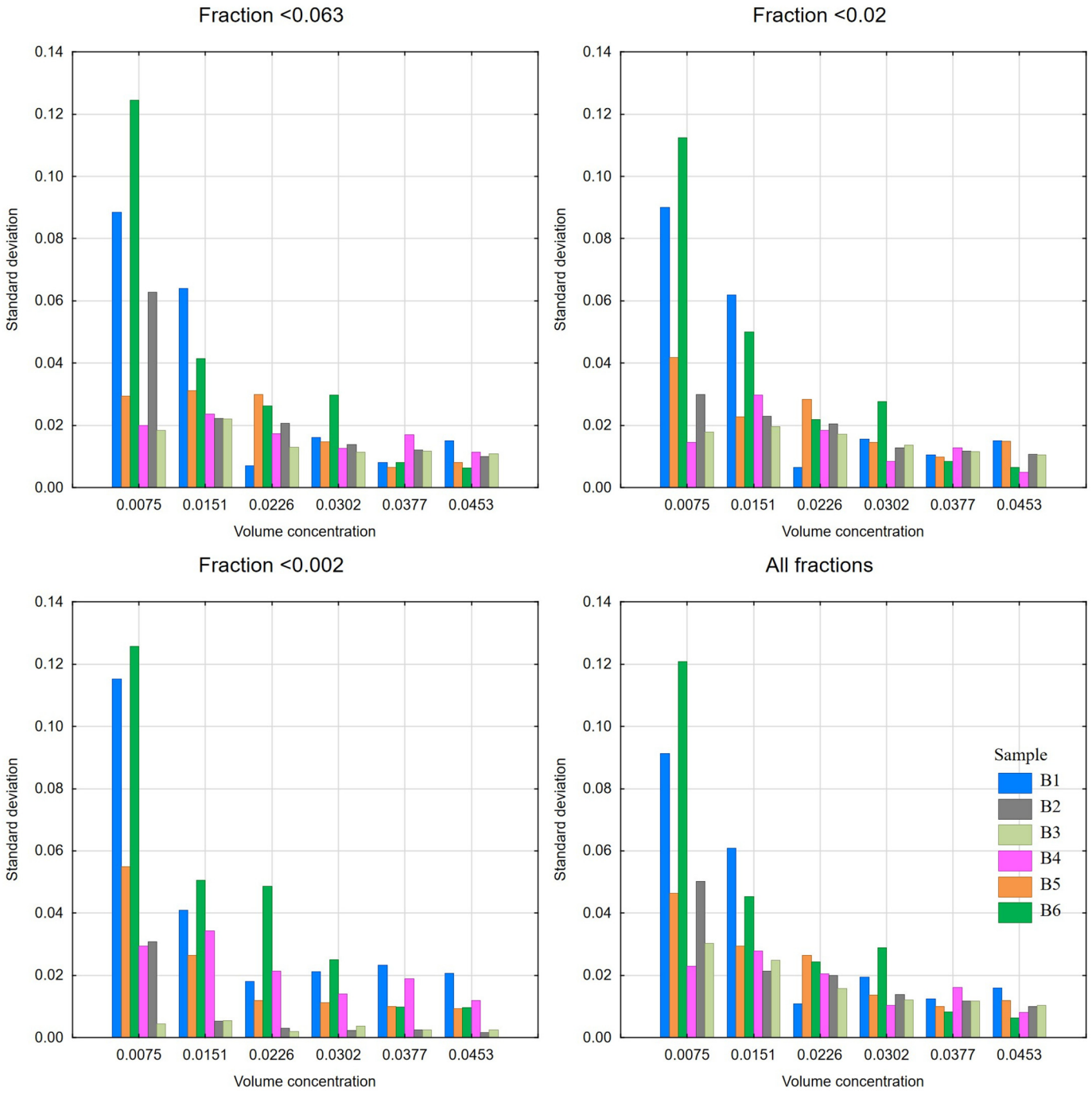

Fig. 2. Comparison of standard deviations for selected fractions.

Table 3
Change of suspension density during measurements depending on the initial concentration.

Soil sample	Change in suspension density during measurements (fractions 0.1–0.002 mm) [g·cm^{-3}]					
	0.0075	0.0151	0.0226	0.0302	0.0377	0.0453
1	2	3	4	5	6	7
B1	1.0103–1.0005	1.0223–1.0015	1.0359–1.0031	1.0480–1.0054	1.0573–1.0057	1.0712–1.0076
B2	1.0089–0.9997	1.0145–1.0021	1.0241–1.0037	1.0331–1.0049	1.0427–1.0069	1.0509–1.0076
B3	1.0084–0.9991	1.0189–0.9996	1.0286–1.0005	1.0373–1.0015	1.0491–1.0024	1.0570–1.0034
B4	1.0066–0.9996	1.0190–1.0029	1.0300–1.0069	1.0421–1.0106	1.0526–1.0126	1.0652–1.0172
B5	1.0071–0.9978	1.0185–0.9980	1.0296–0.9988	1.0407–0.9991	1.0527–1.0003	1.0624–1.0012
B6	1.0116–1.0032	1.0222–1.0087	1.0357–1.0153	1.0461–1.0220	1.0568–1.0277	1.0687–1.0341

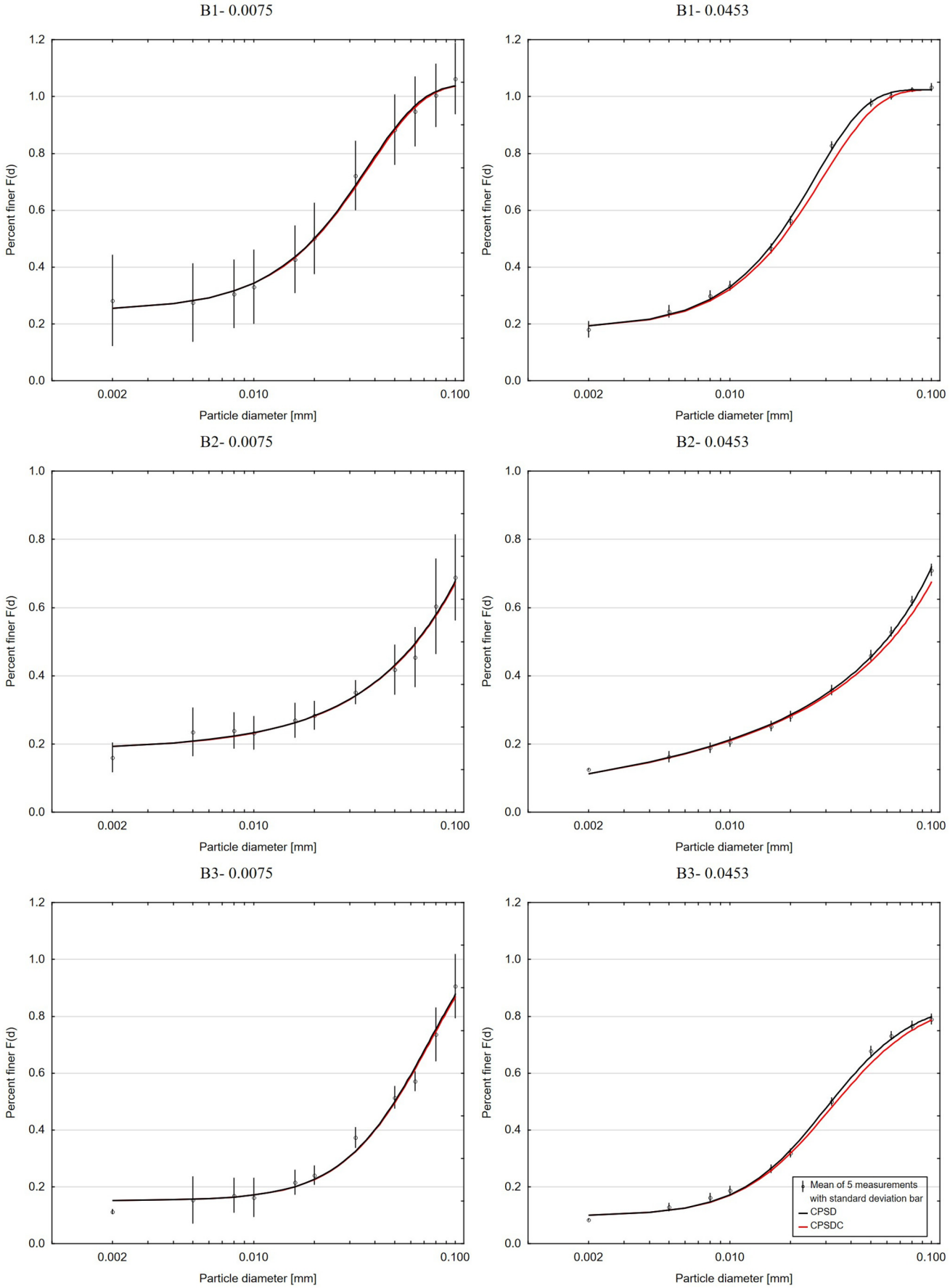

Fig. 3. Cumulative particle size curves for selected soil samples, measured at the lowest and highest applied concentration.

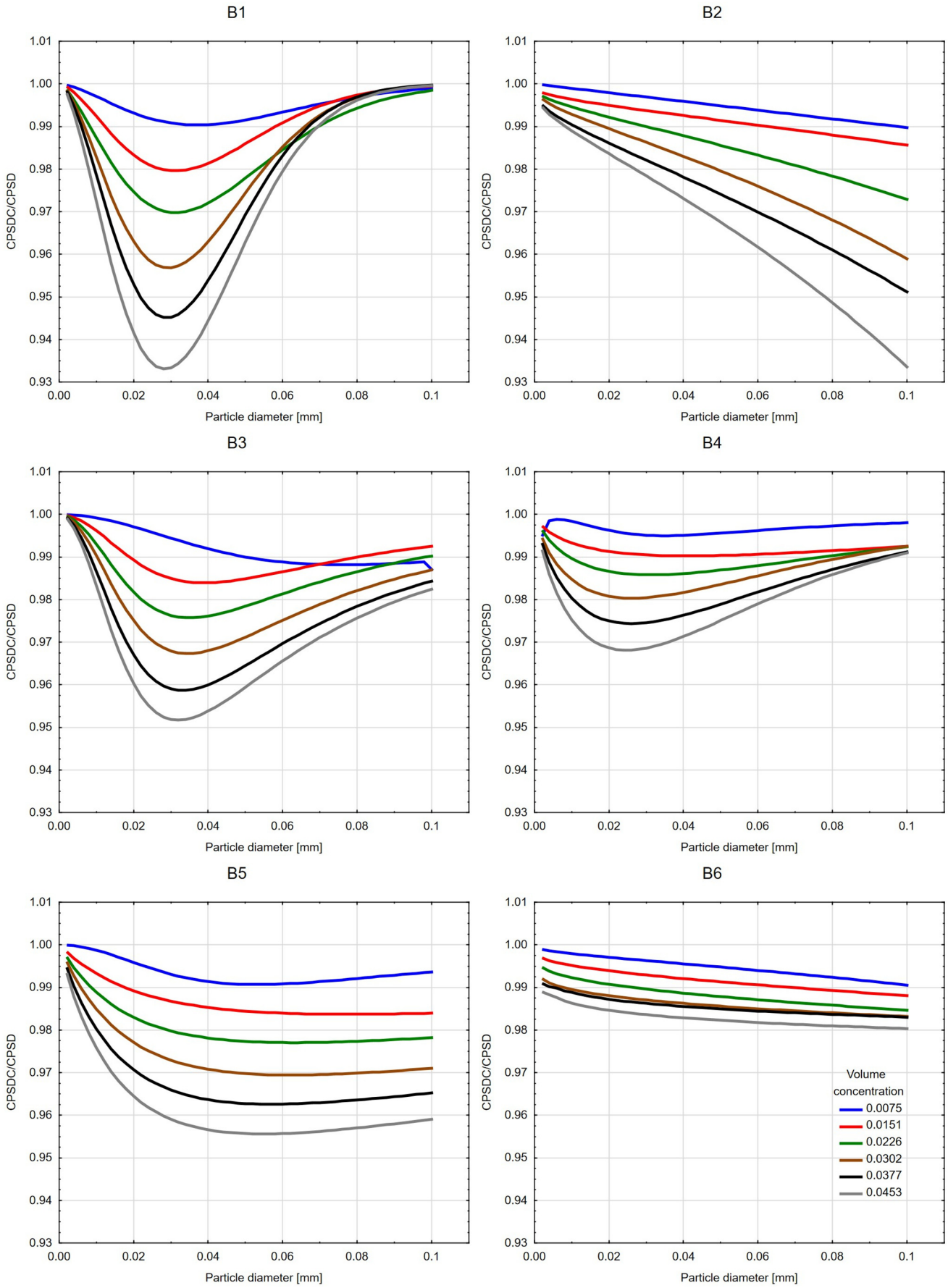

Fig. 4. Ratio of CPSDC/CPSD values as a function of particle diameter, for individual tested samples and concentrations.

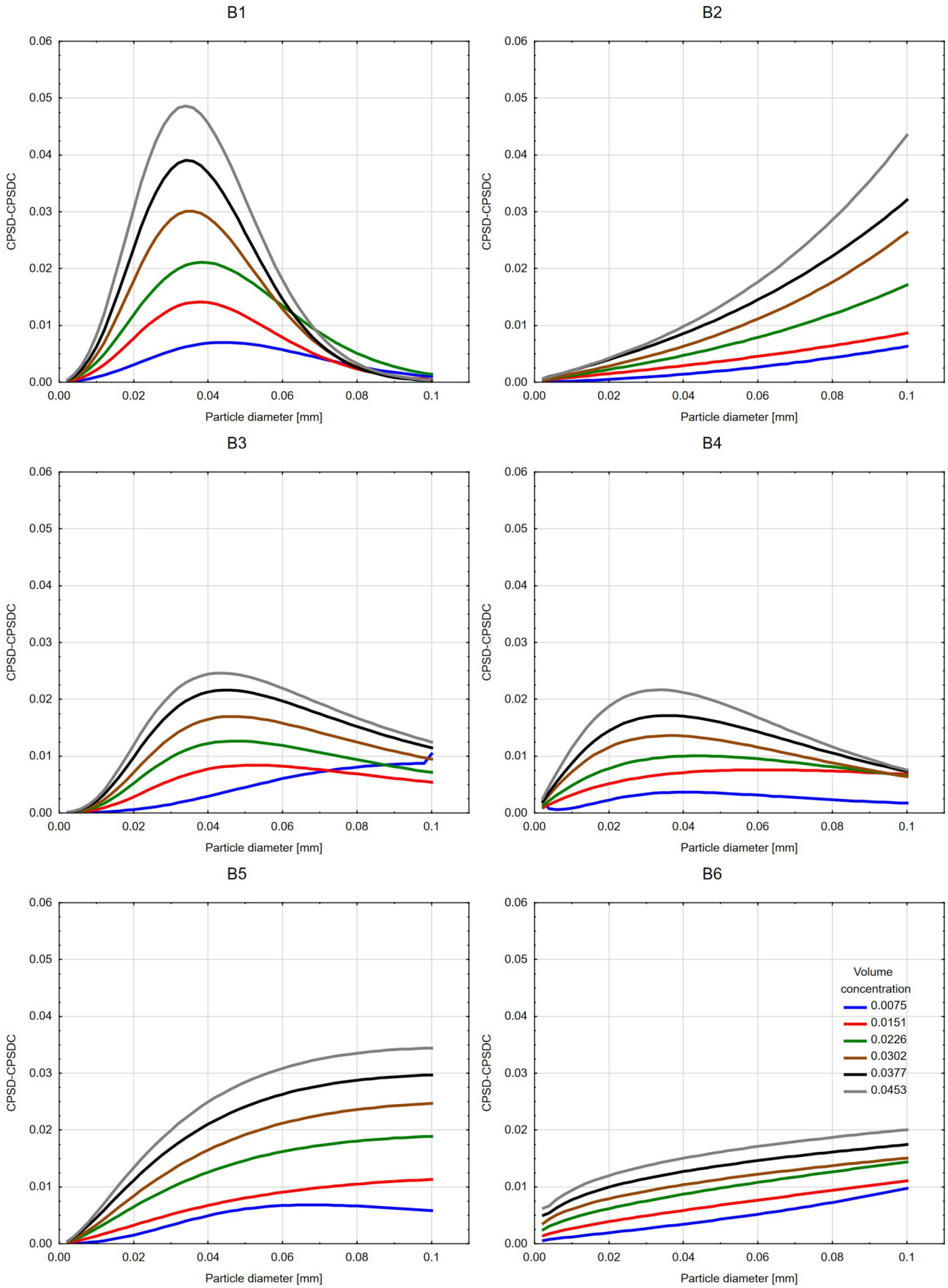

Fig. 5. Difference in CPSD-CPSDC value as a function of particle diameter, for individual tested samples and concentrations.

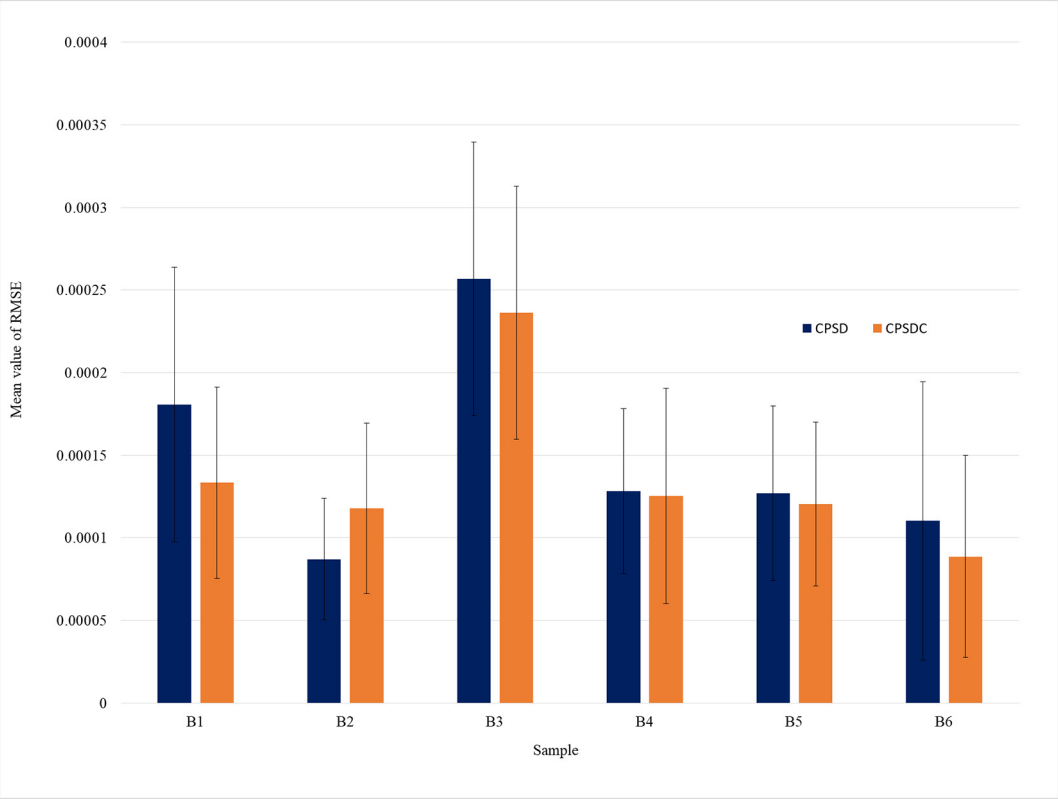

Fig. 6. Mean value of RMSE for the curves with and without correction showed with standard deviation whiskers.

suspension, the results deviate from the others in terms of mode and diameter d_{50}. Also, the curves for the concentration 0.0075 in Figs. 4 and 5 for some samples differ in shape from those obtained for the remaining suspension densities. CPSDC/CPSD and CPSD-CPSDC values for 6 initial concentrations, together with selected characteristics of CPSD and CPSDC curves, are given in Table 4.

The repeatability of the calculation results was tested for 3 selected soils for the suspension concentrations 0.0075, 0.0226 and 0.0453. The convergence of individual CPSDC curves obtained as a result of iterative calculations procedure was assessed. Thus, the curves calculated for 5 individual measurements were compared with the mean values. Correlation coefficients of individual measurements to the mean, mean unbiased standard deviation and mean standard error were adopted as a measures of statistical dispersion. The results are summarized in Table 5.

In all the tested samples, the correlation coefficients were high and exceeded the value of 0.999. The mean unbiased standard deviation and the mean standard error for the mean of the individual CPSDC curves, depended on the initial suspension concentration. For suspensions with the initial concentration of 0.0075, the mean unbiased standard error was 7.58%, while for the suspensions with the initial concentration 0.0226 it did not exceed 1.70%, and for the suspensions with the initial concentration 0.0453 it did not exceed 0.49%. This repeatability of results is related to the larger individual scatter of results for low initial concentrations, not to the properties of the procedure used.

It was expected that the application of the procedure for the correction of the particle settling velocity due to their interactions would result in the particle size curves obtained for the different concentrations being more similar to each other than without its application. This effect was not fully confirmed. Although Mean RMSE value calculated for individual concentrations of suspensions (without 0.0075 concentration with large random errors) in the variant using the correction procedure was smaller than in the variant without the procedure (except for sample B2). The differences were not statistically significant. The results are shown in Fig. 6.

5. Discussion

The results of the conducted research indicate that the correction of the CPSD function related to the application of the procedure described in the Theoretical Basis section is carried out in a different way depending on the examined soil. Both the size of the correction and the range of particle diameters for which the largest correction is observed in the shape of CPSD curves (Figs. 4 and 5, Table 4) are differentiated. Due to the fact that the interactions between sedimentary soil particles always result in a decrease in settling velocity [2,45,46] and therefore, in reality, particles with a certain diameter fall to a given depth over a longer period of time than is indicated by the Stokes equation (CPSDC/CPSD values are always smaller than one), the correction increases (CPSDC/CPSD decreases) with increasing initial suspension concentration. This observation is quite obvious because the increase in the initial concentration of the suspension is manifested by an increase in the coefficient c in eq. (3) and thus by the increase in velocity difference $v^{(3)}(d_i) - v_S(d_i)$. This, in turn, means an increase in the difference in readings of the suspension density $t_i^{(3)} - t_i^{(0)}$ and an increase in the difference in measurements of the suspension density $\rho_z(t_i^{(n)}) - \rho_z(t_i^{(0)})$. The latter therefore causes a greater difference between the calculated values of the CPSD and CPSDC functions.

Another observation is that the highest correction values always occur for particles with dimensions above 0.02 mm, and in the case of 2 out of 6 tested samples for particles with diameters of 0.1 mm. It is important to note that for most of the studied soils, rapid changes in suspension density occur within 10 to 100 s from the beginning of sedimentation. Therefore, even a small change in the measuring time in this range, caused by the application of the proposed procedure,

Table 4
Statistical parameters for individual samples and concentrations.

Parameter	Concentration[a]	Soil sample					
		B1	B2	B3	B4	B5	B6
1	2	3	4	5	6	7	8
d_{50} CPSD[b] ‖ d_{50} CPSDC[b]	0.0075	0.019 ‖ 0.020	0.064 ‖ 0.065	0.050 ‖ 0.050	0.003 ‖ 0.002	0.028 ‖ 0.028	<0.002 ‖ <0.002
	0.0151	0.019 ‖ 0.019	0.056 ‖ 0.057	0.037 ‖ 0.038	0.009 ‖ 0.009	0.026 ‖ 0.027	0.003 ‖ 0.003
	0.0226	0.019 ‖ 0.019	0.055 ‖ 0.057	0.034 ‖ 0.035	0.009 ‖ 0.009	0.026 ‖ 0.027	0.003 ‖ 0.003
	0.0302	0.019 ‖ 0.019	0.058 ‖ 0.060	0.034 ‖ 0.033	0.009 ‖ 0.009	0.028 ‖ 0.029	0.003 ‖ 0.003
	0.0377	0.018 ‖ 0.019	0.054 ‖ 0.056	0.032 ‖ 0.034	0.010 ‖ 0.011	0.026 ‖ 0.028	<0.002 ‖ <0.002
	0.0453	0.017 ‖ 0.018	0.059 ‖ 0.062	0.032 ‖ 0.034	0.009 ‖ 0.010	0.027 ‖ 0.028	<0.002 ‖ <0.002
Distribution mode PSD[c] ‖	0.0075	0.020 ‖ 0.020	0.004 ‖ 0.004	0.044 ‖ 0.044	0.004 ‖ 0.004	0.022 ‖ 0.022	0.002 ‖ 0.002
Distribution mode PSDC[c]	0.0151	0.018 ‖ 0.018	0.004 ‖ 0.004	0.024 ‖ 0.022	0.004 ‖ 0.004	0.004 ‖ 0.004	0.004 ‖ 0.004
	0.0226	0.016 ‖ 0.016	0.004 ‖ 0.004	0.020 ‖ 0.020	0.004 ‖ 0.004	0.004 ‖ 0.004	0.004 ‖ 0.004
	0.0302	0.017 ‖ 0.017	0.004 ‖ 0.004	0.020 ‖ 0.020	0.004 ‖ 0.004	0.004 ‖ 0.004	0.004 ‖ 0.004
	0.0377	0.018 ‖ 0.018	0.004 ‖ 0.004	0.020 ‖ 0.020	0.004 ‖ 0.004	0.004 ‖ 0.004	0.004 ‖ 0.004
	0.0453	0.016 ‖ 0.016	0.004 ‖ 0.004	0.018 ‖ 0.018	0.004 ‖ 0.004	0.004 ‖ 0.004	0.004 ‖ 0.004
Min (CPSDC/CPSD)[d] ‖	0.0075	0.9914 ‖ 0.038	0.9908 ‖ 0.100	0.9894 ‖ 0.077	0.9953 ‖ 0.002	0.9917 ‖ 0.053	0.9915 ‖ 0.100
d for which the minimum has been reached	0.0151	0.9820 ‖ 0.032	0.9871 ‖ 0.100	0.9857 ‖ 0.038	0.9914 ‖ 0.042	0.9841 ‖ 0.072	0.9894 ‖ 0.100
	0.0226	0.9735 ‖ 0.030	0.9758 ‖ 0.100	0.9785 ‖ 0.036	0.9876 ‖ 0.032	0.9791 ‖ 0.063	0.9865 ‖ 0.100
	0.0302	0.9623 ‖ 0.030	0.9634 ‖ 0.100	0.9712 ‖ 0.034	0.9830 ‖ 0.028	0.9731 ‖ 0.061	0.9853 ‖ 0.100
	0.0377	0.9523 ‖ 0.029	0.9567 ‖ 0.100	0.9637 ‖ 0.032	0.9778 ‖ 0.026	0.9673 ‖ 0.056	0.9830 ‖ 0.100
	0.0453	0.9420 ‖ 0.028	0.9411 ‖ 0.100	0.9576 ‖ 0.032	0.9727 ‖ 0.024	0.9613 ‖ 0.054	0.9803 ‖ 0.100
Max (CPSD -CPSDC)[e] ‖	0.0075	0.0069 ‖ 0.045	0.0063 ‖ 0.100	0.0087 ‖ 0.100	0.0036 ‖ 0.040	0.0067 ‖ 0.068	0.0096 ‖ 0.100
d for which the minimum has been reached	0.0151	0.0138 ‖ 0.038	0.0085 ‖ 0.100	0.0083 ‖ 0.052	0.0074 ‖ 0.062	0.0151 ‖ 0.100	0.0109 ‖ 0.100
	0.0226	0.0205 ‖ 0.038	0.0168 ‖ 0.100	0.0124 ‖ 0.048	0.0098 ‖ 0.044	0.0184 ‖ 0.100	0.0140 ‖ 0.100
	0.0302	0.0290 ‖ 0.035	0.0258 ‖ 0.100	0.0165 ‖ 0.046	0.0131 ‖ 0.036	0.0239 ‖ 0.100	0.0146 ‖ 0.100
	0.0377	0.0374 ‖ 0.034	0.0313 ‖ 0.100	0.0210 ‖ 0.044	0.0165 ‖ 0.036	0.0286 ‖ 0.100	0.0175 ‖ 0.100
	0.0453	0.0463 ‖ 0.034	0.0423 ‖ 0.100	0.0238 ‖ 0.044	0.0206 ‖ 0.034	0.0330 ‖ 0.100	0.0201 ‖ 0.100
Range CPSD[f] ‖ Range CPSDC[f]	0.0075	0.782 ‖ 0.781	0.485 ‖ 0.479	0.725 ‖ 0.716	0.543 ‖ 0.544	0.670 ‖ 0.694	0.599 ‖ 0.590
	0.0151	0.808 ‖ 0.807	0.504 ‖ 0.496	0.670 ‖ 0.665	0.647 ‖ 0.641	0.847 ‖ 0.832	0.560 ‖ 0.551
	0.0226	0.848 ‖ 0.847	0.547 ‖ 0.530	0.691 ‖ 0.684	0.610 ‖ 0.605	0.858 ‖ 0.840	0.549 ‖ 0.538
	0.0302	0.825 ‖ 0.825	0.573 ‖ 0.548	0.699 ‖ 0.690	0.621 ‖ 0.616	0.862 ‖ 0.838	0.521 ‖ 0.510
	0.0377	0.809 ‖ 0.809	0.587 ‖ 0.557	0.714 ‖ 0.703	0.630 ‖ 0.624	0.867 ‖ 0.838	0.479 ‖ 0.467
	0.0453	0.830 ‖ 0.830	0.605 ‖ 0.564	0.699 ‖ 0.687	0.633 ‖ 0.628	0.867 ‖ 0.835	0.477 ‖ 0.463

[a] Concentration of suspension as a initial ratio of suspended particles volume to the suspension volume.
[b] Ratio of particle median diameter read of uncorrected and corrected CPSD
[c] Mode of uncorrected and corrected particle size distribution.
[d] Minimum value of the ratio $F^*(d)/F(d)$ for all analysed values of d, when $F^*(d)$ is the CPSDC and $F(d)$ is the CPSD.
[e] Maximum value of the difference $F(d) - F^*(d)$ for all analysed values of d.
[f] Difference between maximum and minimum values of function CPSD - $F_{max}(d) - F_{min}(d)$ and difference between maximum and minimum values of function CPSDC - $F^*_{max}(d) - F^*_{min}(d)$.

results in a significant change in the reading of suspension density. As before, this in turn results in a significant difference between the calculated CPSD and CPSDC values. Soil particles with the smallest diameters (starting their movement from the surface) fall in the most diluted suspension, and therefore their movement is correctly described by the Stokes equation. This means that rapidly falling particles with diameters close to 0.1 mm make the greatest contribution to the formation of return flow that reduces the actual settling velocity of all other particles. [47,48].

In a specific layer of constant density, which falls from the surface of the suspension, there are initially particles with diameters greater than those measured for that layer. These particles, settling at a velocity higher than that of the tested particle, will leave the layer relatively quickly and from that moment on the tested particle will already move in the layer with a constant velocity. The conducted computational experiments allow us to state that for particles with a diameter of 0.016 mm, the density of the layer in which they move is stabilized after about 5 s, and for particles with a diameter of 0.008 mm after about 20 s from the start of sedimentation. At a measuring depth of 120 mm they therefore move for another 1800 s in the constant density layer.

The limit to the application of this calculation procedure is the applicability of the Batchelor equation [30,49]. Its author suggests that it can be used for initial concentrations of $c < 0.05$. However, as results from the presented study shows, the difference between the CPSD and CPSDC curves for the suspension concentration $c \le 0.0151$ is less than

Table 5
Statistical parameters of repeatability of the iterative procedure for selected soils.

Soil sample	B1			B2			B6		
1	2	3	4	5	6	7	8	9	10
Suspension concentration	0.0075	0.0226	0.0453	0.0075	0.0226	0.0453	0.0075	0.0226	0.0453
$\rho(z,t)$ approximation[a]	$\frac{(\alpha+\theta t^{\eta})}{(\kappa^{\eta}+t^{\eta})}$			$\frac{(a+bt)}{(1+ct+dt^2)}$		$\frac{(ab+ct^d)}{(b+t^d)}$	$exp(a+\frac{b}{t}+c\ \ln(t))$	$\frac{(ab+ct^d)}{(b+t^d)}$	
Correlation coefficient[b]	0.9991	0.9996	1.0000	0.9941	0.9997	0.9999	0.9980	0.9985	0.9999
Standard deviation[c]	0.0957	0.0137	0.0109	0.0555	0.0225	0.0105	0.1694	0.0380	0.0057
Standard error[d]	0.0428	0.0061	0.0049	0.0248	0.0101	0.0047	0.0758	0.0170	0.0025

[a] Equation used to approximate the function $\rho = \rho(z, t)$ in the iterative procedure.
[b] Average correlation coefficient of individual measurements in relation to the average of 5 measurements.
[c] Unbiased standard deviation for 5 individual curves, averaged over all (50) points of calculation.
[d] Mean unbiased standard error for 5 individual curves, averaged over all (50) points of calculation.

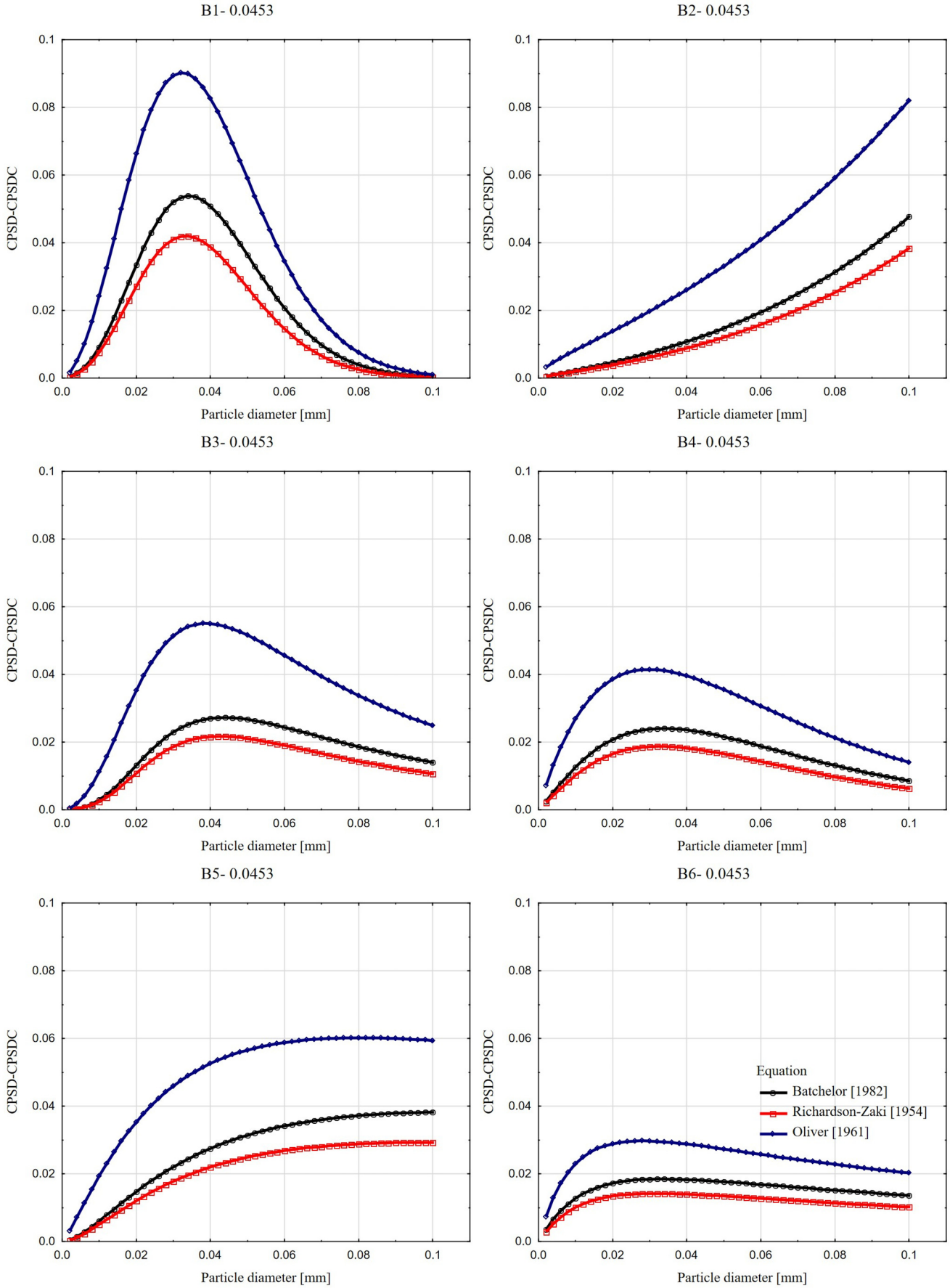

Fig. 7. Differences between the values of CPSD and CPSDC functions calculated on the basis of the Batchelor, Richardson-Zaki and Oliver equations.

1.51%, and the ratio of the content of individual fractions of CPSDC/CPSD does not fall below 0.9820. Also, the results obtained with low initial concentrations of the suspension are characterized by significant random errors. Therefore, it seems that in order to limit random errors occurring during the determination of particle size distribution, it is justified to apply the proposed procedure to suspensions with initial volume concentrations in the range of 0.0302–0.0453.

The Batchelor equation used in this paper [30] is one of several possibly applicable ones. A procedure analogous to that described can be carried out using the Richardson-Zaki Eq. [35]:

$$v = v_S(1-c)^{\vartheta} \tag{13}$$

in which ϑ is a hindered settling exponent. According to Richardson-Zaki, its value for an $Re < 0.2$ is 4.65 while for $0.2 < Re < 1$ this value depends on the Reynolds number and is $4.4 \cdot Re^{-0.03}$. The equation proposed by Oliver (1961) can also be used.

$$v = v_S(1-2.15c)(1-0.75c^{0.33}) \tag{14}$$

It should be remembered that the Batchelor Eq. [30] was proposed for suspensions with low particle size variation [45], and that the Richardson Zaki Eq. [35] is postulated for almost monodispersive suspensions. Applying them to a real soil suspension involves a certain amount of approximation. In the literature, there are also more complex equations that make the hindered settling velocity dependent on the suspension concentration, the Reynolds number, the median particle diameter d_{50}, or a combination of these parameters [34,37,50–52]. However, their use in the proposed model (calculation procedure) is made difficult (albeit possible) by the need to calculate an adjusted velocity for each particle diameter separately.

Fig. 7 shows the differences between the values of CPSD and CPSDC functions calculated on the basis of the 3 mentioned equations for 6 studied samples, for the highest initial concentration used (0.0453). As we can see, the correction obtained in the course of application of the proposed procedure using the Batchelor [30] and Richardson-Zaki [35] formulas is similar and does not exceed the value of 0.055. Oliver Eq. [36], due to the highest reduction of particle hindered settling velocity [53], gives significantly higher values of correction, which reach as much as 0.09 for sample B1. It should be noted that with the remaining (smaller) initial concentrations of the suspension, the correction values are smaller than those presented in Fig. 7.

The aim of the proposed iterative procedure was to take into account the influence of mutual interactions of sedimenting particles on their hindered settling velocity. As can be seen in Figs. 3 and 4, as a result of the procedure, the CPSDC curves (obtained by calculation) are shifted towards larger values of d diameters in relation to the CPSD curves. Thus, the procedure reduces the systematic error resulting from the assumption of too high particle settling speed, while it has a much smaller impact on random errors. These are related to the specificity of measurements, and also with the use of various approximating functions $\rho = \rho(z,t)$ for different initial suspension concentrations (Table 5).

According to the authors, the question of choosing an appropriate equation for correcting the rate of particle drop in relation to the density of the suspension used is still open and should be based on a wider range of experimental material. The choice of a particular equation may depend on the range of fractions to be measured and the initial concentration of the suspension used. The proposed procedure allows for the use of different equations, giving a similar correction of the CPSD curves calculated on the basis of changes in the suspension density. Of course, the problem of particle shape deviation from the spherical and its influence on the settling velocity remains unresolved [54–56]. It was expected that the application of the procedure for the correction of the particle settling velocity due to their interactions would result in the particle size curves obtained for the different concentrations being more similar to each other than without its application. This effect was not fully confirmed. Nevertheless, the variance for the concentration c = 0.0302, 0.0377 and 0.0453 as tested with a paired Student's *t*-test were smaller with the iterative procedure than without it, and the difference was statistically significant at $p = 0.1$ (Fig. 6).

6. Conclusions

The use of suspensions with low volume concentrations in measurement of soil particle size distribution results in significant random errors. The results obtained are characterized by a significant degree of spreading, and obtaining satisfactory results requires observing strict measurement regimes. On the other hand, an increase in the suspension concentration causes mutual interactions of particles to begin having a significant impact on the particle settling velocity, and the use of the Stokes equation to describe the velocity is associated with a significant systematic error.

The iterative calculation method proposed by the authors, using the correction of the settling velocity of particles based on the Batchelor equation, allows the use of suspensions with volume concentration up to 0.0453 in measurements of particle size distribution. At increased suspension concentrations, random errors were reduced. The curves obtained for different concentrations of suspensions had similar shapes. The limitations of the presented method are only due to the scope of applicability of the equation used in the iterative procedure.

CRediT authorship contribution statement

Krzysztof Papuga: Conceptualization, Methodology, Validation, Formal analysis, Investigation, Visualization, Writing - original draft, Writing - review & editing. **Jarosław Kaszubkiewicz**: Conceptualization, Methodology, Supervision, Writing - review & editing. **Dorota Kawałko**: Investigation, Supervision.

Declaration of Competing Interest

The authors declare that they have no known competing financial interests or personal relationships that could have appeared to influence the work reported in this paper.

Acknowledgements

The authors would like to acknowledge the financial support of Wrocław City Hall, municipal programme to support partnerships between higher education and science and the business sector.

References

[1] W.E. Dietrich, Settling velocity of natural particles, Water Resour. Res. 18 (1982) 1615–1626, https://doi.org/10.1029/WR018i006p01615.
[2] S. Dey, S. Zeeshan Ali, E. Padhi, Terminal fall velocity: the legacy of stokes from the perspective of fluvial hydraulics, Proc. R. Soc. A. 475 (2019) 20190277, https://doi.org/10.1098/rspa.2019.0277.
[3] G.F. Coates, C.A. Hulse, A comparison of four methods of size analysis of fine-grained sediments, N. Z. J. Geol. Geophys. 28 (1985) 369–380, https://doi.org/10.1080/00288306.1985.10422234.
[4] L.P. Reeuwijk, Procedures for Soil Analysis, Wageningen FAO ISRIC, 2002.
[5] Y. Yang, L. Wang, O. Wendroth, B. Liu, C. Cheng, T. Huang, Y. Shi, Is the laser diffraction method reliable for soil particle size distribution analysis? Soil Sci. Soc. Am. J. 83 (2019) 276–287, https://doi.org/10.2136/sssaj2018.07.0252.
[6] D. Ashworth, R. Keyes, R. Lessard Kirk, Standard procedure in the hydrometer method for particle size analysis, Commun. Soil Sci. Plant Anal. 32 (2001) 633–642, https://doi.org/10.1081/CSS-100103897.
[7] M. Ryżak, P. Bartmiński, A. Bieganowski, Methods for determination of particle size distribution of mineral soils, Acta Agrophysica 175 (4) (2009) 5–84.
[8] C. Di Stefano, V. Ferro, S. Mirabile, Comparison between grain-size analyses using laser diffraction and sedimentation methods, Biosyst. Eng. 106 (2010) 205–215, https://doi.org/10.1016/j.biosystemseng.2010.03.013.
[9] A.N. Beretta, A.V. Silbermann, L. Paladino, D. Torres, D. Bassahun, R. Musselli, A. García-Lamohte, Soil texture analyses using a hydrometer: modification of the

Bouyoucos method, Cienc. Inv. Agr. 41 (2014) 25–26, https://doi.org/10.4067/S0718-16202014000200013.
[10] P.P. Brown, D.F. Lawler, Sphere drag and settling velocity revisited, J. Environ. Eng. 129 (2003) 222–231, https://doi.org/10.1061/(ASCE)0733-9372(2003)129:3(222).
[11] S. Zhiyao, W. Tingting, X. Fumin, L. Ruijie, A simple formula for predicting settling velocity of sediment particles, Water Sci. Eng. 1 (2008) 37–43, https://doi.org/10.1016/S1674-2370(15)30017-X.
[12] I.N. McCave, J.P.M. Syvitski, Principles and methods of geological particle size analysis, in: J.P.M. Syvitski (Ed.), Principles, Methods and Application of Particle Size Analysis, 1st ed.Cambridge University Press 1991, pp. 3–21, https://doi.org/10.1017/CBO9780511626142.003.
[13] L. David Suits, T. Sheahan, B. Wen, A. Aydin, N. Duzgoren-Aydin, A comparative study of particle size analyses by sieve-hydrometer and laser diffraction methods, Geotech. Test. J. 25 (2002) 10036, https://doi.org/10.1520/GTJ11289J.
[14] J. Quispe, F. Concha, P.G. Toledo, Discrete sedimentation model for ideal suspensions, Chem. Eng. J. 80 (2000) 135–140, https://doi.org/10.1016/S1383-5866(00)00082-4.
[15] T.E. Baldock, M.R. Tomkins, P. Nielsen, M.G. Hughes, Settling velocity of sediments at high concentrations, Coast. Eng. 51 (2004) 91–100, https://doi.org/10.1016/j.coastaleng.2003.12.004.
[16] T. Allen, Powder sampling and particle size measurement, in: T. Allen (Ed.), Particle Size and Measurement, Chapman and Hall, London, UK 1997, pp. 216–219.
[17] R.F. Conley, Some inherent errors in hydrometer sedimentation analysis, Powder Technol. 3 (1969) 102–106, https://doi.org/10.1016/0032-5910(69)80061-6.
[18] J. Kaszubkiewicz, W. Wilczewski, T.J. Novák, P. Woźniczka, K. Faliński, J. Belowski, D. Kawałko, Determination of soil grain size composition by measuring apparent weight of float submerged in suspension, Int. Agrophys. 31 (2017) 61–72, https://doi.org/10.1515/intag-2016-0027.
[19] K. Papuga, J. Kaszubkiewicz, W. Wilczewski, M. Staś, J. Belowski, D. Kawałko, Soil grain size analysis by the dynamometer method – a comparison to the pipette and hydrometer method, Soil Sci. Annu. 69 (2018) 17–27, https://doi.org/10.2478/ssa-2018-0003.
[20] J. Kaszubkiewicz, K. Papuga, D. Kawałko, P. Woźniczka, Particle size analysis by an automated dynamometer method integrated with an x-y sample changer, Measurement. 157 (2020) 107680, https://doi.org/10.1016/j.measurement.2020.107680.
[21] T. Allen, Particle size, shape and distribution, Particle Size Measurement, Springer Netherlands, Dordrecht 1990, pp. 124–191, https://doi.org/10.1007/978-94-009-0417-0_4.
[22] W. Durner, S.C. Iden, G. von Unold, The integral suspension pressure method (ISP) for precise particle-size analysis by gravitational sedimentation: ISP method for particle-size analysis, Water Resour. Res. 53 (2017) 33–48, https://doi.org/10.1002/2016WR019830.
[23] B.V. Balakin, A.C. Hoffmann, P. Kosinski, L.D. Rhyne, Eulerian-Eulerian CFD model for the sedimentation of spherical particles in suspension with high particle concentrations, Eng. Applic. Comput. Fluid Mech. 4 (2010) 116–126, https://doi.org/10.1080/19942060.2010.11015303.
[24] N.-S. Cheng, Effect of concentration on settling velocity of sediment particles, J. Hydraul. Eng. 123 (1997) 728–731, https://doi.org/10.1061/(ASCE)0733-9429(1997)123:8(728).
[25] M. Pavlik, The Dependence of Suspension Viscosity on Particle Size, Shear Rate, and Solvent Viscosity, College of Liberal Arts & Social Sciences Theses and Dissertations 71, 2011 https://via.library.depaul.edu/etd/71 (Accessed 16 September 2020).
[26] M.C. Ruzicka, On buoyancy in dispersion, Chem. Eng. Sci. 61 (2006) 2437–2446, https://doi.org/10.1016/j.ces.2005.11.011.
[27] L. Mazzei, P. Lettieri, A drag force closure for uniformly dispersed fluidized suspensions, Chem. Eng. Sci. 62 (2007) 6129–6142, https://doi.org/10.1016/j.ces.2007.06.028.
[28] G.K. Batchelor, J.T. Green, The determination of the bulk stress in a suspension of spherical particles to order c 2, J. Fluid Mech. 56 (1972) 401, https://doi.org/10.1017/S0022112072002435.
[29] M. Rhodes, Introduction to Particle Technology, John Wiley & Sons, Ltd, Chichester, UK, 2008https://doi.org/10.1002/9780470727102.
[30] G.K. Batchelor, Sedimentation in a dilute polydisperse system of interacting spheres. Part 1. General theory, J. Fluid Mech. 119 (1982) 379–408, https://doi.org/10.1017/S0022112082001402.
[31] G.K. Batchelor, C.-S. Wen, Sedimentation in a dilute polydisperse system of interacting spheres. Part 2. Numerical results, J. Fluid Mech. 124 (1982) 495, https://doi.org/10.1017/S0022112082002602.
[32] M.A. Al-Naafa, M.S. Selim, Sedimentation of monodisperse and bidisperse hard-sphere colloidal suspensions, AICHE J. 38 (1992) 1618–1630, https://doi.org/10.1002/aic.690381012.
[33] R.H. Davis, K.H. Birdsell, Hindered settling of semidilute monodisperse and polydisperse suspensions, AICHE J. 34 (1988) 123–129, https://doi.org/10.1002/aic.690340114.
[34] Z. Ha, S. Liu, Settling velocities of Polydisperse concentrated suspensions, Can. J. Chem. Eng. 80 (2008) 783–790, https://doi.org/10.1002/cjce.5450800501.
[35] J.F. Richardson, W.N. Zaki, Sedimentation and fluidisation: part I, Chem. Eng. Res. Des. 75 (1997) S82–S100, https://doi.org/10.1016/S0263-8762(97)80006-8.
[36] D.R. Oliver, The sedimentation of suspensions of closely-sized spherical particles, Chem. Eng. Sci. 15 (1961) 230–242, https://doi.org/10.1016/0009-2509(61)85026-4.
[37] Ronald J. Gibbs, Martin D. Matthews, The Relationship Between Sphere Size And Settling Velocity, SEPM JSR. Vol. 41, 1971https://doi.org/10.1306/74D721D0-2B21-11D7-8648000102C1865D.
[38] E. Obata, Y. Ohira, M. Ohta, New measurement of particle size distribution by a buoyancy weighing-bar method, Powder Technol. 196 (2009) 163–168, https://doi.org/10.1016/j.powtec.2009.07.015.
[39] M.O.F. Murad, E.J. Jones, B. Minasny, Automated soil particle-size analysis using time of flight distance ranging sensor, Soil Sci. Soc. Am. J. 84 (2020) 690–699, https://doi.org/10.1002/saj2.20053.
[40] A. Nemes, I. Czinkota, G.Y. Czinkota, et al., Outline of an automated system for the quasi-continuous measurement of particle-size distribution, Agrokém. Talajt. 51 (2002) 37–46, https://doi.org/10.1556/agrokem.51.2002.1-2.5.
[41] R. Di Felice, E. Parodi, Wall effects on the sedimentation velocity of suspensions in viscous flow, AICHE J. 42 (1996) 927–931, https://doi.org/10.1002/aic.690420405.
[42] R.H. Davis, H. Gecol, Hindered settling function with no empirical parameters for polydisperse suspensions, AICHE J. 40 (1994) 570–575, https://doi.org/10.1002/aic.690400317.
[43] D. Pal, K. Ghoshal, Hindered settling with an apparent particle diameter concept, Adv. Water Resour. 60 (2013) 178–187, https://doi.org/10.1016/j.advwatres.2013.08.003.
[44] Z. Zhu, H. Wang, D. Peng, J. Dou, Modelling the hindered settling velocity of a falling particle in a particle-fluid mixture by the Tsallis entropy theory, Entropy. 21 (2019) 55, https://doi.org/10.3390/e21010055.
[45] R. Di Felice, The sedimentation velocity of dilute suspensions of nearly monosized spheres, Int. J. Multiphase Flow 25 (1999) 559–574, https://doi.org/10.1016/S0301-9322(98)00084-6.
[46] F. Concha Arcil, Settling velocities of particulate systems, KONA 27 (2009) 18–37, https://doi.org/10.14356/kona.2009006.
[47] P.J.T. Dankers, J.C. Winterwerp, Hindered settling of mud flocs: theory and validation, Cont. Shelf Res. 27 (2007) 1893–1907, https://doi.org/10.1016/j.csr.2007.03.005.
[48] S. Xu, R. Sun, Y. Cai, H. Sun, Study of sedimentation of non-cohesive particles via CFD–DEM simulations, Granul. Matter 20 (2018) 4, https://doi.org/10.1007/s10035-017-0769-7.
[49] R. Silva, F.A.P. Garcia, P.M.G.M. Faia, M.G. Rasteiro, Settling suspensions flow modelling: a review, KONA 32 (2015) 41–56, https://doi.org/10.14356/kona.2015009.
[50] Y.Q. Sha, Introduction to Sediment Dynamics, Industry Press, Beijing, China, 1965.
[51] J. Garside, M.R. Al-Dibouni, Velocity-Voidage relationships for fluidization and sedimentation in solid-liquid systems, Ind. Eng. Chem. Proc. Des. Dev. 16 (1977) 206–214, https://doi.org/10.1021/i260062a008.
[52] N.-S. Cheng, Simplified settling velocity formula for sediment particle, J. Hydraul. Eng. 123 (1997) 149–152, https://doi.org/10.1061/(ASCE)0733-9429(1997)123:2(149).
[53] R. Blazejewski, Apparent viscosity and settling velocity of suspensions of rigid monosized spheres in stokes flow, Int. J. Multiphase Flow 39 (2012) 179–185, https://doi.org/10.1016/j.ijmultiphaseflow.2011.10.006.
[54] M. Jonasz, Nonsphericity of suspended marine particles and its influence on light scattering1: nonsphericity of particles, Limnol. Oceanogr. 32 (1987) 1059–1065, https://doi.org/10.4319/lo.1987.32.5.1059.
[55] J.P. Ahrens, A fall-velocity equation, J. Waterw. Port Coast. Ocean Eng. 126 (2000) 99–102, https://doi.org/10.1061/(ASCE)0733-950X(2000)126:2(99.
[56] J.A. Jiménez, O.S. Madsen, A simple formula to estimate settling velocity of natural sediments, J. Waterw. Port Coast. Ocean Eng. 126 (2003) 70–78, https://doi.org/10.1061/(ASCE)0733-950X(2003)129:2(70).

UNIWERSYTET
PRZYRODNICZY
WE WROCŁAWIU

INSTYTUT NAUK O GLEBIE, ŻYWIENIA ROŚLIN I OCHRONY ŚRODOWISKA

Wrocław 04.04.2022

Mgr inż. Krzysztof Papuga
Instytut Nauk o Glebie, Żywienia Roślin
i Ochrony Środowiska
Uniwersytet Przyrodniczy we Wrocławiu

OŚWIADCZENIE

Oświadczam, że w pracy: Papuga, K., Kaszubkiewicz, J., Kawałko, D., 2021. Do we have to use suspensions with low concentrations in determination of particle size distribution by sedimentation methods? Powder Technology 389, 507–521 (doi: 10.1016/j.powtec.2021.05.060) mój udział polegał na opracowaniu koncepcji, metodologii, wykonaniu analiz laboratoryjnych i obliczeniowych, opracowaniu merytorycznym i graficznym rezultatów analiz oraz przygotowaniu treści manuskryptu.

.....Papuga.....
Podpis

UNIWERSYTET
PRZYRODNICZY
WE WROCŁAWIU

Wrocław 04.04.2022

Prof. Dr hab. Jarosław Kaszubkiewicz
Instytut Nauk o Glebie, Żywienia Roślin
i Ochrony Środowiska
Uniwersytet Przyrodniczy we Wrocławiu

OŚWIADCZENIE

Oświadczam, że w pracy: Papuga, K., Kaszubkiewicz, J., Kawałko, D., 2021. Do we have to use suspensions with low concentrations in determination of particle size distribution by sedimentation methods? Powder Technology 389, 507–521 (doi: 10.1016/j.powtec.2021.05.060) mój udział polegał na opracowaniu nadzorowaniu przy opracowaniu koncepcji, metodologii i doboru analiz laboratoryjnych. Nadzór merytoryczny obejmował także poprawność interpretacji wyników oraz przygotowanie treści manuskryptu.

.....
Podpis

UNIWERSYTET
PRZYRODNICZY
WE WROCŁAWIU

INSTYTUT NAUK O GLEBIE, ŻYWIENIA ROŚLIN I OCHRONY ŚRODOWISKA

Wrocław 04.04.2022

Dr inż. Dorota Kawałko
Instytut Nauk o Glebie, Żywienia Roślin
i Ochrony Środowiska
Uniwersytet Przyrodniczy we Wrocławiu

OŚWIADCZENIE

Oświadczam, że w pracy: Papuga, K., Kaszubkiewicz, J., Kawałko, D., 2021. Do we have to use suspensions with low concentrations in determination of particle size distribution by sedimentation methods? Powder Technology 389, 507–521 (doi: 10.1016/j.powtec.2021.05.060)mój udział polegał na nadzorowaniu przy opracowaniu metodologii, doboru analiz laboratoryjnych oraz przygotowaniu treści manuskryptu.

Dorota Kawałko
.....
Podpis

UNIWERSYTET PRZYRODNICZY WE WROCŁAWIU
INSTYTUT NAUK O GLEBIE, ŻYWIENIA ROŚLIN I OCHRONY ŚRODOWISKA
UL. GRUNWALDZKA 53, 50-357 WROCŁAW
tel. 71 320 56 04
e-mail: igleb@upwr.edu.pl • https://ingos.upwr.edu.pl/

agriculture

MDPI

Article

Effect of Organic Matter Removal by Hydrogen Peroxide on the Determination of Soil Particle Size Distribution Using the Dynamometer Method

Krzysztof Papuga [1,*], Jarosław Kaszubkiewicz [1], Dorota Kawałko [1] and Maria Kreimeyer [2]

[1] Institute of Soil Science and Environment Protection, Wrocław University of Environmental and Life Sciences, 25 Norwida St., 50-375 Wrocław, Poland; jaroslaw.kaszubkiewicz@upwr.edu.pl (J.K.); dorota.kawalko@upwr.edu.pl (D.K.)
[2] Agrolab Agrar und Umwelt GmbH, Breslauer Str. 60, 31157 Sarstedt, Germany; maria.kreimeyer@agrolab.de
* Correspondence: krzysztof.papuga@upwr.edu.pl

Abstract: The dynamometer method of determining particle size distribution was developed several years ago. The principles of sample preparation for this method are based on those used in other sedimentation methods. With improvements in these procedures, an investigation of the effect on obtained particle size distribution results by removing organic matter using hydrogen peroxide was proposed. For this purpose, the particle size distributions were determined in 50 soil samples with varying organic matter content, before and after organic matter removal. A comparative analysis of the results, including calculation of the Euclidean distance, was performed on both groups. It was found that differences in the particle size distributions of the soils after the application of hydrogen peroxide were difficult to predict, and irregular in both magnitude and direction. However, in light soils, the process of organic matter removal caused an increase in the clay fraction at the expense of the silt fraction, which decreased. In soils with a higher initial clay fraction, there were decreases in the clay and sand fractions, while the silt fraction increased.

Keywords: particle size distribution; dynamometer method; grain size analysis; soil organic matter

Citation: Papuga, K.; Kaszubkiewicz, J.; Kawałko, D.; Kreimeyer, M. Effect of Organic Matter Removal by Hydrogen Peroxide on the Determination of Soil Particle Size Distribution Using the Dynamometer Method. *Agriculture* **2022**, *12*, 226. https://doi.org/10.3390/agriculture12020226

Academic Editor: Sara Marinari

Received: 15 January 2022
Accepted: 2 February 2022
Published: 4 February 2022

1. Introduction

The particle size distribution is the most important property of soil. Over the past 100 years, several different sedimentation methods have been developed to determine soil particle size distributions [1,2]. These methods include the pipette, hydrometer, Atterberg and photo-sedimentation methods, and the sedimentation balance and centrifugation. The first two are the most commonly used, with the pipette method being considered to be the reference technique [3–5]. Sedimentation methods use the Stokes equation, which describes the dependence of the falling velocity of a spherical body on its diameter and density in relation to the dynamic viscosity and density of the fluid it is falling through [6–8]. The direct use of Stokes equation in the natural sciences requires certain assumptions to be made that do not fully represent the actual process of particle sedimentation. The Stokes equation concerns the settling of particles in a fluid that fulfil the following conditions: the falling particle has a perfectly spherical shape; the particle falls with uniform motion; the particle is smooth and inelastic; the Reynolds number is <2; the falling particle is not in contact with other particles; and the particle falls in a vessel with a diameter many times the diameter of the particle [9–12]. When using the Stokes equation in the pipette and hydrometer methods, it is assumed that the soil particle fulfils the assumptions described above. Furthermore, at the beginning of any sedimentation experiment, the soil sample suspension is completely homogenised (i.e., all particles are evenly distributed throughout the medium they are suspended in). In addition, it is only possible to determine fractions consisting of particles of measurable size using the pipette and hydrometer methods.

The upper limit is a diameter of 0.1–0.3 mm, as particles with a larger diameter fall off too quickly [13–15]. The smallest diameter of the determinable particles is 0.002 mm, below which free fall is significantly affected by Brownian motion [13,16]. It is also assumed that there is no return flow phenomenon affecting the settling velocity of soil particles [17].

Soil does not only consist of mineral grains, which are the subject of the above considerations on the determination of particle size distributions. Soil also contains soil organic matter (SOM), carbonates, salts, and other organic and inorganic compounds. Therefore, the determination of particle size distributions using sedimentation methods requires the appropriate preparation of the soil samples. For each method, there is a different sample preparation procedure; however, practically each method includes the removal of SOM. This is due to two facts. Firstly, it has a specific density of 1.0–1.5 $g \cdot cm^{-3}$, which significantly differs from the density of the mineral fractions. Secondly, the organic matter causes soil particles to stick together in microaggregates, making full dispersion of the soil sample impossible [18].

Hydrogen peroxide is the most common chemical used to remove SOM, and must be added in appropriate amounts [9,19–21]. Then, excess hydrogen peroxide is removed from the sample by heating until no CO_2 is released or a much lighter coloured suspension is obtained. Heating the sample also allows the organic matter to decompose more intensively. The process of removing organic matter is time-consuming, thus significantly increasing the sample preparation time. The addition of hydrogen peroxide also strongly influences the properties of the tested soil. Inorganic substances are decomposed and new minerals are formed. It increases the content of Al_2O_3 and Fe_2O_3, and affects the particle size distribution of the soil [22–24].

Other methods that use the sedimentation process are currently under development that minimise the disadvantages of the methods developed so far [25,26]. In particular, there is a focus on automating the entire process and minimising human involvement [27–29]. One of the automated sedimentation methods is the dynamometer method, developed several years ago by the authors. The dynamometer method is based on the measurement of changes in the apparent weight of a float immersed in a sediment soil suspension. The apparent weight of the float is measured using a dynamometer, and a cumulative particle size distribution curve is calculated using the Stokes formula. The advantages of the method are strong compliance with the results of the reference sedimentation method, the ability to analyse multiple fractions, recording results in digital form, and shortening the analysis time in relation to other sedimentation methods. Still a disadvantage of the method is the need for manual sample preparation, as in other sedimentation methods. A detailed description of the method is provided in Kaszubkiewicz et al. [30,31] and Papuga et al. [32]. The developed method requires checking the influence of organic matter removal on the obtained results of particle size distribution. Consequently, the authors attempted to determine the extent to which the organic matter removal process affects the results obtained using the dynamometer method. Moreover, it was checked whether the dynamometer method differed from the other sedimentation methods in this respect, and whether the amount of organic matter in soil samples significantly affects the results of the analysis of particle size distribution using the dynamometer method.

2. Materials and Methods

The 50 samples used in this study were taken from the surface horizon (0–30 cm depth) of agriculturally cultivated soils in the Lower Silesian area (Poland). The soils varied in particle size distribution and soil organic carbon (SOC) content. The samples were air-dried, crushed in mortar, and sifted through a 2 mm sieve. Analyses of the following parameters that influence the sedimentation of soil particles were performed: the SOC content (measured by gas chromatography); the calcium carbonate content (analysed using the volumetric method and a Scheibler apparatus); and the pH in 1:1 soil:water mixture by weight of one part to one part distilled water (by potentiometric pH meter).

The particle size distribution in the samples was then determined using the dynamometer method, with and without SOM removal. The soil suspension was prepared according to the dynamometer method described in Kaszubkiewicz et.al. [31]. An aliquot of 60 g of the sieved soil were weighed and transferred to a glass beaker, to which 25 cm^3 of dispersant (sodium hexametaphosphate) and 700 cm^3 of distilled water were added (for samples with the organic matter removed, a weight of >60 g was used, in proportion to the SOC content of each soil sample, in order to obtain 60 g of dry soil after organic matter removal). The contents of the beaker were stirred in a laboratory stirrer for 15 min, and then transferred to a measuring cylinder with a capacity of 1000 cm^3. The suspension was filled to a volume of 1000 cm^3 with distilled water, which was at ambient laboratory temperature. Measurements were taken at a depth of 120 mm. The particle size distribution of the soil samples was determined using the dynamometer method with an automatic sample changer. A detailed description of the method is presented in Kaszubkiewicz et al. [31]. The fractions with equivalent diameters of <0.063, <0.05 and <0.002 mm were measured. The granulometric groups were determined according to the US Department of Agriculture's classification [33].

The results were verified by comparing the <0.063 fraction content obtained by the dynamometer method with the results obtained by the sieve method. The 2.0–0.063 mm fraction was determined by wet sieving over a sieve with a mesh diameter of 0.063 mm. After rinsing, the soil residue on the sieve was dried, weighed and then the <0.063 mm fraction was calculated (the weight of the dried soil remaining on the sieve was subtracted from the individual weight of soil sample). Comparisons were made for all samples, both those with and without organic matter.

The organic matter was removed according to a procedure reported in the literature, appropriately modified to accommodate the soil weights used (which were heavier than those used in other sedimentation methods) [3,10,34]. To the air-dried soil, 50 mL of distilled water was added, and then 50 mL of 30% hydrogen peroxide. After 24 h, another 50 mL of hydrogen peroxide was added. Then, after another 24 h, the samples were transferred to a heating plate where they were heated to 90 °C until the remaining hydrogen peroxide was completely removed (i.e., until there were no gas bubbles in the suspension).

The results were used to determine the magnitude of the differences between the different fractions of samples subjected to SOM removal and those in which the organic matter was retained. For this purpose, a reduced main axis (RMA) analysis is suggested, instead of simple regression when both variables (in this study, the two variables are the contents of a specific fraction in samples with and without SOM) are affected by measurement errors [35,36]. The regression line is determined in such a way that the sum of the areas of right-angled triangles formed between the measurement points and the line (triangle sum of squares (TSS)) is the smallest. Changes in all three fractions (<0.063, <0.05, and <0.002 mm) were also analysed by determining the Euclidean distance between points. Points are the contents of each fraction measured in samples with and without SOM [37]. The distribution of the Euclidean distances, and the selected statistical parameters that characterised them, were determined (mean, median, range, and Pearson correlation coefficient).

3. Results

3.1. pH, Carbonates and Soil Organic Matter Content

The pH values of the analysed samples ranged from 3.4 to 7.2. Only three samples were classed as strongly acidic and six as acidic. The remaining samples were slightly acid (21) and neutral (20). Classification determined according to the US Department of Agriculture's classification [33]. The calcium carbonate content in the investigated soils ranged from 0 to 3.8%. In 24 samples, the calcium carbonate content was below detection level (i.e., less than 0.1%). Moreover, a calcium carbonate content in the range of 0.1 to 1% was found in 19 samples. For the remaining seven samples, this value exceeded 1%. The mean calcium carbonate content for all samples was 0.4%, with the median being only 0.1%.

Based on the results, it was found that there was no need to remove the calcium carbonate before proceeding with analysis of the particle size distribution. The samples differed in their SOC contents, which ranged from 0.88 to 4.5%. Eighteen samples were from soils containing up to 1.4% organic carbon. The organic carbon content in 21 samples ranged from 1.5 to 2.4%. The remaining 11 samples contained more than 2.4% organic carbon. The mean SOC content was 1.9% and the median was 1.6%. Details of these properties are included in Table 1.

Table 1. pH, soil organic carbon (SOC) and calcium carbonate content of the investigated soils.

No. Sample	pH	SOC (%)	$CaCO_3$ (%)	No. Sample	pH	SOC (%)	$CaCO_3$ (%)
1	5.7	4.5	0.0	26	7.0	0.9	0.5
2	6.7	2.8	1.6	27	6.3	3.3	0.2
3	6.6	3.6	0.1	28	4.2	1.6	0.0
4	6.7	3.2	1.7	29	6.6	1.4	0.0
5	7.0	3.1	0.2	30	6.7	1.1	0.2
6	6.3	1.5	0.0	31	6.3	1.5	3.8
7	7.2	1.2	1.2	32	5.6	2.2	0.0
8	6.8	1.7	0.6	33	6.2	0.9	0.0
9	6.2	2.1	0.3	34	4.6	1.6	0.0
10	5.9	1.8	0.1	35	4.5	1.1	0.0
11	6.6	1.9	0.3	36	5.9	1.6	0.0
12	6.2	2.5	0.0	37	7.0	1.4	0.5
13	3.6	1.1	0.0	38	6.6	1.2	0.2
14	5.5	1.0	0.0	39	6.8	2.3	0.4
15	6.7	1.7	0.0	40	4.4	1.7	0.2
16	6.0	2.1	0.0	41	6.0	0.9	0.0
17	6.1	1.5	0.0	42	6.6	1.9	0.0
18	6.4	1.2	0.0	43	6.4	1.4	0.3
19	5.8	1.3	0.0	44	6.7	2.3	1.2
20	6.4	1.4	0.0	45	6.7	2.4	0.2
21	5.4	1.5	0.0	46	5.5	1.5	0.0
22	6.0	1.2	0.2	47	6.2	2.6	0.0
23	6.4	1.2	0.2	48	7.0	2.5	1.9
24	6.3	1.3	0.7	49	7.1	3.5	1.9
25	5.5	1.8	0.0	50	6.9	2.9	0.4

3.2. Particle Size Distribution with and without Soil Organic Matter Removal

Based on determinations of particle size distribution in samples without the SOM removed, the following granulometric groups were distinguished: sandy loam, 18 samples; silt loam, 10; loamy sand, 12; loam, 8; sand, 1; and clay loam, 1. After SOM removal, the classes were: sandy loam, 22 samples; silt loam, 14; loamy sand, 7; loam, 6; and sand, 1. There was no tendency towards a change in category in any particular direction after SOM removal. For example, a sample containing SOM, classed as a clay loam, met the guidelines for loam after removal of the SOM. In four cases, samples that were identified as loam changed the category to silt loam after SOM removal. In five samples, the category changed from loamy sand to sandy loam after removal of the SOM. The classes for each sample are shown in Table 2.

Table 2. Granulometric groups of the investigated soils with SOM and after SOM removal.

No. Sample	Granulometric Group with SOM	Granulometric Group without SOM	No. Sample	Granulometric Group with SOM	Granulometric Group without SOM
13	Sand	Loamy Sand	29	Sandy Loam	Sandy Loam
20	Loamy Sand	Loamy Sand	30	Sandy Loam	Sandy Loam
23	Loamy Sand	Loamy Sand	35	Sandy Loam	Sandy Loam
32	Loamy Sand	Loamy Sand	36	Sandy Loam	Sandy Loam
33	Loamy Sand	Loamy Sand	37	Sandy Loam	Sandy Loam
38	Loamy Sand	Loamy Sand	42	Sandy Loam	Loam
40	Loamy Sand	Loamy Sand	3	Loam	Loam
27	Loamy Sand	Sandy Loam	4	Loam	Loam
28	Loamy Sand	Sandy Loam	25	Loam	Loam
39	Loamy Sand	Sandy Loam	50	Loam	Loam
41	Loamy Sand	Sandy Loam	5	Loam	Silt Loam
15	Loamy Sand	Sandy Loam	8	Loam	Silt Loam
34	Loamy Sand	Sand	9	Loam	Silt Loam
1	Sandy Loam	Sandy Loam	31	Loam	Silt Loam
6	Sandy Loam	Sandy Loam	7	Silt Loam	Silt Loam
10	Sandy Loam	Sandy Loam	17	Silt Loam	Silt Loam
11	Sandy Loam	Sandy Loam	18	Silt Loam	Silt Loam
12	Sandy Loam	Sandy Loam	43	Silt Loam	Silt Loam
14	Sandy Loam	Sandy Loam	44	Silt Loam	Silt Loam
16	Sandy Loam	Sandy Loam	45	Silt Loam	Silt Loam
19	Sandy Loam	Sandy Loam	46	Silt Loam	Silt Loam
21	Sandy Loam	Sandy Loam	47	Silt Loam	Silt Loam
22	Sandy Loam	Sandy Loam	48	Silt Loam	Silt Loam
24	Sandy Loam	Sandy Loam	49	Silt Loam	Silt Loam
26	Sandy Loam	Sandy Loam	2	Clay Loam	Loam

The clay fraction (<0.002 mm) in all the samples with SOM ranged from 0.8 to 27.3%, the mean content being 11.1%, and the median 9.4%. After SOM removal, the range in clay content was from 4.6 to 24.3%, while the mean content (11.6%) changed minimally, and the median increased to 11.4%.

For the silt (0.05–0.002 mm) and sand (2–0.05 mm) fractions, the range was much greater. The silt fraction in all the samples with SOM ranged from 2.1 to 63.2%, the mean content being 31.7%, and the median 28.9%. After SOM removal, the range in silt content was from 5.3% to 65.0%, while the mean silt content (33.5%) was almost identical. The median increased to 30.7%.

The sand fraction in all the samples with SOM ranged from 22.0 to 89.5%, the mean content being 57.2%, and the median 58.1%. After SOM removal, the range in sand content was from 18.9 to 89.2%, while the mean content (54.8%) decreased, and the median decreased to 57.7%. The three fractions in the different samples are shown in Table 3.

Table 3. Content of the three fractions in the samples with SOM, and after SOM removal.

No. Sample	Sand Content (%)	Silt Content (%)	Clay Content (%)	Sand Content (%)	Silt Content (%)	Clay Content (%)
	Samples with SOM			Samples after SOM Removal		
1	52.5	29.3	18.2	53.1	31.2	15.7
2	35.8	36.9	27.3	31.7	44.0	24.3
3	43.0	38.3	18.7	36.1	48.2	15.7
4	46.0	37.2	16.8	35.4	41.8	22.8
5	36.0	45.6	18.4	31.5	53.1	15.4
6	61.0	27.1	11.9	59.7	30.1	10.2
7	22.0	59.2	18.8	19.0	65.0	16.0
8	40.0	46.4	13.6	36.9	50.1	13.0
9	35.0	49.2	15.8	30.8	54.4	14.8
10	62.0	25.7	12.3	63.7	26.5	9.8
11	56.0	29.5	14.5	61.0	24.8	14.2
12	73.5	12.8	13.7	64.9	26.6	8.5
13	89.5	2.1	8.4	85.9	8.3	5.8
14	59.5	24.7	15.8	55.5	31.2	13.3
15	78.7	13.2	8.1	76.4	16.0	7.6
16	67.5	24.1	8.4	67.3	26.5	6.2
17	24.4	63.2	12.4	21.7	63.8	14.5
18	34.6	51.4	14.0	34.3	51.2	14.5
19	63.2	26.9	9.9	60.2	28.3	11.5
20	82.4	10.6	7.0	81.7	12.1	6.2
21	65.8	28.5	5.7	66.2	25.9	7.9
22	67.9	25.1	7.0	68.1	25.8	6.1
23	79.7	12.5	7.8	82.6	10.4	7.0
24	71.1	20.7	8.2	67.9	25.0	7.1
25	51.4	40.3	8.3	48.0	42.5	9.5
26	73.5	14.4	12.1	73.4	18.6	8.0
27	84.6	9.0	6.4	79.6	9.0	11.4
28	79.9	11.3	8.8	75.4	10.0	14.6
29	56.6	35.7	7.7	53.4	39.2	7.4
30	53.7	32.6	13.7	55.7	32.9	11.4
31	43.5	48.1	8.4	36.0	58.4	5.6
32	79.9	13.4	6.7	85.0	9.7	5.3
33	79.1	14.3	6.6	83.6	10.2	6.2
34	84.3	8.7	7.0	89.2	5.3	5.5
35	73.9	21.7	4.4	71.9	17.9	10.2
36	55.5	42.2	2.3	53.9	36.7	9.4
37	70.9	25.4	3.7	66.7	28.7	4.6
38	84.9	14.3	0.8	83.5	11.9	4.6
39	76.2	21.3	2.5	77.3	15.0	7.7
40	84.4	14.6	1.0	82.2	11.5	6.3
41	80.3	12.1	7.6	80.3	8.3	11.4
42	51.5	42.0	6.5	47.1	39.3	13.6
43	40.2	51.0	8.8	37.2	50.1	12.7
44	37.0	52.7	10.3	29.7	53.0	17.3
45	26.7	57.7	15.6	18.9	58.4	22.7
46	26.3	56.7	17.0	20.3	63.8	15.9
47	25.9	54.5	19.6	27.3	53.8	18.9
48	27.2	50.4	22.4	20.5	59.4	20.1
49	31.5	52.1	16.4	20.5	63.4	16.1
50	35.8	47.1	17.1	32.9	49.4	17.7

3.3. Differences in the Particle Size Distributions in Samples with and without SOM

Of the 50 samples tested, the granulometric categories of 13 samples after SOM removal were changed. In 11 of these, there was a decrease in sand content after SOM removal. Only in one sample was there an increase in the sand fraction, with a simultaneous

decrease in the silt and clay fractions. In one sample, the sand fraction increased, whilst the clay fraction also increased. These re-categorised samples were characterised by at least one fraction being close to the category limit for a particular granulometric group.

The effect of SOM removal on the different fractions showed that the mean sand fraction in the different samples decreased as a result of the SOM removal process by −2.41 percentage points (pps) (minimum −11.0 pps, maximum 5.1 pps). At the same time, the mean silt fraction increased by 1.86 pps (minimum −6.3 pps, maximum 13.8 pps), and the mean clay fraction increased by 0.56 pps (minimum −5.2 pps, maximum 7.1 pps). However, when considering the changes relative to the initial fraction (in samples with SOM) for each sample, the relative changes were much greater for the clay fraction. The mean difference in the clay fraction of different samples was as high as 36.5% (minimum −38.0%, maximum 530.0%). This is due to the fact that the finest fraction was the least abundant, so every 1 pp difference translated into a large relative difference. For the silt fraction, this value was 9.6% (minimum −39.0%, maximum 295.0%). Such a large maximum difference occurred in sample 13, which contained only 2.1% silt in the variant with SOM. For sand, this value was −6.3% (minimum −34.9%, maximum 8.9%). The average sand and silt fractions were much more abundant than the clay fractions.

The change (value after SOM removal—value before SOM removal) in the sand fraction as a result of SOM removal was positively correlated with its initial content and negatively correlated with the initial contents of silt and clay. These correlations were statistically significant at $p < 0.05$. The change in silt content was, in turn, negatively correlated with the initial sand content and positively correlated with the initial silt and clay contents. These correlations were statistically significant at $p < 0.05$. For the change in silt content and initial clay content, the correlation coefficient was 0.6029 and the linear regression equation had the form $y = 0.4860x - 3.5305$ (increasing trend). Furthermore, the change in clay content due to SOM removal was negatively correlated with initial clay content. These correlations were statistically significant at $p < 0.05$. The correlation coefficient for these two quantities was 0.4717, and the linear regression equation had the form $y = -0.2778x + 3.6368$ (decreasing trend). Thus, in light soils (sandy, containing <10% clay fraction), the process of SOM removal caused an increase in the clay fraction at the same time as a decrease in the silt fraction. On the other hand, in soils with a higher initial clay fraction (medium and heavy soils, containing >10% clay), the SOM removal process caused a decrease in the clay and sandy fractions, while the silt fraction increased (Figure 1). A correlation between changes in the three fractions as a result of SOM removal and the initial SOC content of the soil samples was also tested. It was found that there was a negative, statistically significant correlation for the sand fraction ($r = -0.3718$, $p = 0.008$) and a positive correlation for the silt fraction ($r = 0.3171$, $p = 0.025$).

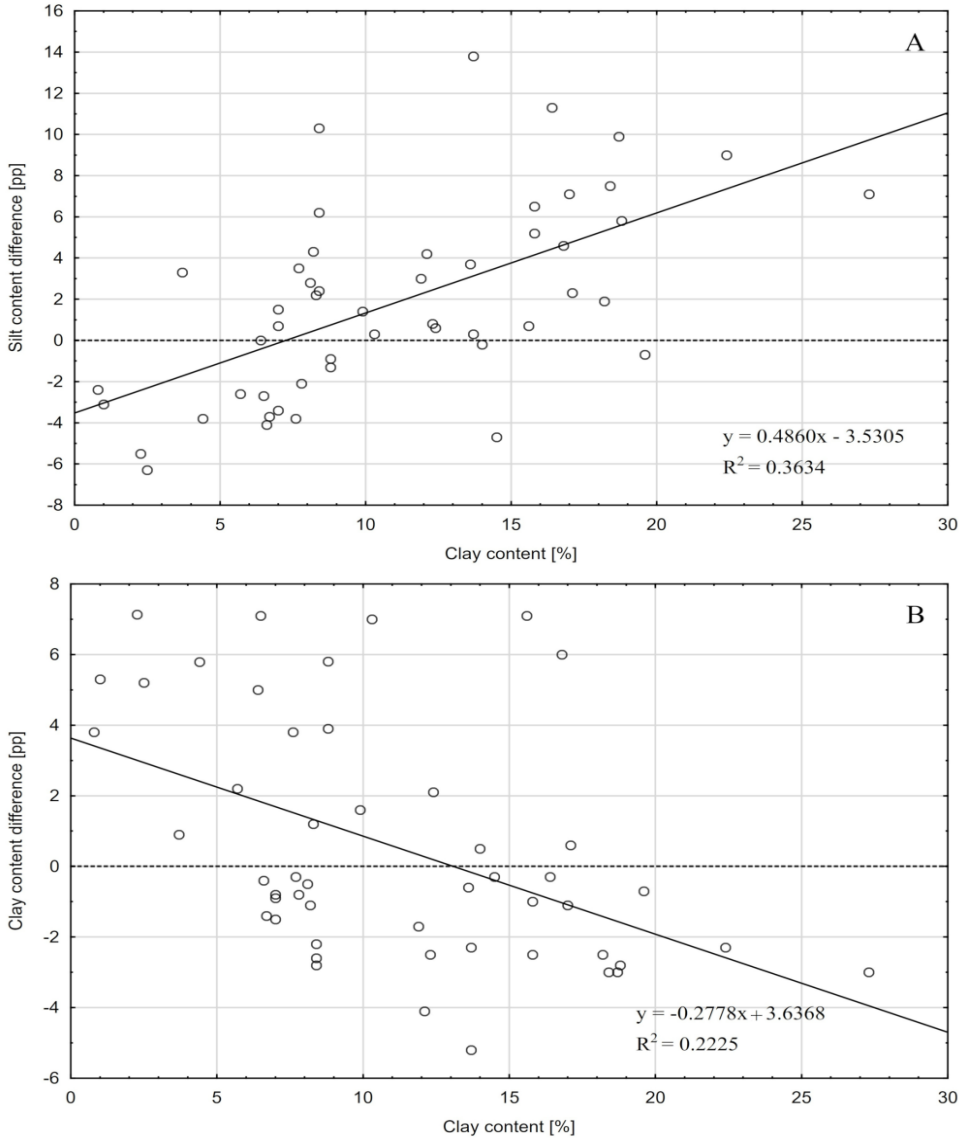

Figure 1. Difference in the silt (**A**) and clay (**B**) fractions between samples with SOM and after SOM removal relative to the clay fraction in the different soils.

The Euclidean distance was used to provide an overall assessment of the influence of the SOM removal process on the results of the dynamometer method. In this study, the distance was between points in a three-dimensional space describing the particle size distribution through three parameters (the sand, silt, and clay fractions). The points represented the differences between these fractions in samples with and without SOM. The Euclidean distance thus calculated for the 50 samples ranged from 0.6 to 17.1%, with a mean value of 6.6% and a standard deviation of 3.6%. The Euclidean distance between the means of the different fractions calculated before and after SOM removal was also determined, and found to be 3.1%, with the ratio of the two values being 2.13 (2.13 = 6.6%/3.1%). Thus, it can be concluded that, while the individual sample results sometimes changed significantly during the SOM removal process, the change in the means of the different fractions was much smaller. In other words, the changes in the different fractions were irregular and did not show an overall trend. The Euclidean distance was found to be correlated with the organic matter content of the samples. These correlations were statistically significant (r = 0.3998 and p = 0.004) (Figure 2).

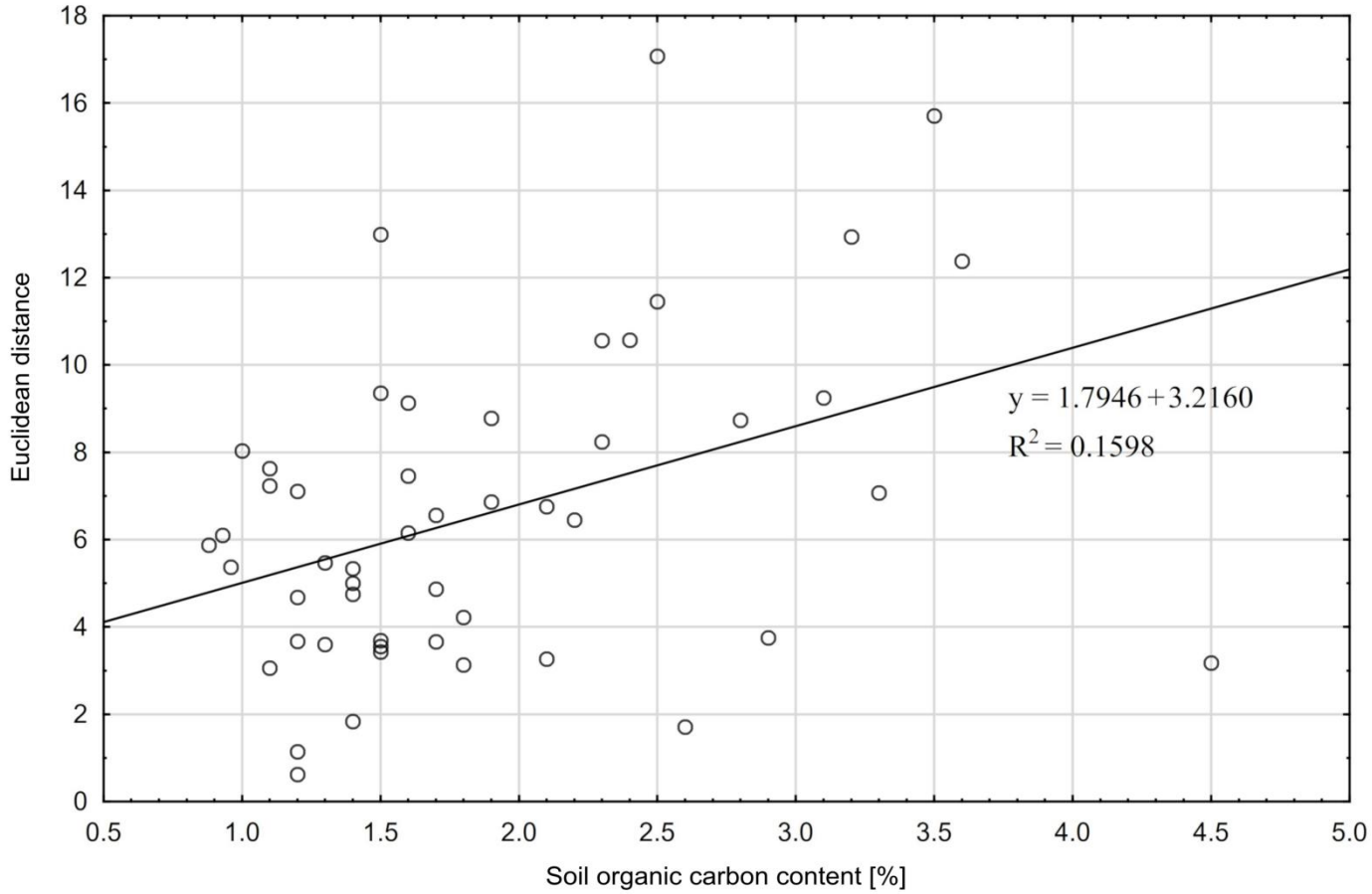

Figure 2. Euclidean distance between the points representing particle size distribution with SOM and after SOM removal, relative to initial soil organic carbon content.

3.4. Fractions <0.063 mm Obtained by the Dynamometer and Sieve Methods

To control the quality of the results of the particle size analysis using the dynamometer method, a comparison was made between data from the <0.063 mm fraction determined by dynamometer and those of the same fraction determined by wet sieving. For samples with SOM, the fraction determined using both methods correlated at r = 0.9954, and the trend line for their mutual relation had the form $y = 0.9324x + 1.8313$ (where x is the <0.063 fraction measured by wet sieving, and y is the same fraction measured by dynamometer. A similar correlation was occurred for the two methods after SOM removal, with r = 0.9938 and the trend line being $y = 0.9512x + 1.1197$ (Figure 3).

Using this regression model [35,36], for the samples with SOM, the equation $y = 0.9367x + 1.6203$ was obtained (determinations as above), and the TSS value was 111.6. The average for one measurement was 2.232. For the samples after SOM removal, the regression line determined by the RMA method was described by the equation $y = 0.9571x - 1.4117$, and the TSS value was 158.7. The average TSS for one measurement was 3.175. In both cases, agreement between the sieve and dynamometer determinations was high, with similar values, and only slightly affected by the SOM removal process.

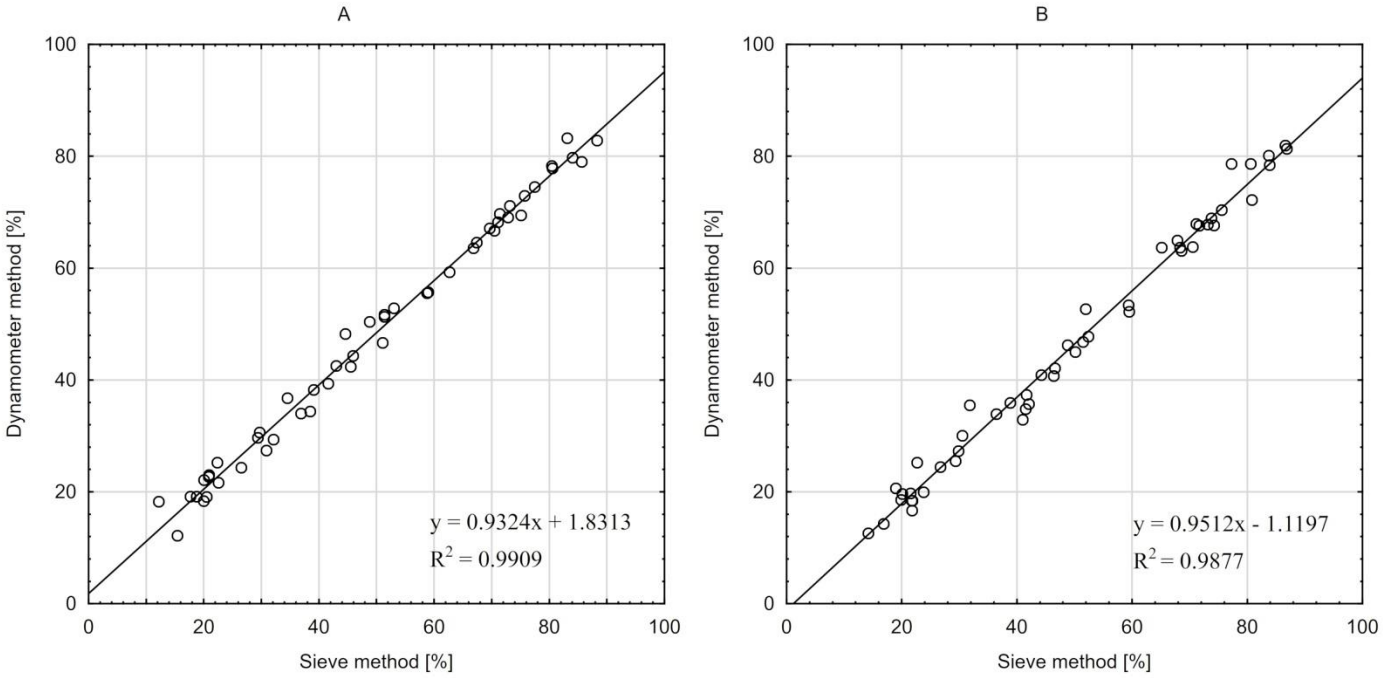

Figure 3. Comparison between the <0.063 mm fractions determined by the dynamometer and sieve methods for all samples: with SOM (**A**), and after SOM removal (**B**).

4. Discussion

When considering SOM, in terms of its influence on the results of the sedimentary analysis of particle size distribution, it is important to note that it occurs in particulate organic matter (POM) and mineral-associated organic matter (MAOM) forms. Additionally, dissolved organic matter is present, but its proportion is small in relation to total organic matter [38]. MAOM and POM differ in density and particle size. MAOM is associated with silt and clay fractions and its particles are smaller than 0.057 mm. POM is composed of organic matter particles with sizes in the range 0.0057–2.0 mm and is not bound in microaggregates [39–41]. These differ in their properties, including in their influence on the results of particle size analysis by sedimentation methods [42]. The different properties of these fractions strongly complicate the effect of SOM removal on the results of soil particle size distribution using sedimentation methods. The authors consider that the changes in the different fractions resulting from SOM removal were caused by two factors.

The first factor is the mineralisation of organic matter with the removal of its decomposition products. In the measurement process of samples containing SOM, its particles were determined as mineral grains. Their lower density value caused the organic particles and organic-mineral complexes to fall with velocities lower than their equivalent diameters would suggest. Therefore, they were interpreted as small particles, while in reality, they are particles with larger diameters. The results of the tests only partially confirmed this observation because, although the average sum of the <0.063 mm fractions measured by dynamometer method and the >0.063 mm fractions measured by sieving was higher for samples with SOM (98.51%) than for those after SOM removal (96.33%), both indicated numbers below 100%.

The Stokes [43] equation shows that particles with densities ρ_{s1} and ρ_{s2} have equal falling velocities when their diameters, D_1 and D_2, satisfy the equation:

$$\frac{D_1}{D_2} = \sqrt{\frac{(\rho_{s2} - \rho_w)}{(\rho_{s1} - \rho_w)}} \quad (1)$$

where ρ_w is the water density.

Therefore, SOM particles with diameters slightly larger than 0.063 mm are shown as <0.063 mm in the sedimentation analysis and simultaneously as >0.063 mm in the sieve analysis. As a result, the sum of the <0.063 mm fraction measured by sedimentation dynamometer and the >0.063 mm fraction measured by sieve analysis should be greater than 100%. However, this is not confirmed by the results obtained. Two explanations are possible. The first is that SOM particles are generally smaller in diameter than 0.063 mm, so they would appear only once during the analysis. This is consistent with data from the literature. Barthès et al. [44] reported that SOM particle diameters are mostly smaller than 0.02 mm. A second explanation is that the dynamometer method underestimated the fractions. It is highly likely that both effects might occur simultaneously, and the absence of SOM particles with dimensions not much larger than 0.063 mm.

The second factor is the effect of the SOM removal process on the mineral particles associated with organic matter. SOM particles are found in soil in a form associated with different granulometric fractions which affects the interpretation of their equivalent diameters in sedimentation measurements [45]. Some SOM (especially that which is less than 6 years of age) may be responsible for the ability of soil particles and aggregates to stick together [46]. The simple peptisation process does not significantly affect their stability. The process of SOM oxidation using H_2O_2 can break it down, causing the mineral particles (actually aggregates) to break down into smaller fragments, thus changing the sedimentation velocity of the associated mineral particles [47]. Organic-mineral complexes containing MAOM have a lower average density than mineral soil particles. Mineralisation of their organic fraction causes an increase in density, and thus an increase in sedimentation velocity in aqueous suspension. Such particles can therefore be interpreted in the sedimentation analysis as being larger than they originally were, despite the loss of some mass. The results of the sedimentation analysis may also have been influenced by the heating of the suspension and the contact time with the aqueous peptiser solution, which was longer than in the samples from which SOM was not removed. The preparation of the samples may not have disintegrated all the aggregates, which disintegrated later in the organic matter removal process. Moreover, the interpretation of results may be hindered by the shape of clay grains, which may significantly deviate from the spherical shape (which is one of the conditions for the application of the Stokes equation). Despite the existence of a modified Stokes equation [12], the currently used algorithms of the dynamometer method do not contain equations correcting the deviation of clay particles from the spherical shape.

Removal of the SOM therefore resulted in a relative increase in the mineral fractions and a decrease in the content of grains with dimensions corresponding to the diameters of substitute grains of POM and MAOM. The results of these processes are complex, depending not only on the SOM content, but also on the diameters of its substitute grains, their association with different mineral fractions, and the particle size distribution of the mineral fractions. Obviously, this effect should have had a decreasing significance as the initial SOM content decreased. Beuselinck et al. [48] found that the process of SOC removal from samples containing <1% SOC (SOC equivalent to 1.7% SOM) did not significantly affect the results of their study; the results of the present study at least partly support that finding. In samples containing up to 0.9% SOC, the application of hydrogen peroxide did not affect the results of the particle size distribution analysis. An even higher value was reported by Jensen et al. [49], who concluded that the organic carbon limit above which organic matter should be removed was 2%. They also found that, above this content, there was a large increase in the underestimation of the silt and clay fractions in samples that the organic matter had not been removed from. Similar conclusions were reached by Hereter et al. [50]. SOM should be removed if the SOM content is greater than 2% and the sample has a <0.002 mm fraction greater than 25%. Such sample properties result in an underestimation of the clay fraction in samples that have not been pre-treated. However, our results did not confirm this observation. On the other hand, Zimmermann and Horn [24] reported significant differences in the different fractions in their study, with the removal of SOM causing an increase in the clay fraction and a decrease in the silt and sand fractions.

5. Conclusions

Changes in the particle size distribution of soils due to the removal of SOM using 30% hydrogen peroxide were irregular in both magnitude and direction. Only in light soils (containing an initial <10% clay fraction) was it found that the SOM removal process caused an increase in the clay fraction and a decrease in the silt fraction. In soils with a higher initial clay fraction (>10%), the SOM removal process caused a decrease in the clay and sand fractions, with a simultaneous increase in the silt fraction.

It was observed that there was a negative, statistically significant correlation between the initial SOM content and the change in the sand fraction, and a positive correlation between the initial SOM content and the change in the silt fraction. This suggests that the SOM particles in the soil had diameters smaller than 0.063 mm in most cases.

The mechanisms responsible for changes in the particle size distributions resulting from the removal of SOM are complex, with their orientation resulting from the SOM content and properties, and the nature of the links between SOM and the soil mineral fraction. Potentially important influences on the results may include the breakdown of microaggregates bound by young SOM, a change in the average density of mineral organic particles in the mineralisation of their organic parts, or a relative increase in some soil fractions. All this indicates that, in soils with different origins, compositions and content of different types of organic matter, the effect of SOM removal may be difficult to predict. Therefore, there was no rationale for removing SOM in samples containing less than 2% SOM. The effect of organic matter removal on the results obtained by the dynamometer method is consistent with that presented in work on other sedimentation methods.

Author Contributions: Conceptualization, K.P. and J.K.; methodology, K.P. and J.K.; validation, K.P. and J.K.; formal analysis, K.P.; investigation, K.P. and M.K.; resources, K.P.; data curation, J.K.; writing—original draft preparation, K.P.; writing—review and editing, K.P. and J.K.; visualization, K.P.; supervision, J.K. and D.K.; project administration, J.K. All authors have read and agreed to the published version of the manuscript.

Funding: This research received no external funding.

Institutional Review Board Statement: Not applicable.

Informed Consent Statement: Not applicable.

Data Availability Statement: Not applicable.

Acknowledgments: We would like to thank Michał Staś for valuable assistance in the data collection. The APC is co-financed by Wroclaw University of Environmental and Life Sciences.

Conflicts of Interest: The authors declare no conflict of interest. The funders had no role in the design of the study; in the collection, analyses, or interpretation of data; in the writing of the manuscript, or in the decision to publish the results.

References

1. Ryżak, M.; Walczak, R.T.; Niewczas, J. Comparison of particle size distribution in soils from laser diffraction and sedimentation methods. *Acta Agrophys.* **2004**, *4*, 509–518.
2. Dipova, N. Determining the grain size distribution of granular soils using image analysis. *Acta Geotech. Slov.* **2017**, *1*, 29–37.
3. Ryżak, M.; Bartmiński, P.; Bieganowski, A. Methods for determination of particle size distribution of mineral soils. *Acta Agrophys.* **2009**, *175*, 5–84.
4. Taubner, H.; Roth, B.; Tippkötter, R. Determination of Soil Texture: Comparison of the Sedimentation Method and the Laser-Diffraction Analysis. *J. Plant Nutr. Soil Sci.* **2009**, *172*, 161–171. [CrossRef]
5. Elfaki, J.T.; Gafer, M.A.; Sulieman, M.M.; Ali, M.E. Hydrometer method against pipette method for estimating soil particle size distribution in some soil types selected from Central Sudan. *Int. J. Eng. Res.* **2016**, *2*, 25–41.
6. McCave, I.N.; Syvitski, J.P.M. Principles and Methods of Geological Particle Size Analysis. In *Principles, Methods and Application of Particle Size Analysis*; Syvitski, J.P.M., Ed.; Cambridge University Press: Cambridge, UK, 1991; pp. 3–21. ISBN 978-0-521-36472-0.
7. Buchan, G.; Grewal, K.; Claydon, J.; Mcpherson, R. A Comparison of Sedigraph and Pipette Methods for Soil Particle-Size Analysis. *Soil Res.* **1993**, *31*, 407. [CrossRef]
8. Stokes, G.G. *Mathematical and Physical Papers*; Cambridge University Press: Cambridge, UK, 2009; ISBN 978-0-511-70226-6.

9. McKenzie, N.; Coughlan, K.; Cresswell, H. *Soil Physical Measurement and Interpretation for Land Evaluation*; CSIRO Publishing: Clayton, Australia, 2002; ISBN 978-0-643-06987-9.
10. Di Stefano, C.; Ferro, V.; Mirabile, S. Comparison between Grain-Size Analyses Using Laser Diffraction and Sedimentation Methods. *Biosyst. Eng.* **2010**, *106*, 205–215. [CrossRef]
11. Sochan, A.; Bieganowski, A.; Bartmiński, P.; Ryżak, M.; Brzezińska, M.; Dębicki, R.; Stuczyński, T.; Polakowski, C. Use of the Laser Diffraction Method for Assessment of the Pipette Method. *Soil Sci. Soc. Am. J.* **2015**, *79*, 37–42. [CrossRef]
12. Faroughi, S.A.; Huber, C.A. Theoretical Hydrodynamic Modification on the Soil Texture Analyses Obtained from the Hydrometer Test. *Géotechnique* **2016**, *66*, 378–385. [CrossRef]
13. Allen, T. Particle Size, Shape and Distribution. In *Particle Size Measurement*; Springer: Dordrecht, The Netherlands, 1990; pp. 124–191. ISBN 978-94-010-6673-0.
14. Van Rijn, L. *Principles of Sediment Transport in Rivers, Estuaries and Coastal Seas*; Aqua Publications: Amsterdam, The Netherlands, 1993; ISBN 9080035629.
15. Jillavenkatesa, A.; Dapkunas, S.J.; Lum, L.S.H. *NIST Recommended Practice Guide—Particle Size Characterization*; National Institute of Standards and Technology: Washington, DC, USA, 2001.
16. Shein, E.V. The Particle-Size Distribution in Soils: Problems of the Methods of Study, Interpretation of the Results, and Classification. *Eurasian Soil Sci.* **2009**, *42*, 284–291. [CrossRef]
17. Papuga, K.; Kaszubkiewicz, J.; Kawałko, D. Do We Have to Use Suspensions with Low Concentrations in Determination of Particle Size Distribution by Sedimentation Methods? *Powder Technol.* **2021**, *389*, 507–521. [CrossRef]
18. Hassink, J.; Whitmore, A.P.; Kubat, J. Size and density fractionation of soil organic matter and the physical capacity of soils to protect organic matter. *Eur. J. Agron.* **1997**, *7*, 189–199. [CrossRef]
19. Van Reeuwijk, L.P. *Procedures for Soil Analysis*, 6th ed.; ISRIC: Wageningen, The Netherlands, 2002.
20. Blott, S.J.; Croft, D.J.; Pye, K.; Saye, S.E.; Wilson, H.E. Particle Size Analysis by Laser Diffraction. *Geol. Soc. Lond. Spec. Publ.* **2004**, *232*, 63–73. [CrossRef]
21. Vdovic, N.; Pikelj, K.; Jurina, I.; Ivanic, M.; Dunato, N. The Implications of Sample Preparation on the Particle Size Distribution of Soil. *J. Plant Nutr. Soil Sci.* **2019**, *9*, 277–285. [CrossRef]
22. Sasaki, S. Hydrogen peroxide treatment on typical Hokkaido soils. *Soil Sci. Plant Nutr.* **1961**, *6*, 106–113. [CrossRef]
23. Mikutta, R.; Kleber, M.; Kaiser, K.; Jahn, R. Review: Organic Matter Removal from Soils Using Hydrogen Peroxide, Sodium Hypochlorite, and Disodium Peroxodisulfate. *Soil Sci. Soc. Am. J.* **2005**, *69*, 16. [CrossRef]
24. Zimmermann, I.; Horn, R. Impact of Sample Pretreatment on the Results of Texture Analysis in Different Soils. *Geoderma* **2020**, *371*, 114379. [CrossRef]
25. Durner, W.; Iden, S.C.; von Unold, G. The Integral Suspension Pressure Method (ISP) for Precise Particle-Size Analysis by Gravitational Sedimentation: ISP Method for Particle-Size Analysis. *Water Resour. Res.* **2017**, *53*, 33–48. [CrossRef]
26. Ghasemy, A.; Rahimi, E.; Malekzadeh, A. Introduction of a New Method for Determining the Particle-Size Distribution of Fine-Grained Soils. *Measurement* **2019**, *132*, 79–86. [CrossRef]
27. Turlej, T. Automation of Sedimentation Test. *Water Sci. Technol.* **2018**, *77*, 1960–1966. [CrossRef]
28. Murad, M.O.F.; Jones, E.J.; Minasny, B. Automated Soil Particle-size Analysis Using Time of Flight Distance Ranging Sensor. *Soil Sci. Soc. Am. J.* **2020**, *84*, 690–699. [CrossRef]
29. Orhan, U.; Kılınç, E. Estimating Soil Texture with Laser-Guided Bouyoucos. *Automatika* **2020**, *61*, 1–10. [CrossRef]
30. Kaszubkiewicz, J.; Wilczewski, W.; Novák, T.J.; Woźniczka, P.; Faliński, K.; Belowski, J.; Kawałko, D. Determination of Soil Grain Size Composition by Measuring Apparent Weight of Float Submerged in Suspension. *Int. Agrophys.* **2017**, *31*, 61–72. [CrossRef]
31. Kaszubkiewicz, J.; Papuga, K.; Kawałko, D.; Woźniczka, P. Particle Size Analysis by an Automated Dynamometer Method Integrated with an X-y Sample Changer. *Measurement* **2020**, *157*, 107680. [CrossRef]
32. Papuga, K.; Kaszubkiewicz, J.; Wilczewski, W.; Staś, M.; Belowski, J.; Kawałko, D. Soil Grain Size Analysis by the Dynamometer Method—A Comparison to the Pipette and Hydrometer Method. *Soil Sci. Annu.* **2018**, *69*, 17–27. [CrossRef]
33. Soil Survey Division Staff. *Soil Survey Manual: Soil Conservation Service, U.S. Department of Agriculture Handbook 18*; U.S. Department of Agriculture: Washington, DC, USA, 1993.
34. Coates, G.F.; Hulse, C.A. A Comparison of Four Methods of Size Analysis of Fine-Grained Sediments. *N. Z. J. Geol. Geophys.* **1985**, *28*, 369–380. [CrossRef]
35. Smith, R.J. Use and misuse of the reduced major axis for line-fitting. *Am. J. Biol. Anthropol.* **2009**, *140*, 476–486. [CrossRef]
36. Harper, W.V. Reduced Major Axis Regression: Teaching Alternatives to Least Squares. In Proceedings of the Ninth International Conference on Teaching Statistics (ICOTS9), Flagstaff, AZ, USA, 13–18 July 2014.
37. Iglesias, F.; Kastner, W. Analysis of Similarity Measures in Times Series Clustering for the Discovery of Building Energy Patterns. *Energies* **2013**, *6*, 579–597. [CrossRef]
38. Bolan, N.S.; Adriano, D.C.; Kunhikrishnan, A.; James, T.; McDowell, R.; Senesi, N. Dissolved Organic Matter. In *Advances in Agronomy*; Elsevier: Amsterdam, The Netherlands, 2011; Volume 110, pp. 1–75. ISBN 978-0-12-385531-2.
39. Six, J.; Conant, R.T.; Paul, E.A.; Paustian, K. Stabilization mechanisms of soil organic matter: Implications for C-saturation of soils. *Plant Soil* **2002**, *241*, 155–176. [CrossRef]
40. Totsche, K.U.; Amelung, W.; Gerzabek, M.H.; Guggenberger, G.; Klumpp, E.; Knief, C.; Lehndorff, E.; Mikutta, R.; Peth, S.; Prechtel, A.; et al. Microaggregates in Soils. *J. Plant Nutr. Soil Sci.* **2018**, *181*, 104–136. [CrossRef]

41. Cotrufo, M.F.; Ranalli, M.G.; Haddix, M.L.; Six, J.; Lugato, E. Soil Carbon Storage Informed by Particulate and Mineral-Associated Organic Matter. *Nat. Geosci.* **2019**, *12*, 989–994. [CrossRef]
42. Lavallee, J.M.; Soong, J.L.; Cotrufo, M.F. Conceptualizing Soil Organic Matter into Particulate and Mineral-associated Forms to Address Global Change in the 21st Century. *Glob. Change Biol.* **2020**, *26*, 261–273. [CrossRef] [PubMed]
43. Stokes, G.G. On the effect of the internal friction of fluids on the motion of pendulums. *Trans. Camb. Philos. Soc.* **1850**, *9*, 8–106.
44. Barthès, B.G.; Brunet, D.; Hien, E.; Enjalric, F.; Conche, S.; Freschet, G.T.; d'Annunzio, R.; Toucet-Louri, J. Determining the Distributions of Soil Carbon and Nitrogen in Particle Size Fractions Using Near-Infrared Reflectance Spectrum of Bulk Soil Samples. *Soil Biol. Biochem.* **2008**, *40*, 1533–1537. [CrossRef]
45. Yang, X.M.; Drury, C.F.; Reynolds, W.D.; MacTavish, D.C. Use of Sonication to Determine the Size Distributions of Soil Particles and Organic Matter. *Can. J. Soil Sci.* **2009**, *89*, 413–419. [CrossRef]
46. Puget, P.; Chenu, C.; Balesdent, J. Dynamics of Soil Organic Matter Associated with Particle-Size Fractions of Water-Stable Aggregates: Dynamics of Soil Organic Matter in Water-Stable Aggregates. *Eur. J. Soil Sci.* **2000**, *51*, 595–605. [CrossRef]
47. Schmidt, M.W.I.; Rumpel, C.; Kögel-Knabner, I. Particle Size Fractionation of Soil Containing Coal and Combusted Particles. *Eur. J. Soil Sci.* **1999**, *50*, 515–522. [CrossRef]
48. Beuselinck, L.; Govers, G.; Poesen, J.; Degraer, G.; Froyen, L. Grain-Size Analysis by Laser Diffractometry: Comparison with the Sieve-Pipette Method. *CATENA* **1998**, *32*, 193–208. [CrossRef]
49. Jensen, J.L.; Schjønning, P.; Watts, C.W.; Christensen, B.T.; Munkholm, L.J. Soil Texture Analysis Revisited: Removal of Organic Matter Matters More than Ever. *PLoS ONE* **2017**, *12*, e0178039. [CrossRef]
50. Hereter, A.; Josa, R.; Candela, X. Changes in Particle-Size Distribution Influenced by Organic Matter and Mechanical or Ultrasonic Dispersion Techniques. *Commun. Soil Sci. Plant Anal.* **2002**, *33*, 1351–1362. [CrossRef]

UNIWERSYTET
PRZYRODNICZY
WE WROCŁAWIU

INSTYTUT NAUK O GLEBIE, ŻYWIENIA ROŚLIN I OCHRONY ŚRODOWISKA

Wrocław 04.04.2022

Mgr inż. Krzysztof Papuga
Instytut Nauk o Glebie, Żywienia Roślin
i Ochrony Środowiska
Uniwersytet Przyrodniczy we Wrocławiu

OŚWIADCZENIE

Oświadczam, że w pracy: Papuga K., Kaszubkiewicz J., Kawałko D., Kreimeyer M., 2022. Effect of Organic Matter Removal by Hydrogen Peroxide on the Determination of Soil Particle Size Distribution Using the Dynamometer Method. Agriculture, 12, 226 (doi: 10.3390/agriculture12020226) mój udział polegał na opracowaniu koncepcji, metodologii, wykonaniu analiz laboratoryjnych i obliczeniowych, opracowaniu merytorycznym i graficznym rezultatów analiz oraz przygotowaniu treści manuskryptu.

Papuga
.....
Podpis

UNIWERSYTET PRZYRODNICZY WE WROCŁAWIU
INSTYTUT NAUK O GLEBIE, ŻYWIENIA ROŚLIN I OCHRONY ŚRODOWISKA
UL. GRUNWALDZKA 53, 50-357 WROCŁAW
tel. 71 320 56 04
e-mail: igleb@upwr.edu.pl • https://ingos.upwr.edu.pl/

UNIWERSYTET
PRZYRODNICZY
WE WROCŁAWIU

Wrocław 04.04.2022

Prof. Dr hab. Jarosław Kaszubkiewicz
Instytut Nauk o Glebie, Żywienia Roślin
i Ochrony Środowiska
Uniwersytet Przyrodniczy we Wrocławiu

OŚWIADCZENIE

Oświadczam, że w pracy: Papuga K., Kaszubkiewicz J., Kawałko D., Kreimeyer M., 2022. Effect of Organic Matter Removal by Hydrogen Peroxide on the Determination of Soil Particle Size Distribution Using the Dynamometer Method. Agriculture, 12, 226 (doi: 10.3390/agriculture12020226) mój udział polegał na nadzorowaniu przy opracowaniu koncepcji, metodologii i doboru analiz laboratoryjnych. Nadzór merytoryczny obejmował także poprawność interpretacji wyników oraz przygotowanie treści manuskryptu.

.....
Podpis

UNIWERSYTET
PRZYRODNICZY
WE WROCŁAWIU

INSTYTUT NAUK O GLEBIE, ŻYWIENIA ROŚLIN I OCHRONY ŚRODOWISKA

Wrocław 04.04.2022

Dr inż. Dorota Kawałko
Instytut Nauk o Glebie, Żywienia Roślin
i Ochrony Środowiska
Uniwersytet Przyrodniczy we Wrocławiu

OŚWIADCZENIE

Oświadczam, że w pracy: Papuga K., Kaszubkiewicz J., Kawałko D., Kreimeyer M., 2022. Effect of Organic Matter Removal by Hydrogen Peroxide on the Determination of Soil Particle Size Distribution Using the Dynamometer Method. Agriculture, 12, 226 (doi: 10.3390/agriculture12020226) mój udział polegał na nadzorowaniu przy opracowaniu metodologii, doboru analiz laboratoryjnych oraz przygotowaniu treści manuskryptu.

Dorota Kawałko

Podpis

UNIWERSYTET PRZYRODNICZY WE WROCŁAWIU
INSTYTUT NAUK O GLEBIE, ŻYWIENIA ROŚLIN I OCHRONY ŚRODOWISKA
UL. GRUNWALDZKA 53, 50-357 WROCŁAW
tel. 71 320 56 04
e-mail: igleb@upwr.edu.pl • https://ingos.upwr.edu.pl/